1994

Behaviour of precast reinforced concrete beam-column connections under static and repeated loading

Han Qian
University of Wollongong

UNIVERSITY OF WOLLONGONG

BEHAVIOUR OF PRECAST REINFORCED CONCRETE BEAM-COLUMN CONNECTIONS UNDER STATIC AND REPEATED LOADING

by

HAN QIAN, B.E.

A thesis submitted in fulfilment of the requirements
for the award of the degree of

MASTER OF ENGINEERING (HONOURS)

in

DEPARTMENT OF CIVIL AND MINING ENGINEERING

February 1994

DECLARATION

I hereby declare that this work has not been submitted for a higher degree to any other University or Institute.

Han Qian

February, 1994

ACKNOWLEDGMENTS

The author wishes to express her heartfelt gratitude to Associate Professor Y.C. Loo, her supervisor, for his invaluable guidance, constant encouragement and patient assistance during the research and writing of this thesis.

The author acknowledges the assistance given by Professor R.N. Singh, Head of the Department of Civil and Mining Engineering at the University of Wollongong.

The author would like to thank Ms. Bao Zhong Yao and Mr. R. Piyasena who aided immensely in conducting the tests, and Mr. Don Lu for checking the thesis presentation.

The author would like to thank laboratory technical officers, Messrs. Richard Webb and Frank Hornung for their unquestioned help and in conducting laboratory experiments.

Unqualified appreciation goes to the author's husband, Dong Qiu, whose constant endearment, financial assistance and understanding helped considerably in the preparation of this thesis.

ABSTRACT

Connection design is one of the most important considerations for the successful construction of precast concrete structures. The configuration details of the connection affect the strength, stability, ductility as well as load redistribution of the structure under loading.

Since the 1980's, extensive laboratory testing and research work has been conducted to study the seismic behaviour of beam-column connections in cast-in-place reinforced concrete building frames. However, only a limited number of studies have been conducted on the performance of precast concrete connections, and into a lesser extent on moment resistant precast concrete beam-column connections. This is in spite of the fact that precast concrete connections have been in use all over the world since the 1950's. Reliable connection behaviour can only be verified by testing, although the ACI Manual[62,63] and the Australian Manual[5] describe nearly 40 beam-column connections fulfilling many functions. Therefore, it is desirable to perform tests on more precast beam-column subassemblies.

This study investigates the performance of two types of moment-resisting connections for joining precast beams and columns, which were recommended by the American Prestressed Concrete Institute (PCI) and Australian Prestressed Concrete Group (APCG) for use in precast reinforced concrete building frames. A total of twelve half-scale model connections, divided into two groups according to the type of loading were designed, manufactured and tested to failure under static and repeated loadings. Each group had two monolithic models for the purpose of comparison and two models of each type of precast connections. The beam and column dimensions, the strength of precast concrete and configuration details were kept constant to afford a direct comparative study of connection behaviour. The only variable used in the study was the steel ratio of tension bar in the connecting beams. Each type of connection in

each group had two steel ratios corresponding to the two cases, p_t-p_c=2/3 p_{all} and p_t-p_c=p_{all}, respectively to study the effect of the amount of reinforcement in the subassemblies. Note that (p_t-p_c) is the steel ratio difference between the tension and compression bars and p_{all} is the tension steel ratio allowed by the Australian Standard.

The objective of this study is to develop a moment-resisting precast concrete beam-column connection that is economical and can be easily constructed. The connections are evaluated based on their performance in terms of strength, deformation ductility, crack features, failure modes and energy dissipation characteristics as well as their constructibility.

From the comparative study, it is found that both types of precast connections performed satisfactorily in that their bending strength capacity and energy absorbing capacity are, without exception, better than the monolithic ones. In addition, their ductility, in general, is superior to their monolithic counterparts. This indicates that both types of precast connections can be considered as moment-resisting ductile precast concrete beam-column connections and can be safely applied to precast reinforced concrete building frame construction.

Finally, in light of the test results, the relative merits of the two types of precast connections are discussed and recommendations given.

CONTENTS

LIST OF FIGURES

LIST OF PLATES

LIST OF TABLES

NOTATION

a = depth of the rectangular stress block or a segment of the critical shear perimeter parallel to the x-axis

A_{sc} = cross sectional area of compression steel

A_{st} = cross sectional area of tension steel

b = width of the section

D = overall depth of the section

d = effective depth of the section

E_s = modulus of elasticity of steel

f_{sy} = yield strength of tension steel

f_{sy}' = yield strength of compression steel

f_c' = characteristic compressive strength of precast concrete

f_c'' = characteristic compressive strength of cast-in-place concrete

k_{uB} = neutral axis parameter for a section with balanced steel ratio

k_u = neutral axis parameter

L = span of cantilever connecting beam

M_{max} = calculated ultimate bending moment of connecting beam

M_u = measured ultimate bending moment of connecting beam

P = concentrated load

P_{all} = maximum allowable steel ratio

P_B = balanced steel ratio

P_b = vertical load on the connecting beam

Pc = vertical load on the column

p_c = compression steel ratio

p_c' = normalised compression steel ratio

P_u = measured ultimate vertical load of connecting beam

P_{max} = calculated ultimate vertical load of connecting beam

γ = ratio of the depth of the rectangular stress block to $k_u d$

v_1 = ratio of the maximum load applied to the specimen at each cycle to the maximum load applied at first cycle

v_2 = ratio of the maximum load applied to the specimen at each cycle to the theoretical maximum load P_{max}

Δ_y = deflection of connecting beam at initial yield for tensioning steel bars

Δ_{Hu} = ultimate horizontal deflection of connecting beam

Δ_{Hy} = horizontal deflection of connecting beam at initial yield for tensioning steel bars.

Δ_u = ultimate vertical deflection of connecting beam

ε_{cu} = ultimate strain of concrete in compression

θ_u = ultimate beam end rotation of connecting beam

θ_y = beam end rotation of connecting beam at initial yield for tensioning steel bars

Δ = deflection of connecting beam at load point

CHAPTER 1

INTRODUCTION

1.1 General Remarks

In a relatively short period of time, precast concrete has become a very important material of framing structures. The wide application of this technique is based on the advantages of prefabrication such as the reduction in construction time, quantities of materials and manpower and the improvement of the quality of the products. Construction with precast concrete can proceed almost independently of weather conditions. All these eventually result in a reduction of costs and better working conditions for the building operatives.

In recent years, more and more attention has been focussed on the connections of precast concrete structures, since the design of connection is one of the most critical engineering phases in the design of precast concrete structures. Satisfactory performance and economy of precast concrete structures depends to a great extent on the proper selection and design of each connection. The function of a connection is to transfer load from one precast member to another and to provide stability. A good connection must not only have enough strength to resist the force to which it will be subjected during its lifetime, but also enough ductility to undergo large deformations prior to failure. In addition, a good connection must be required to meet other criteria such as volume change accommodation, durability, fire resistance, fabrication simplicity and erection swiftness. Furthermore, reliable connection behaviour can only be verified by testing. It is desirable for precast reinforced concrete ductile frames to possess more reliable connection types to match the individual structural requirements. Therefore, performing tests on more precast beam-column connections is essential to establish the necessary requirement for adequate design of precast reinforced concrete connections.

1.2 Objectives and Scope

The beam-column connections investigated in this study were examined for structural performance, as measured by load and deflection behaviour, and for cost effectiveness and constructibility. Emphasis was placed on the behaviour of the connection subjected to static and repeated loading, which was designed considering the gravity loading and lateral loading due to wind or equivalent moderate seismic loading. The specimens were chosen based on a previous investigation[82]. The two types of connections studied are recommended by American Prestressed Concrete Institute[62,63] and Australian Prestressed Concrete Group[5] for use in precast reinforced concrete building frames.

The intention behind the work reported herein was to investigate the following:

(a) comparison between the precast concrete beam-column connections to monolithic connections on the behaviour of strength, deformation, ultimate loading capacity, ductility, energy dissipation, crack features, failure modes and construction properties;

(b) comparison between the performance of connections under static loading to repeated loading;

(c) comparison between the performance of connections with different steel ratios;

(d) comparison between the performance of precast concrete beam-column connections using two types of configurations;

(e) identification of a precast concrete beam-column connection which has adequate strength and ductility to be classified as an economical, easily constructed, ductile and moment-resisting connection in the context of seismic design.

The research consisted of an experimental program in which twelve half-scale specimens were designed, manufactured and tested. These specimens were divided

into two groups according to the different types of loading. Each group had six specimens, including two monolithic beam-column connections for the purpose of comparison and four precast beam-column assemblies with two different configurations, in which the connections were made out of precast beam and column elements assembled in the connection zone by cast-in-place concrete.

The beam and column dimensions, the strength of precast concrete and configuration detail were kept constant to afford a direct comparison. The only difference was the steel ratio of the tension bar in the connecting beams.

1.3 Summary of Contents

Before conducting these tests, a brief review of previous investigations on monolithic and precast reinforced concrete beam-column connections was carried out. This is presented in Chapter 2.

Details of all the specimens are described in Chapter 3, which also contains the description of test set-up and experimental procedure of the connection tests.

Results of all the tests and the observed behaviour of the test specimens under static and repeated loading are given in Chapters 4 and 5 respectively.

Summary and conclusions are presented in Chapter 6, which also contains the recommendations for further study.

CHAPTER 2

LITERATURE REVIEW

2.1 General Remarks

Precast concrete has proven to be an economical form of construction. It is a building process ideally suited for the future. Materials are inexpensive and the method of construction, involving factory manufacture of components and rapid site erection, leads itself to innovations in design and construction. Advanced technology, including robotic and the use of computer-aided manufacture, will lead to more efficient erection procedures. The potential for significant reductions in building costs is apparent. The high technology and low labour content make it suitable for the conditions and technological strengths of many countries. Without necessarily losing the flexibility of construction form that has resulted from mass produced " strength building " developed in countries that are technologically less advanced, precast concrete is now becoming a fundamental method of civil engineering construction and will also develop as leading construction technique into the next century.

The use of precast concrete dates back to the 19th century when precast infill panels were used between insitu columns as perimeter walls on industrial buildings. However, the development of the concept was restricted by lack of mobile cranage and was generally limited to units that could be hoisted by block and tackle and shear-legs.[16]

A notable example incorporating this concept of precast structures in Australia was the Dennys Lescelles Wool store in Geelong, a three-storey building designed and constructed in 1901-1911, which was surely one of the most technically advanced reinforced concrete building of its time.[16]

With the development of mobile cranes in the 1920's and 30's, numerous systems of structural precast concrete were developed in Europe and the United States of

America. The precast concrete building frames have been confirmed to have a number of attractive features such as better quality control of the product, savings in formwork and construction time. In the 1950's, with the development of prestressed concrete and the availability of large capacity mobile cranes, precast concrete came into its own and by 1960 there were major plants operating in all main cities over the world.[16]

Since the early 1960's there has been a steady and remarkable increase in the use of precast concrete for structural components. However, until the late 1970's to early 1980's, lack of information on the behaviour of moment-resisting connections between precast elements made the use of precast elements for seismic resistance in moment resisting frames and walls to be the exception rather than the rule.[34]

The boom years of the mid-1980's produced a significant increase in structural applications of precast concrete, which had the advantages of familiar materials and methods, high quality factory made units and speed of construction. With this increased use of precast concrete structural elements came an increasing concern that some of the design solutions being used should be more fully researched. Even if there was no reason to doubt the validity of extrapolating cast-in-place results, the number of major buildings employing precast concrete for seismic resistance demanded that more research and testing be done to justify confidence in the structural systems.[34]

2.2 Previous Study on Beam-Column Connection

As early as the 1960's, the structural engineers have been interested in studying the beam-column connection. This is because the connection is a very important part of reinforced concrete framed structures. The successful structural performance of a reinforced concrete frame largely depends on the connection behaviour. The configuration of the connections affects the constructibility, stability, strength flexibility and residual forces in the structure. Furthermore, connections play an important role in the dissipation of energy and redistribution of loads as the structure is loaded in seismic

zones. Connector types are crucial not only to the behaviour of the completed structure but also to the economical development of the building system.

The investigation of beam-column connections carried out in recent decades, can be divided into two groups,namely, the studying of monolithic reinforced concrete beam-column connections and the studying of precast or prestressed reinforced concrete beam-column connections.

2.2.1 Study on Monolithic Reinforced Concrete Beam-Column Connections

Investigation of the behaviour of reinforced concrete beam-column connections has attracted many researchers in the past 30 years. When a reinforced concrete ductile moment-resisting frame is subjected to large seismic lateral forces, the beam-column connections must be capable of carrying large forces which are accompanied by large deformations. The first behaviour studies of beam-column connections were conducted in the United States by the Poland Cement Association in the early 1960's and were published by Hanson and Conner in 1976. These tests have become the standard reference for subsequent investigation[51]. Since then the problem has been studied by other investigators in the U.S. as well as in Canada, Japan and New Zealand. Although the objectives have varied, the main emphasis of these studies has been to develop guidelines which would ensure proper anchorage of beam bars in the joint and provide ductile behaviour under repeated cyclic loading.

In 1970's ACI-ASCE Joint Committee 352[66] published the recommendations for design of beam-column joints in monolithic reinforced concrete structures. In recent years, extensive laboratory testing and research work have been conducted to study the seismic behaviour of beam-column connections in view of several collapses around the world. They include the connection mechanisms and load path, computer programs in simulating earthquake on a structural frame, earthquake simulation testing of small-scale

reinforced concrete structures, epoxy repair technique for moderate earthquake damage and using fibre reinforced concrete in seismic beam-column joints.

A review, chronologically, of some experimental investigations on beam-column connection is summarised in Table 2.1.

Table 2.1 Test Programs on R/C Beam-Column Connections

Date	Authors	Institution	Connec-tion	ref-erence
1967	Hanson, Conner	PCA Labs, Skokie, Illinois	exterior	38
1969	Higashi, Ohwada	Tokyo Metropolitan Univ., Japan	interior	41
1971	Hanson	PCA Labs, Skokie, Illinois	interior exterior	37
1971	Megget, Park	Univ. of Canterbury, New Zealand	exterior	52
1971	Brown, Jirsa	Rice University,	exterior	12
1972	Hanson, Conner	PCA Labs, Skokie, Illinois	interior exterior	39
1972	Kirdina, Schaaff	Technical univ.-Braunschweig, W. Germany	exterior	44
1972	Patton	Univ. of Canterbury, New Zealand	exterior	58
1972	Renton	Univ. of Canterbury, New Zealand	exterior	67
1972	Smith	Univ. of Canterbury, New Zealand	exterior	71
1974	Park , Thompson	Univ. of Canterbury, New Zealand	interior	57
1974	Uzumeri, Seckin	Univ. of Toronto,Canada	exterior	81

1975	Preistley	Ministry of Works, New Zealand	interior	61
1976	Gulkan	Mid. East Tech. Univ., Ankara,Turkey	interior	36
1977	Fenwick and Irvine	Univ. of Auckland, New Zealand	interior	28
1977	Lee, Wight, Hanson	Univ. of Michigan, Ann Arbor	exterior	47
1977	Meinheit , Jirsa	Univ. of Texas at Austin	interior	50
1977	Townsend, Hanson	Univ. of Michigan, Ann Arbor	exterior	78
1977	Uzumeri	Univ. of Toronto, Canada	exterior	80
1978	Birss, Paulay, Park	Univ. of Canterbury, New Zealand	interior	10
1978	Keong and Park	Univ. of Canterbury, New Zealand	interior	43
1978	Paulay, Park, Priestly	Univ. of Canterbury, New Zealand	interior	59
1979	Soleimani, Popov, Bertero	Univ. of California, Berkeley	interior	72
1980	Bertero, Popov, Forzani	Univ. of California at Berkeley	interior	7
1980	Scribner,Wight	Univ. of Illinois, Urbana, Ill,	exterior	69
1981	Park, Gaerly, Stevenson	Univ. of Canterbury , New Zealand	interior	55
1981	Meinheit, Jirsa	Univ. of Texas at Austin	interior	51
1981	Scarpas	Univ. of Canterbury, New Zealand	exterior	68

1982	Ehsani, Wight	Univ. of Michigan	exterior	23
1982	Durrani, Wight	Univ. of Michigan	interior	19
1985	Ehsani, Wight	Univ. of Michigan	exterior	21
1986	Filippou, Popov, Vertero	Univ. of California, Berkeley	interior	29
1987	Abrams	Univ. of Illinois, Urbana-Champaign.	interior	1
1987	Durrani, Wight	Rice univ., Houston, Texas,	interior	20
1988	Metwally, Chen	Pudue Univ.	interior	24
1988	Soroushian, et al.	Michigan State Univ. U.S.A.	exterior	73
1989	Gefken, Ramey	Univ. of California	exterior	33
1989	Paulay	Univ. of Canterbury, Christchurch New Zealand	interior	60
1990	French, Thorp,Tsai	Univ. of Minnesota	interior	32
1990	Leon	Univ. of Minnesota	interior	47
1991	Alameddine, et al.,	Univ. of Arizona, Tucson, AZ	exterior	3
1991	Ehsani, Alameddine	Univ. of Arizona, Tucson.	exterior	22
1991	Soroushian, Choi	Michigan State Univ. U.S.A.	exterior	74
1992	Guimaraes, Kreger Jirsa	Univ. of Texas at Austin	interior	35
1992	Tsonos, Tegos, Penelis	Aristotle Univ. Thessaloniki, Greece	exterior	79
1993	Adin, et al.,	Technion-Israel Institute of Technology,	exterior	2

1993	Cheung, Paulay, Park	Univ. of Canterbury, New Zealand	exterior interior	15

2.2.2 Study on Precast R/C Beam-Column Connections

Because the basic problem in design of precast R/C building frames is finding an economical and practical method for connecting precast components together, beam-column connection detail is the key to the construction of precast R/C moment-resisting building frames. The function of connections is not only to transfer loads but also to develop continuity and monolithic behaviour in the entire structure. After realising the importance of connections since the early use of precast concrete construction, some studies, even though of only a limited number, were conducted on the performance of precast reinforced concrete beam-column connections.

One of the first experimental studies on precast beam-column connections was undertaken by P.W. Birkeland and H.W.Birkeland[9], at the structural consulting firm of ABAM Engineer, Tocoma, Washington in 1966. The experiments were conducted on a form of bolted connection called the "knife connection". Since then, other investigations have been focused on the proposing of different kinds of connections and with the development of the knowledge of earthquakes, more studies were focused on finding the ductile, moment-resisting connection in the context of seismic design. The boom years were in 1980's.

In 1981, 11 tests on full-scale beam-column connections, including two monolithic specimens for purposes of comparison were conducted by S.U. Pillai and D.W. Kirk[64]. This project was undertaken with the objective of developing a precast concrete beam-column connection which had adequate strength and ductility to be classified as a ductile, moment-resisting connection in the context of seismic design. The tests were conducted on a form of welded connection and the test results indicated that the proposed method of

connection performed satisfactorily and in a manner comparable to the performance of a similar monolithic connection.

Four years later, P.B. Hatt and D.W. Kirk[8], conducted tests on an improved beam-column connection, in an attempt to prove that connections can be designed to behave in a ductile fashion , conducting tests similar to those conducted by S.U. Pillai and D.W. Kirk[64]. Experimental results showed that the joint detail proposed can withstand large ductility demands.

Due to the ever increasing information on the topic of precast concrete, the Precast / Prestressed Concrete Institute (PCI) summarised and described approximately 40 beam-column connections [62,63] and Australia Prestressed Concrete Group (APCG) also published a hand-book which combined with Australian practices[5]. These connections can be mainly classified into seven types according to the different means of connections:

. welded connection;

. bolted connection;

. precast beam constructed into a CIP column;

. precast column constructed into a CIP beam;

. precast beam and precast column connected with CIP concrete;

. post-tensioned connection;

. composite connection.

In 1987, a study sponsored by PCI was conducted by C.W. Dolan, J.F. Stanton and R.G. Anderson at University of Washington[17]. The PCI Specially Funded Research and Development Programs 1 and 4 (PCI 1/4) focused on the actual behaviour of commonly used connections. The two programs were combined in order to devote maximum effort to the physical testing of connections in common use. PCI 1/4 consisted of individual tests of eight simple connections, eight moment resisting connections and one moment resisting frame test. These sixteen connections were all

selected from the PCI Manual. The tests indicated that only the results of the moment resistant connections are applicable to seismic design.

After the late 1980's more studies have been conducted on the behaviour of precast reinforced concrete beam-column connection designed to resist earthquake load mainly in the United States, Japan, New Zealand, Canada and China.

In America, a series of seven precast concrete beam-column connections were tested at the University of Minnesota By C.W. French et al[30,31]. The various connection details used were post-tensioned; threaded rebar; welded; composite-post-tensioned in the bottom of the beam with a cast-in-place top and bolted. All of the structures were subjected to identical cyclic lateral load histories. The tests indicated that the specimens with the plastic hinge occurring at the conventionally reinforced joint region showed better energy dissipation characteristics than those with the plastic hinge occurring in the prestressed concrete beams.

A test program at the University of Michigan conducted by K.S. Soubra, J.K. Wight and A.E.Naaman[75,76] studied the characteristics of fibre reinforced concrete (FRC) composites and examined the use of FRC in the joint between two precast concrete elements. Six beam-type specimens, each consisting of two precast reinforced concrete parts jointed together by a cast-in-place fibre reinforced concrete connector, were tested under cyclic third point loading. Conclusions drawn from the study were that the FRC joint performed better than joint cast with conventional concrete and that FRC joints with steel fibres performed better than FRC joints with plastic fibres.

On October 8, 1986, the PCI, in corporation with the Precast Concrete Manufacturers Association of California (PCMAC) and PCI Seismic Committee, sponsored a one-day workshop in Los Angeles on the Effective Use of Precast Concrete for Seismic Resistance. The workshop was aimed at design professionals, producers / constructors, code writers, building officials and researchers. The overall goal was to provide guidance to the precast concrete industry[25,26].

In 1987, R.E. Englekirk published a paper presenting the basic concepts in developing a precast concrete ductile moment resisting frame for a building situated in a region of high seismicity[27]. In his paper, the design consideration concerning hinged connectors, ductile energy dissipating connectors and strong non-yielding connectors was described. Also the various connector type assemblages including a precast shell with cast-in-place core, cold joints reinforced with mild steel, grouted post-tensioned assemblage of precast components and unbounded post-tensioned assembly of precast components were discussed.

A study was undertaken by C.W. Dolan and S.P. Pessikin in Cornell University, New York in 1989[18]. The purpose of that study was to examine the feasibility of using models to investigate the behaviour of moment resisting connections for precast concrete structures. Tests of one-quarter scale models of a single beam-column connection were conducted and the results were compared to a test of a prototype connection. The model tests accurately reflected both the strength and the moment-rotation behaviour of the prototype connection, demonstrating that models were useful tools for evaluating precast concrete connection behaviour. Test results confirmed that the connections have a low flexural stiffness, and specific research areas were recommended.

A lot of combined work was conducted between United States and Japan. On October 27 through November 1, 1986, the fifth American Concrete Institute-Japan Concrete Institute Seminar on Concrete was held in Japan[40]. The subject of the Seminar was Precast Concrete Construction in Seismic Zones. Conclusions drawn from the Seminar were that:

· the information on the actual dynamic response of precast concrete construction in earthquakes is lacking and there is inadequate correlation between computer predictions of dynamic behaviour and actual behaviour.

• there is a need for a code compatible research program that examines the significance of variations in global ductility forms on dynamic response and the interrelation between such global ductility forms and ductility response characteristics.
•summarised the different studying programs between Japanese investigators and non-Japanese investigators.

After the fifth ACI-JCI Seminar[40], the Precast Seismic Structural Systems (PRESSS) Research Program was initiated as part of the United States - Japan protocol on large scale testing for seismic response of precast concrete buildings. Both American and Japanese research teams developed independent programs which met the needs of the individual countries. These were then examined to determine the areas where cooperative research between the programs could be developed to the maximum degree possible. An essential aspect of this is a clear understanding of the differences in design philosophy between Japanese and American practice. The overall purpose of these coordinated research programs was to develop recommendations for the seismic design of buildings constructed of a particular material, in this case precast concrete, based on sound analytical and experimental research.

The PRESSS Research Program was conceived in three phases. Phase 1, which was funded for a three-year period ending in 1993, was focused on identifying and evaluating the most promising structural concepts for precast concrete building systems in seismically active regions. It consisted of five projects: concept development; connection classification and modelling; PRESSS analytical platform development; preliminary design recommendation coordination. Phase 2 will involve detailed experimental studies of components and subassemblies of precast systems selected during phase 1 for more detailed investigation. Phase 3 is expected to involve one or more multistorey full-size " super-assemblage " experiments and the finalisation of the seismic design recommendations for incorporation into the model building codes[65].

During PRESSS phase 1, several works have been done and a series of papers have been published in PCI journal. The paper prepared by J.F. Stanton et al[77] describes the studies on connections in precast concrete structures being conducted under the PRESSS Research Program. It also classifies and evaluates some existing connections for the purpose of selecting the most promising systems for further development for analysis and ultimately, for testing. The paper prepared by S.D. Nakaki and R.E. Englekirk[53] described the results of the workshops held by ACI in April 1991 as well as the review by the PRESSS Applications Advisory Committee. The paper prepared by L.S. Johal et al[42] presented the impact of past PCI-funded research, and the results of an industry survey conducted by the PCI Committee on research and development to determine the most needed topics for future research in precast and prestressed concrete.

In New Zealand, extensive work has been carried out in relation to the behaviour of precast building frames in seismic regions in which most connections were made in the form of post-tensioned connections. As early as 1971, R.W.G.Blakeley and R. Park[11] conducted a series of four tests on full-scale precast, prestressed concrete beam-column assemblies under reversed cyclic loading of high intensity. The test variables included the amount of transverse confining steel for ductility and the position of the plastic hinge in the members. The results showed that prestressed concrete framed structures are capable of resisting moderate earthquakes without structural damage and of withstanding severe earthquakes, although in this case structural damage may occur.

In 1986, a study on the behaviour of three full-scale exterior precast beam-column connections was conducted by E. Park and P.K. Bull at the University of Canterbury[54]. The specimens were composite connections consisting of a precast prestressed beam shell with a cast-in-place concrete core. The specimens were tested cyclically to determine their seismic performance characteristics when plastic hinge regions occur in the beams adjacent to the columns. The general conclusion from the

tests was that specimens would indeed be satisfactory for use in ductile seismic resisting frames if they were designed for seismic loading.

In 1988, a seminar held in University of Canterbury highlighted a growing need to investigate and verify the performance of precast concrete in structural members for seismic resistance. Following the seminar a study group was formed and in 1991 published their study report " Guide lines for the use of structural precast concrete in buildings " [34].

A series of experimental programs were conducted at the National Institute of Standards and Technology[14]. The overall test program involved the testing of one-third scale model interior beam-column connections. The objective of the study was to develop a moment resistant precast concrete connection that was economical and could be easily constructed.

In Canada, some work has been carried out in recent years. In 1990, M. Seckin and H.C. Fu[70] conducted experiments on interior beam-column assemblies representing a portion of a frame subjected to simulated seismic loading. The differences of behaviour of these types of connections were presented and discussed. Test data showed that properly designed precast beam-column connections maintained ductility and strength and exhibited excellent energy-dissipating capacity when subjected to large inelastic deformations under loads reversals.

In recent years, because of the remarkable labour shortage in Japan, the precast concrete frame systems are increasingly being used for the construction of large scale shopping centres, schools and housing buildings. The recent tendency is the mixing of precast and cast-in-place connection methods. A lot of work has been carried out[13,45,83].

In China, precast concrete has been used in various kinds of civil and industrial buildings for more than 30 years. After a series of tests and investigations of the

results of earthquake hazards, they have worked out some principles and types of joint detail based on calculation[49].

In India, work has also been carried out. 28 tests on post-tensioned grouted keyed connections were conducted by G.Annamalai and R.C. Broun,Jr in 1990[4]. The test indicated that post-tensioned grouted keyed connections exhibited a high degree of monolithic action and could transfer shear satisfactorily across the connection.

2.3 Summary of literature review

Summing up the literature review, it is clear that most of the data available to date are based on experimental and analytical studies on the performance of reinforced monolithic concrete beam-column connections subjected to cyclic inelastic loadings. However, only a limited number of studies have been conducted on the performance of precast concrete connections and to a lesser extent on moment resistant precast concrete beam-column connections. This is true despite the fact that precast concrete connections have been in use all over the world since the 1950's. Furthermore, every kind of connection has its own characteristic. There is no one connection which is absolutely right or wrong. A good connection should not only satisfy the needs of serviceability such as strength, stiffness or ductility, but also satisfy the needs of economy and constructibility. So it is desirable for precast reinforced concrete ductile frames to possess more reliable connection types to match the individual structures. Although the PCI Manual[44,45] and Australia Manual[43] describe nearly 40 beam-column connections fulfilling many functions, reliable connection behaviour can only be verified by testing. Therefore, preforming tests on more precast beam-column subassemblies is essential to establish the necessary requirement for adequate design of precast reinforced concrete connection.

In response to these needs, a study of the behaviour of precast concrete beam-column connections suited for multi-storey residential buildings was initiated at the University of Wollongong. The study was conceived in three phases. Phase 1, which

has been completed, was focused on the behaviour of connection under static loading[82]. Phase 2, which is being studied, is focused on the behaviour of connections under moderate earthquake type loading. Phase 3, which will be done soon, is focused on the behaviour of connections under severe earthquake type loading. The study herein is the work in phase 2.

CHAPTER 3

EXPERIMENTAL INVESTIGATION

3.1 Seismic Design Philosophy

Earthquake is one of nature's unpredictable and disastrous forces. The energy release causes forces which are often greater than the structural resistance of natural and man-made structures. For earthquake or blast resistant design, the recent practice has been to proportion members according to two separate criteria. For moderate earthquakes, the building should be serviceable, therefore, deformations are held to a prescribed minimum. This can be easily done by an elastic analysis procedure. For severe earthquakes, the structures must not collapse. It is possible to design the structures to remain elastic during a major earthquake. However, such a design can be very expensive, and the additional cost involved is seldom justified except perhaps for certain critical systems. On the other hand, it is possible to design the structure so that even though it may suffer considerable inelastic deformation during a severe earthquake, it will not collapse and does not cause excessive structural damage. This criterion imposes demands on the ability of the structure to absorb and dissipate the energy fed into it from ground motion. The manner in which these energy requirements is met varies with the structural system used for the building. For medium-rise reinforced concrete buildings the necessary lateral stiffness and energy capacity requirements can be met by using a ductile moment-resisting frame. This ductile moment-resisting reinforced concrete frame is designed to dissipate seismic energy by flexural yielding at selected plastic hinge positions, since with proper design the plastic hinges can be made adequately ductile. Fig 3.1 shows mechanisms of inelastic deformation that could form in moment-resisting frames due to the formation of plastic hinges. If yielding begins in the columns of a moment-resisting frame before it begins in the beams, a column sidesway mechanism can form. Such a

mechanism can make very large curvature ductility demands on the plastic hinges of the critical storey. On the other hand, if yielding begins in the beams before it begins in the columns, a beam sidesway mechanism will develop, which makes more moderate demands on the curvature ductility required at the plastic hinges in the beams and at the column bases. Therefore a beam sideway mechanism is the preferred mode of inelastic deformation, particularly since ductility can be more easily provided by reinforcing details in beams than in columns. As a result of the above consideration, the columns of multistorey ductile moment-resisting frames should have adequate flexural strength to avoid the formation of column sideway mechanism. Thus a strong column-weak beam approach is advocated.

Dependent on the design philosophy adopted for the design of the connections between the precast elements, precast seismic structural systems can be separated into two basic categories: strong connections and ductile connections[65].

The strong connections are detailed to be effectively rigid and to be stronger than designated locations of inelastic action (plastic hinges). In this case, the design philosophy is to make the structural system behave under seismic loading as though it were an equivalent monolithically constructed structure. If the connection detail is successful, the structural elements could presumably be designed in accordance with existing materials codes. This is the current design philosophy, and it has formed the basis of most recent experimental research on precast seismic structural systems.

The ductile connections are detailed to be weaker than the precast elements, and are intended as locations of ductile inelastic deformation. If the precast elements are designed to have an adequate margin of strength over that of the ductile connection, they will remain elastic under seismic response. As a consequence, the precast elements would not need to be detailed for ductility, resulting in economy. In some cases, it is apparent that ductile connections could be designed to be replaceable after a

major earthquake at a much lower cost than repair of damage to a ductile reinforced concrete frame.

In this study, the connections are detailed to be strong connections.

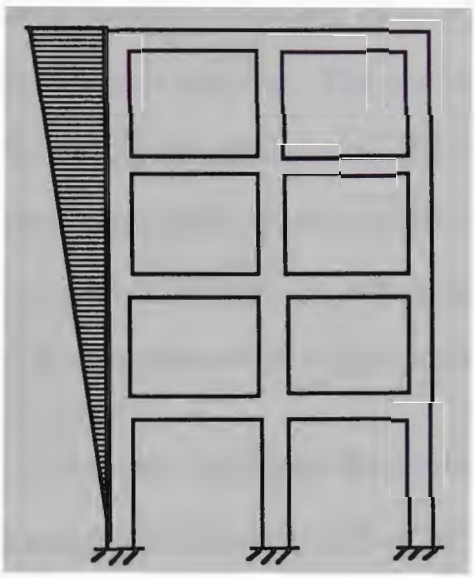

Moment-Resisting Frame

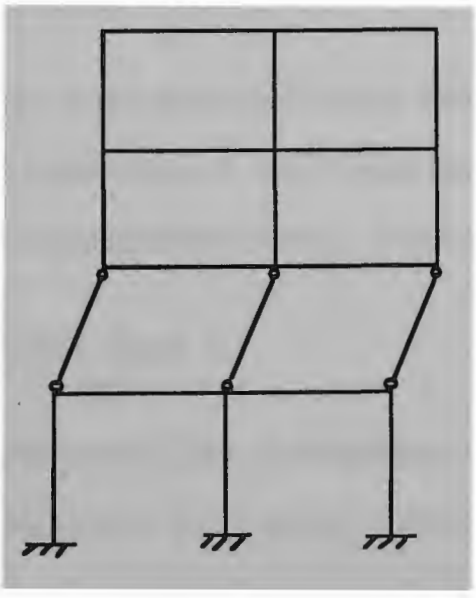

Column Sidesway Mechanisms

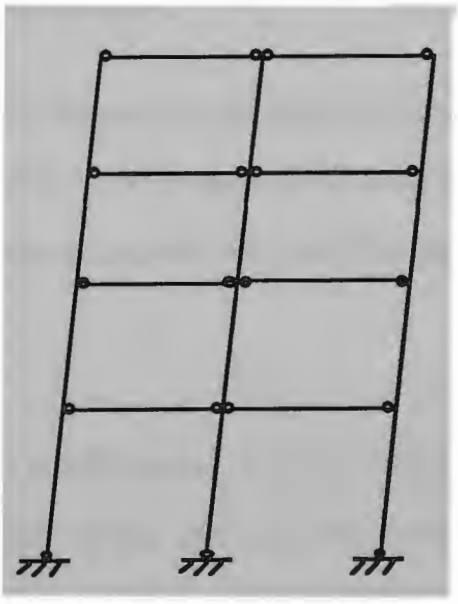

Beam Sidesway Mechanisms

Fig 3.1 Moment resisting frame with horizontal seismic loading and possible mechanisms.

3.2 Selection of Connections

The basic problem in the design of earthquake resistant building structures incorporating precast concrete elements is finding an economical and practical method for connecting the precast elements together. The connection between the elements should ensure satisfactory strength and stiffness against seismic loads and enable the structure to achieve the necessary ductility during cyclic loading in the inelastic range. The connection types are crucial not only to the behaviour of the completed structure but also to the economical development of the building system.

A composite system of concrete buildings combining precast and cast-in-place reinforced concrete, has a number of advantages in construction. The incorporation of precast concrete elements has the advantage of high quality control and speed of construction and the cast-in-place reinforced concrete provides the structural continuity and the ductility necessary for adequate seismic performance.

Based on the description above, two kinds of connections designated as Type A and Type B were selected, which were recommended by PCI and APCG suitable for multistorey residential building. These connections are described in the following.

Connection Type A

In connection Type A the precast column is prefabricated with reinforcing bars projecting out to the required overlapping length at the level of the connection. Similarly, the precast beam is prefabricated with the planes at two ends inclined as shown in Fig. 3.2.1, and the longitudinal reinforcement projecting out. In construction, the column is aligned and the beam is moved into its position, with the bars overlapping. Then the stirrups are placed around the reinforcement at the connection. High early strength cast-in-place concrete is next placed into the form to

complete the rigid connection. In this case, temporary props and formwork are needed during construction.

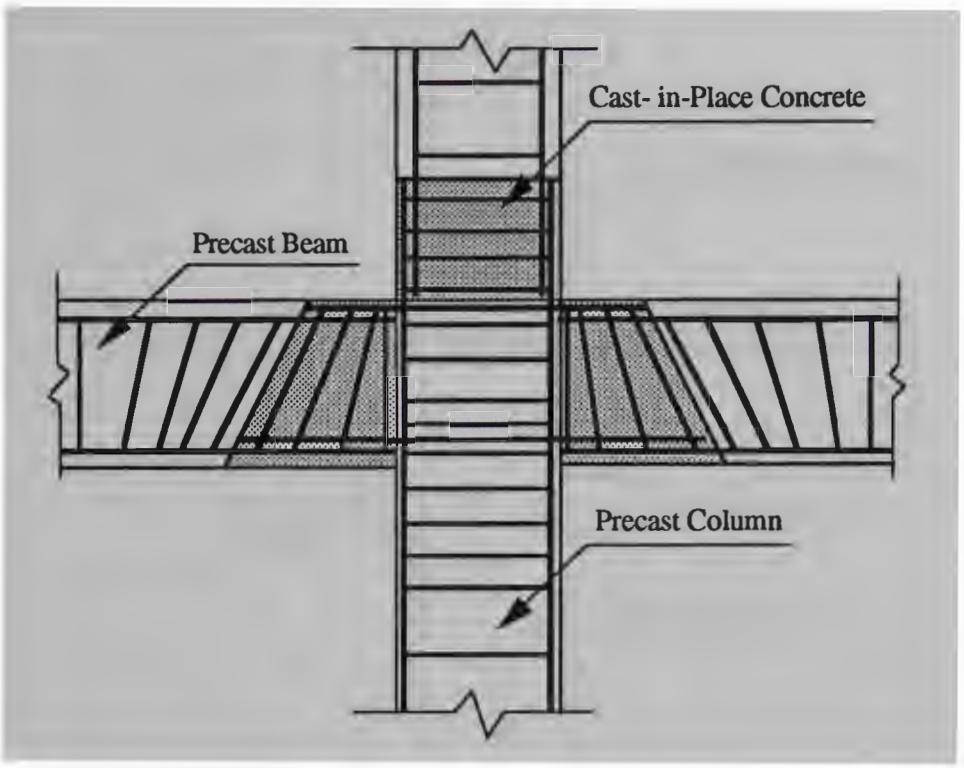

Fig. 3.2.1 Connection Type A

Connection Type B

In connection Type B, the precast column is prefabricated with a corbel at the connection point. The corbel has a large steel angle embedded on the top. The precast beam is also prefabricated with an angle embedded at the bottom of it. The beam is only partially poured and the stirrups are exposed. In construction, when the beam is moved into position, welding work is performed immediately on the two angles. The precast hollow-core-slab units are then positioned on the beam and cast-in-place concrete is then placed on top of the beam together with the top concrete of the hollow-core slabs to form the monolithic systems. In this case, neither formwork nor

temporary props are needed during construction. This offers the opportunity to do the structural and architectural work at the same time and will save both time and money.

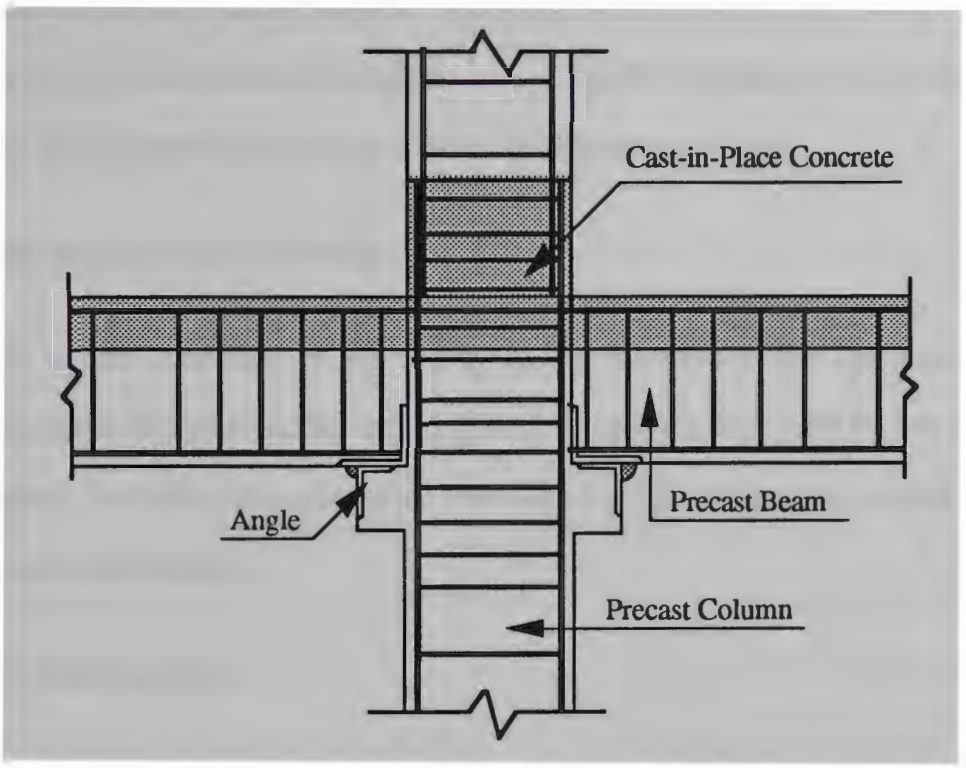

Fig. 3.2.2 Connection Type B

3.3 Design of Test Specimens

3.3.1 Description of test specimens

A good test specimen for the purpose of research in the laboratory should have some main criteria. They are discussed below.

A. Typicality.

The specimen should be the typical unit of the real structure. When the loading is applied, the specimen should have similar internal force, displacement or deformation as those in the real structure. In moment-resisting frames, the inelastic hinges were chosen at the root of the beam. So the investigation reported in this work was carried

out with the objective of studying the inelastic deformation behaviour of the root of the precast beam. Furthermore, in a reinforced concrete frame, there is usually a moment counter-flexural point in the beam and column at which the moment vanishes. Using these concepts, the " cross shaped " specimen was chosen in this study. Thus, when load is applied, the moment is equal to zero at tips of both beam and column whilst the moment is the largest at the roots of these cantilever members.

B. Easy construction and testing

Due to the limitation of test set-up in the laboratory, the specimen cannot be manufactured full scale as the real structure. Moreover, it cannot be too small to lose its reality. So half-scale specimens were chosen. This was done to make it easy for construction and testing.

C. Easy load applying

The connecting beam in the real structure may sustain many kinds of loads. It is impossible and unnecessary to apply all these kinds of loads on the beam in the laboratory. The emphasis of this study is on the moment-resistant beam-column connection. So a concentrated load was applied at the tip of the beam to get the largest moment at the beam-column joint. For some of the specimens, the repeated concentrated loading was applied at the beam tip to simulate earthquake-type loading. Normally, the beam-tip should be applied with repeated reversed loading to simulate earthquake effects. But the investigation reported herein is to study the behaviour of precast beam-column connection suitable for multistorey residential buildings. In this case, the gravity loads are high so that the earthquake loading may not produce any reversed moment at the connections. So, in this study, only single direction repeated loading was applied. Fig. 3.3.1 shows a multistorey frame and a representative distribution of moments in the beams due to gravity loads, earthquake loads and a combination of the two.

As described above, the geometry of the specimen and loading arrangements used in the study are shown in Fig 3.3.2. They are identical to those used by Yao[82]. This was done so that not only the criteria discussed above could be satisfied but also a direct comparison could be made with the results available for different steel ratios and strengths of concrete. Furthermore, the existing test set-up could be utilised.

The test program has two precast specimens namely, Type A and Type B and a monolithic specimen for the purpose of comparison. Each of these three specimens had two sets with the same geometry but with different reinforcement ratios. Six such specimens were tested under static loading. Another identical set of six specimens were tested under repeated loading, making the total number of specimens tested equal to twelve. Each specimen was designated by two or three letters and one number. The first letter, S or R, indicates the type of loading (S for static loading and R for repeated loading); the second letter, P or M, indicates the casting method (P for precast and M for monolithic casting method); the third letter A or B indicates the type of connection (A for Type A and B for Type B). The number indicates the amount of steel ratio (1 for lower ratio and 2 for higher ratio).

Table 3.3.1 lists all the 12 test specimens and their corresponding design variables.

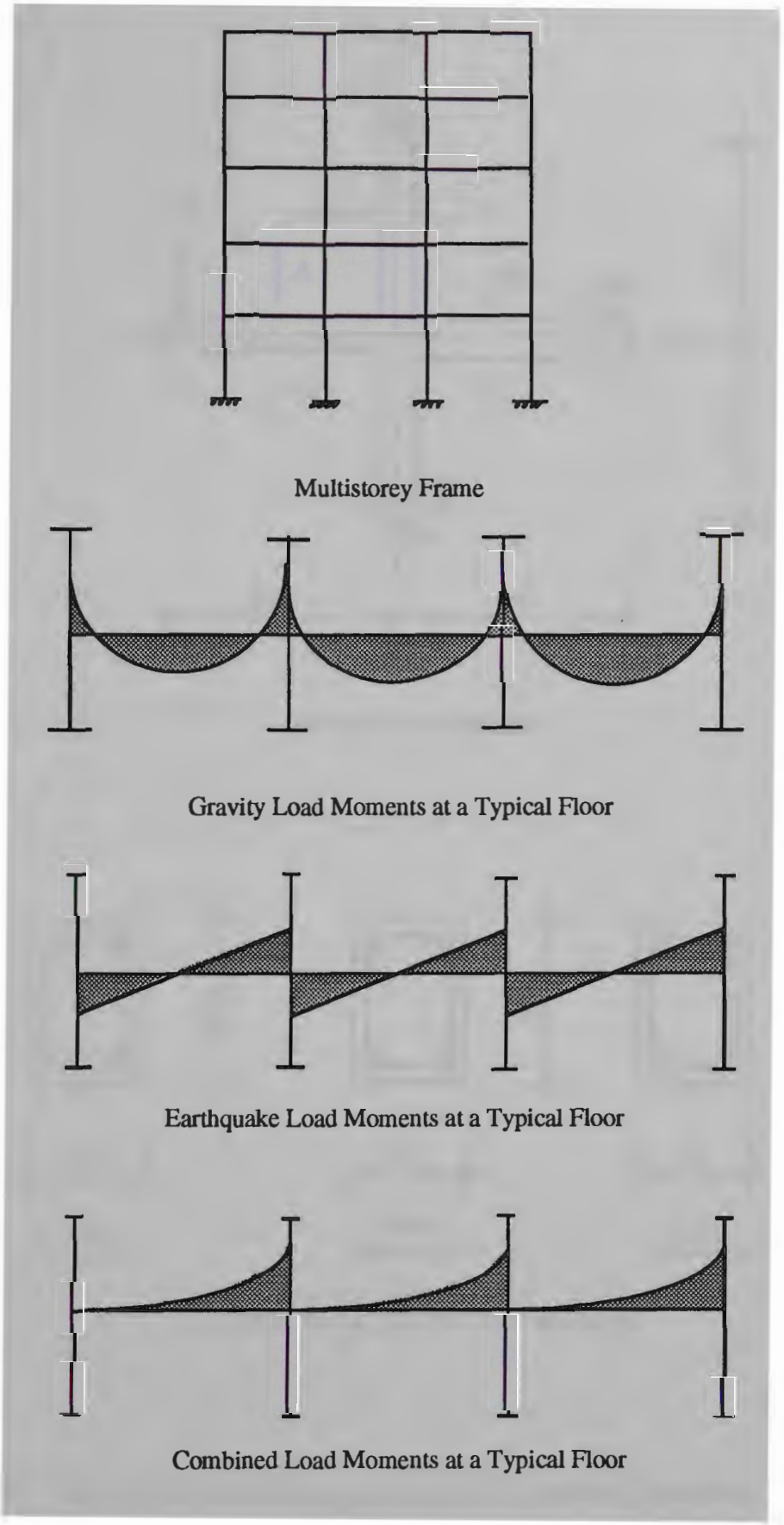

Fig. 3.3.1 Bending Moments at a Typical Floor in a Mulitstorey Frame

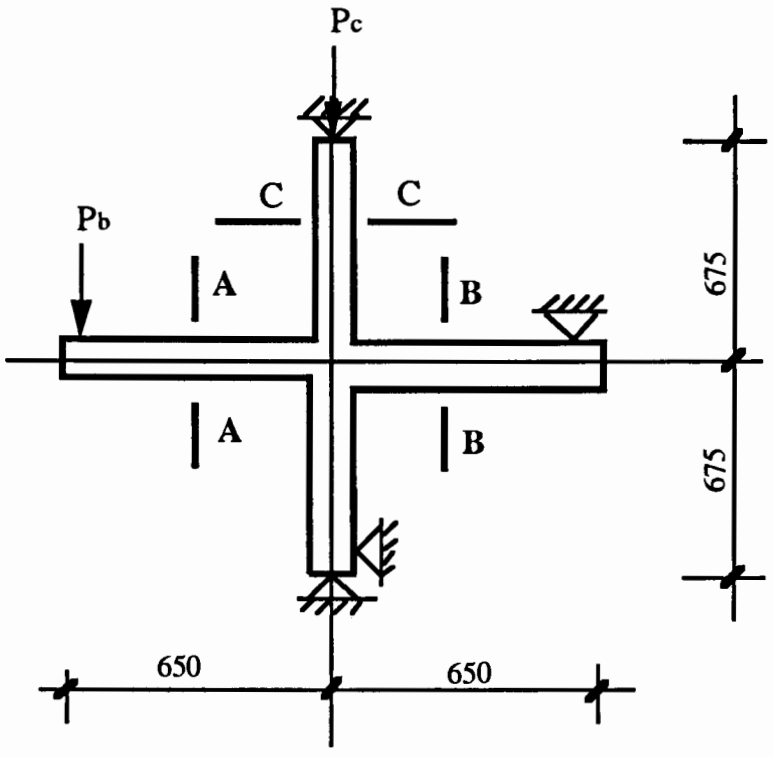

(a) Load Arrangement

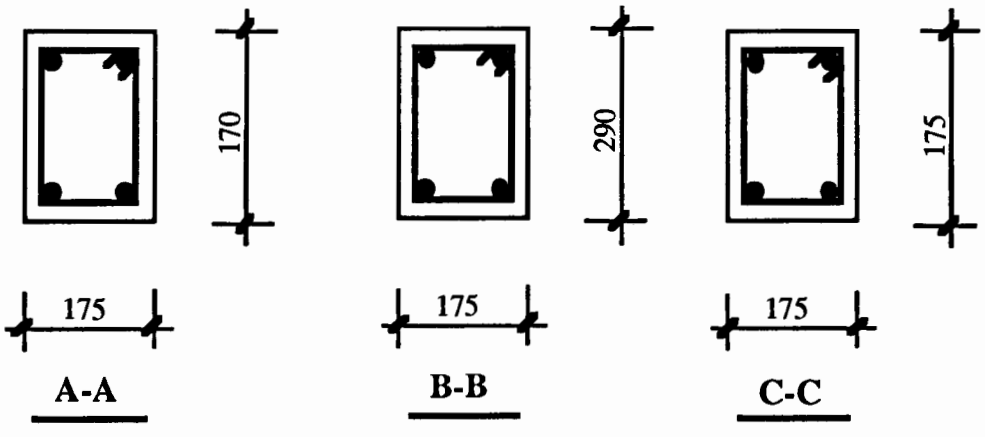

(b) Beam and Column Cross Sections

Fig.3.3.2 Load Arrangements and Details of Specimens

Table 3.3.1 Test and Design Variables of Specimens

Name of specimen	Type of loading	Casting method	Type of connection	Steel ratio
SM1	Static	Monolithic	—	2/3 P_{all}
SPA1	Static	Precast	Type A	2/3 P_{all}
SPB1	Static	precast	Type B	2/3 P_{all}
SM2	Static	Monolithic	—	P_{all}
SPA2	Static	Precast	Type A	P_{all}
SPB2	Static	Precast	Type B	P_{all}
RM1	Repeated	Monolithic	—	2/3 P_{all}
RPA1	Repeated	Precast	Type A	2/3 P_{all}
RPB1	Repeated	Precast	Type B	2/3 P_{all}
RM2	Repeated	Monolithic	—	P_{all}
RPA2	Repeated	Precast	Type A	P_{all}
RPB2	Repeated	Precast	Type B	P_{all}

3.3.2 Materials

A. Concrete

In order to limit the number of variables, the strength of concrete was kept the same in all the specimens. Because of the limitation of formwork, only six specimens were cast at a time. Therefore, slight difference of concrete strengths between models for static loading and those for repeated loading occurred. Concrete strength of 32 MPa was used for the calculation of steel ratio. Table 3.3.2 shows the measured values of strength and slump of precast concrete. They were ordered from a local supplier.

Table 3.3.2 The Strength and Slump of Precast Concrete

No.	Name of specimens	Pouring date	Total vol. (m^3)	Slump (mm)	7 days' strength (MPa)	28 days' strength (MPa)
1	SM,SPA, SPB	12 / 8 / 93	1	150	16.5	28.5
2	RM,RPA, RPB	30 / 8 / 93	1	85	17.4	33.7

Normally, the strength of the cast-in-place concrete should be at least 10 MPa higher than that of the precast concrete for the purpose of avoiding premature connection failure. In order to obtain the required strength and slump some trials were made. Appendix 4 describes the mix design in detail for the cast-in-place concrete. Table 3.3.3 shows the measured values of strength and slump of cast-in-place concrete.

Table 3.3.3 The Strength and Slump of Cast-in-Place Concrete

No.	Name of specimens	Pouring date	Total vol. (m^3)	Slump (mm)	7 days' strength (MPa)
1	SPA2,SPB2	22 / 9 / 93	0.075	85	45.20
2	SPA1,SPB1	22 / 9 / 93	0.075	80	49.42
3	RPA2,RPB2	5 / 10 / 93	0.075	50	58.26
4	RPA1,RPB1	5 / 10 / 93	0.075	100	52.00

B. Reinforcement.

Four types of reinforcing bars were used for the specimens, namely, Y16 deformed bars (as top steel for beams), Y12 deformed bars (as main steel for columns), R10 plain bars (as bottom steel for beams) and R6 plain bars (as stirrups for beams and links for column). They were all obtained from a local supplier.

In designing the details of specimens, two different steel ratios were chosen for all the specimens, i.e., p_{t1}-p_c=2/3 p_{all} and p_{t2}-p_c=p_{all}. The reasons for doing this are explained below.

(1) According to Loo(1990)[48], there are three limiting steel ratios: lower limit p_t=1.4 / f_{sy}; upper limit p_t-p_c=P_{all} and reasonable steel ratio p_t-p_c=2/3 p_{all}. For economy, p_t-p_c=2/3p_{all} is usually chosen in many cases of design and construction.

(2) In some cases, on the other hand, structural engineers have to use the upper limit steel ratio to satisfy architects' aesthetic needs and the safety of structure as well.

Detailed design of the specimens, according to Loo (1990)[48], are as follows.

From Fig. 3.3.2 section A-A,

b = 175 mm, D = 170 mm,

using Y16 bars, d = 170 - 25 - 16/2 = 137 mm,

determine A_{sc} using 2R10 bars, and normalised 2R10 to deformed bars,

Thus A_{sc} = 160x250/400 = 100 mm^2

Assume f_c' = 32 MPa, f_{sy} = 400 MPa,

therefore γ = 0.85 - 0.007 (f_c'-28) = 0.85 - 0.007 (32-28) = 0.822

(1) Using $P_t - P_c = P_{all}$

$$P_{all} = 0.34\,\gamma f_c'/f_{sy} = 0.34x0.822x32/400 = 0.02236$$

therefore $P_t - P_c \leq 0.02236$

$$A_{st} - A_{sc} \leq 0.02236x175x137 = 536$$

therefore, $A_{st} = 536+100 = 637$

Say $A_{st} = 600$ (3Y16)

(2) Using $P_t - P_c = 2/3\ P_{all}$

$$P_t - P_c = 2/3\ P_{all} = 2/3x0.02236 = 0.0149$$

$$A_{st} - A_{sc} = 0.0149x175x137 = 357$$

therefore, $A_{st} = 357 + 100 = 457$

Say A_{st}=400 (2Y16)

Before testing the specimens, the material properties of each type of bar were obtained from the tension test. Appendix 3 gives the original test data and Table 3.3.4 summarises the main results which would be used in calculations for predicting the maximum yield load capacity of the connecting beams during the testing of specimens.

Table 3.3.4 Test Data of Tension Steel Bars

Type of bar	yield load (kN)	yield extension	yield strength (MPa)	max. load (kN)	Es (MPa) $x10^4$
Y16	87.75	2.18×10^{-3}	440	112.95	21.5
Y12	52.20	2.13×10^{-3}	470	63.38	23.03
R10	29.72	1.64×10^{-3}	371.5	38.15	22.76

C. Configuration

In order to satisfy the needs of earthquake-resisting, all the stirrups were doubled at the beam-column zone. Because the lengths of the exposed bars were not long enough to satisfy the length of overlapping, they were welded in connection Type A. Details of the specimens are shown in Fig. 3.3.3 through Fig. 3.3.8.

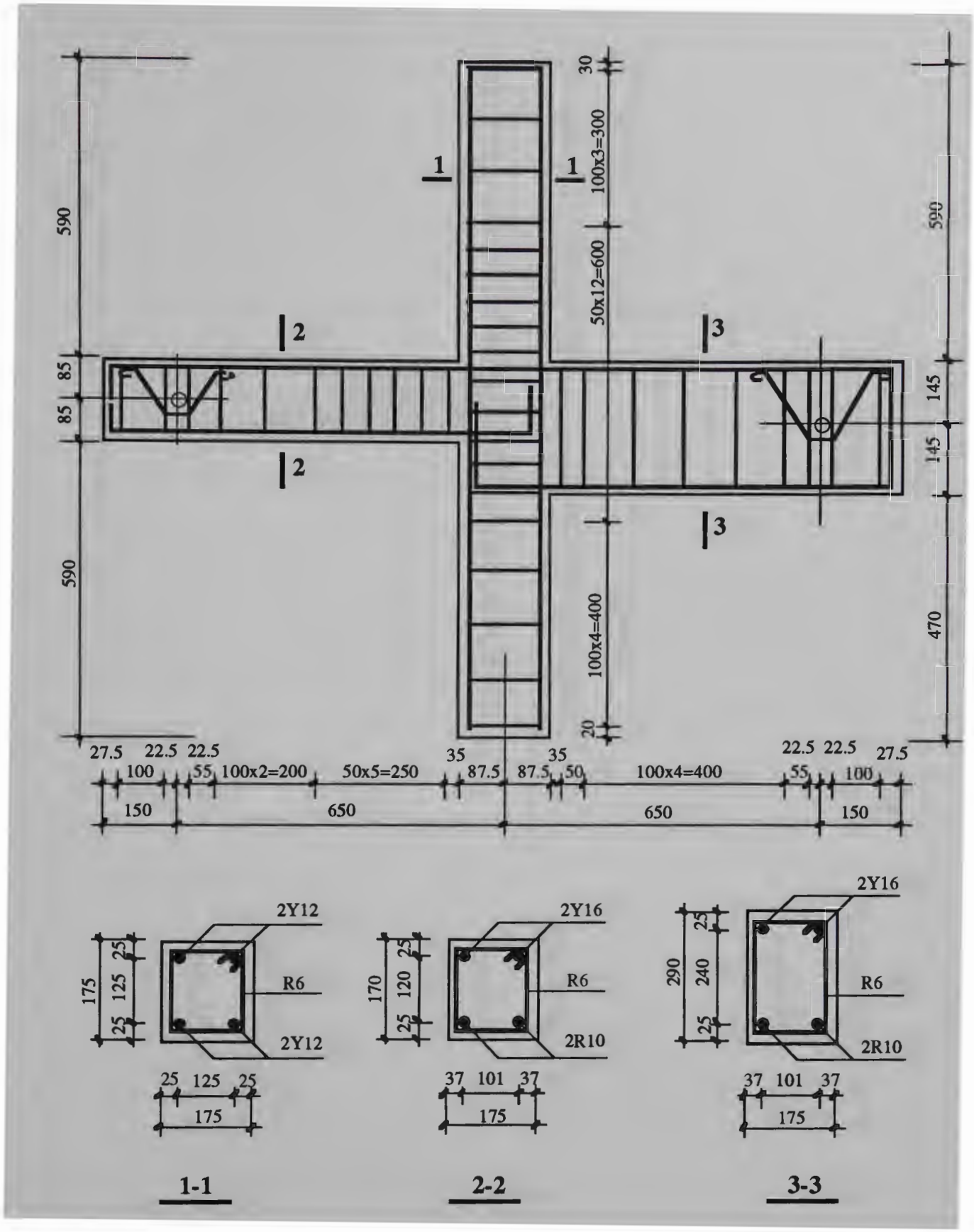

Fig. 3.3.3 Detail of Specimens SM1 & RM1

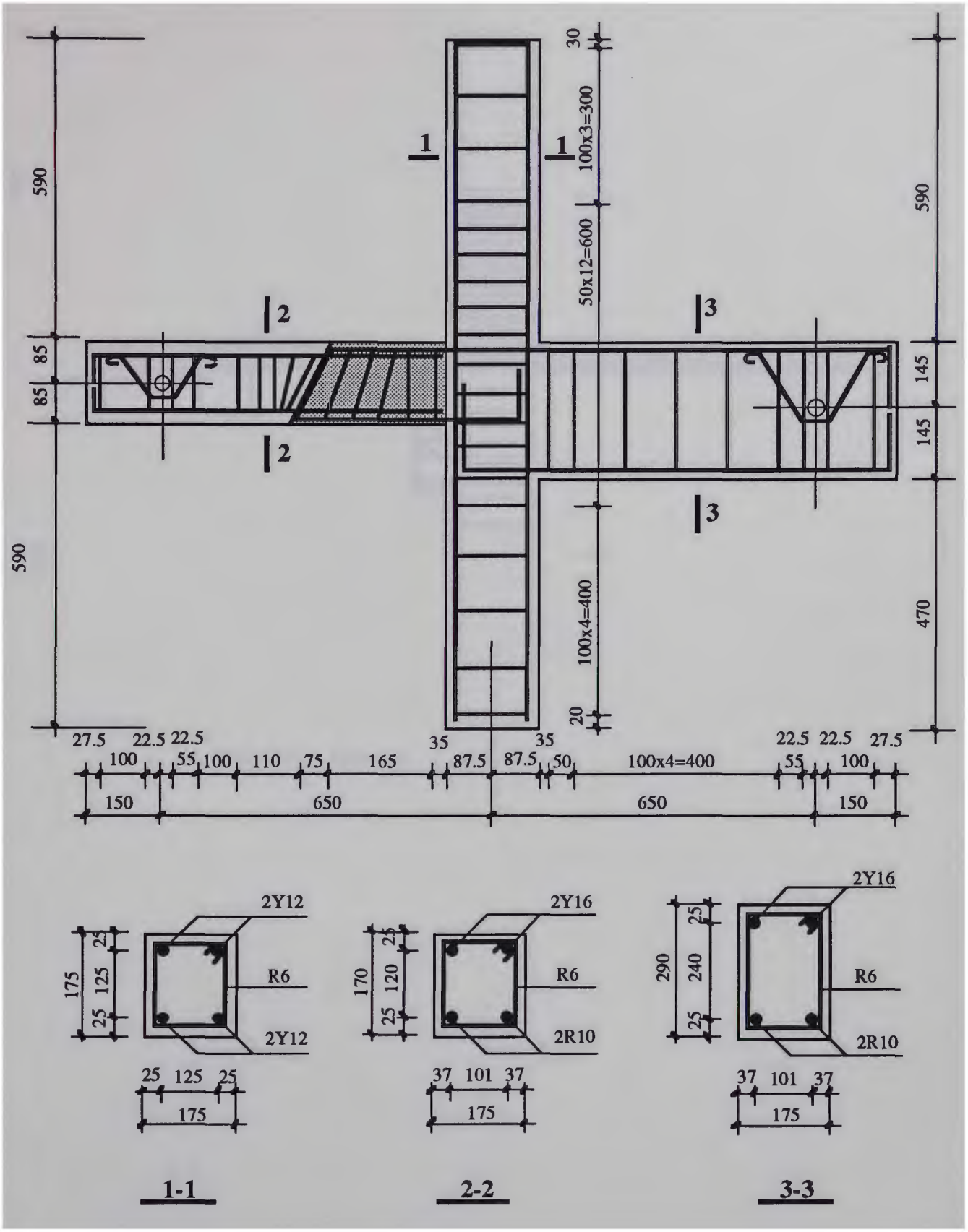

Fig. 3.3.4 Detail of Specimens SPA1 & RPA1

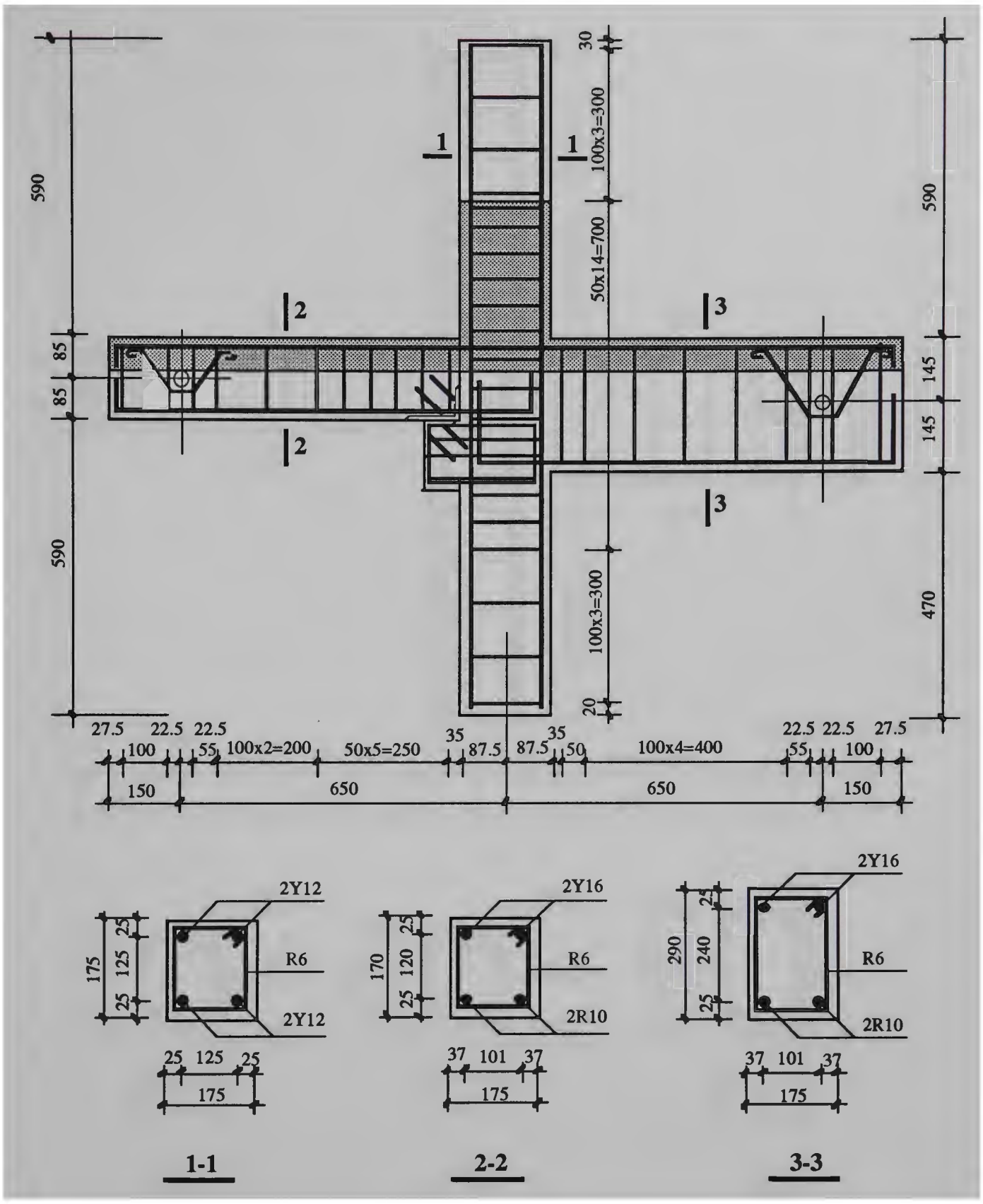

Fig. 3.3.5 Detail of Specimens SPB1 & RPB1

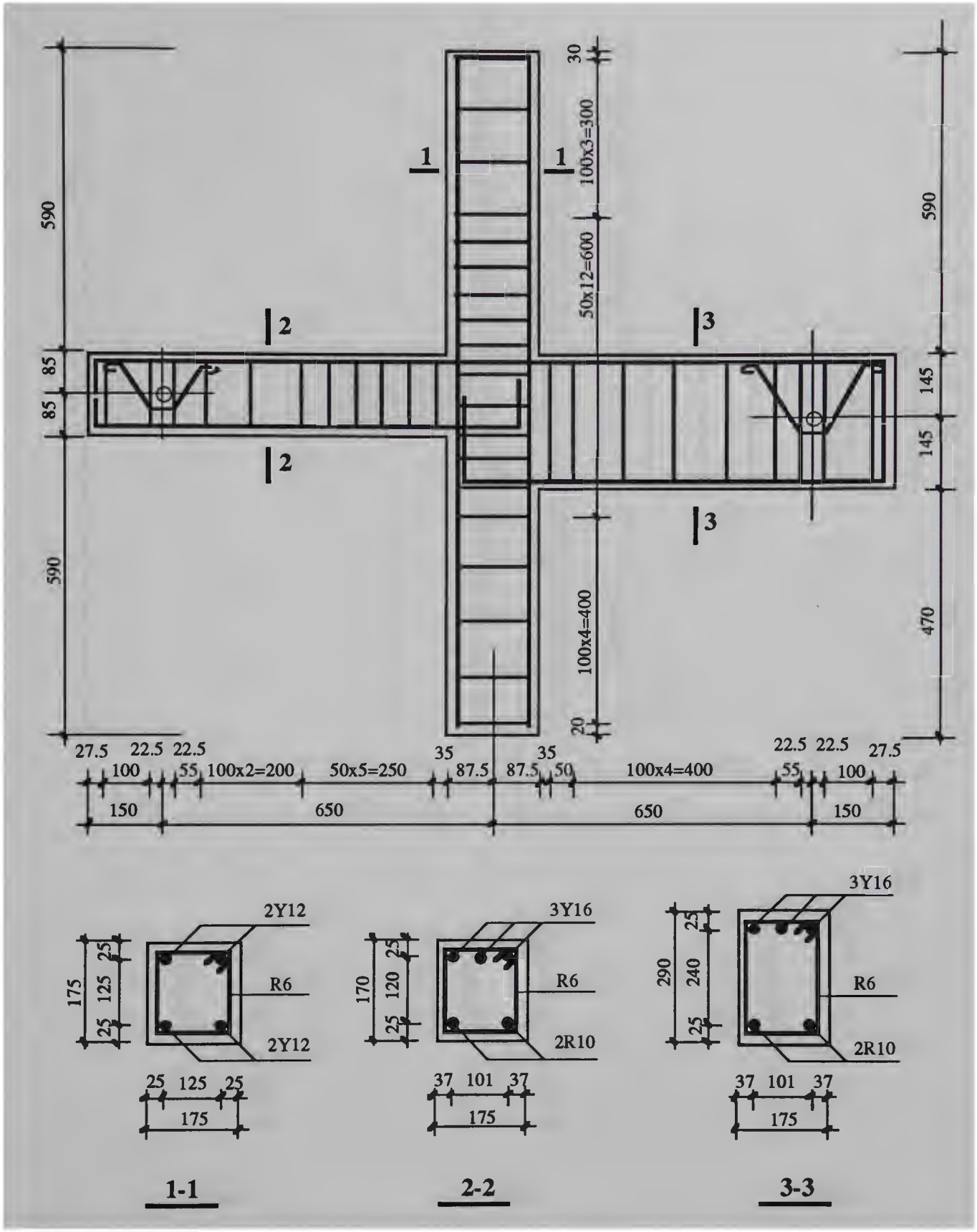

Fig. 3.3.6 Detail of Specimens SM2 & RM2

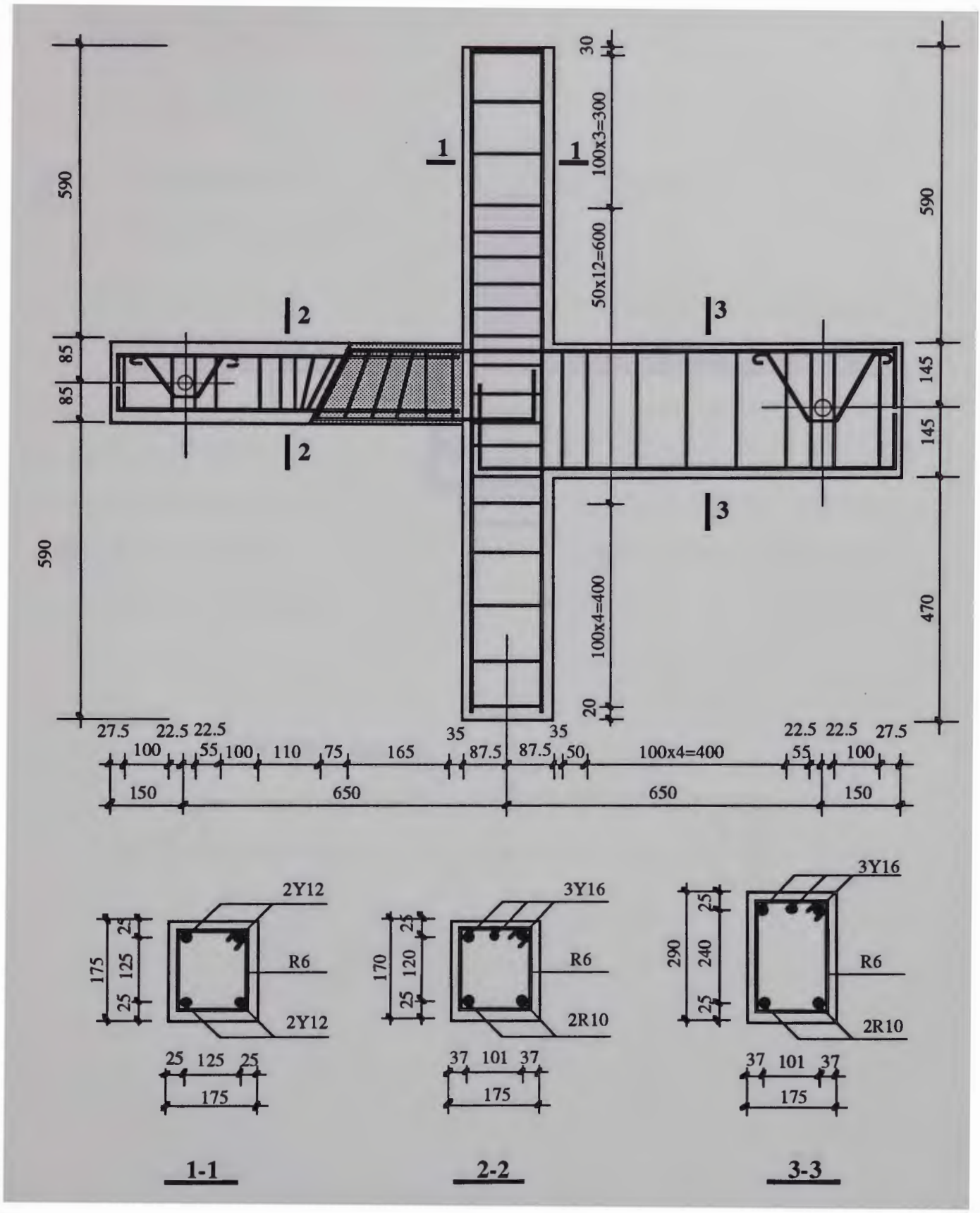

Fig. 3.3.7 Detail of Specimens SPA2 & RPA2

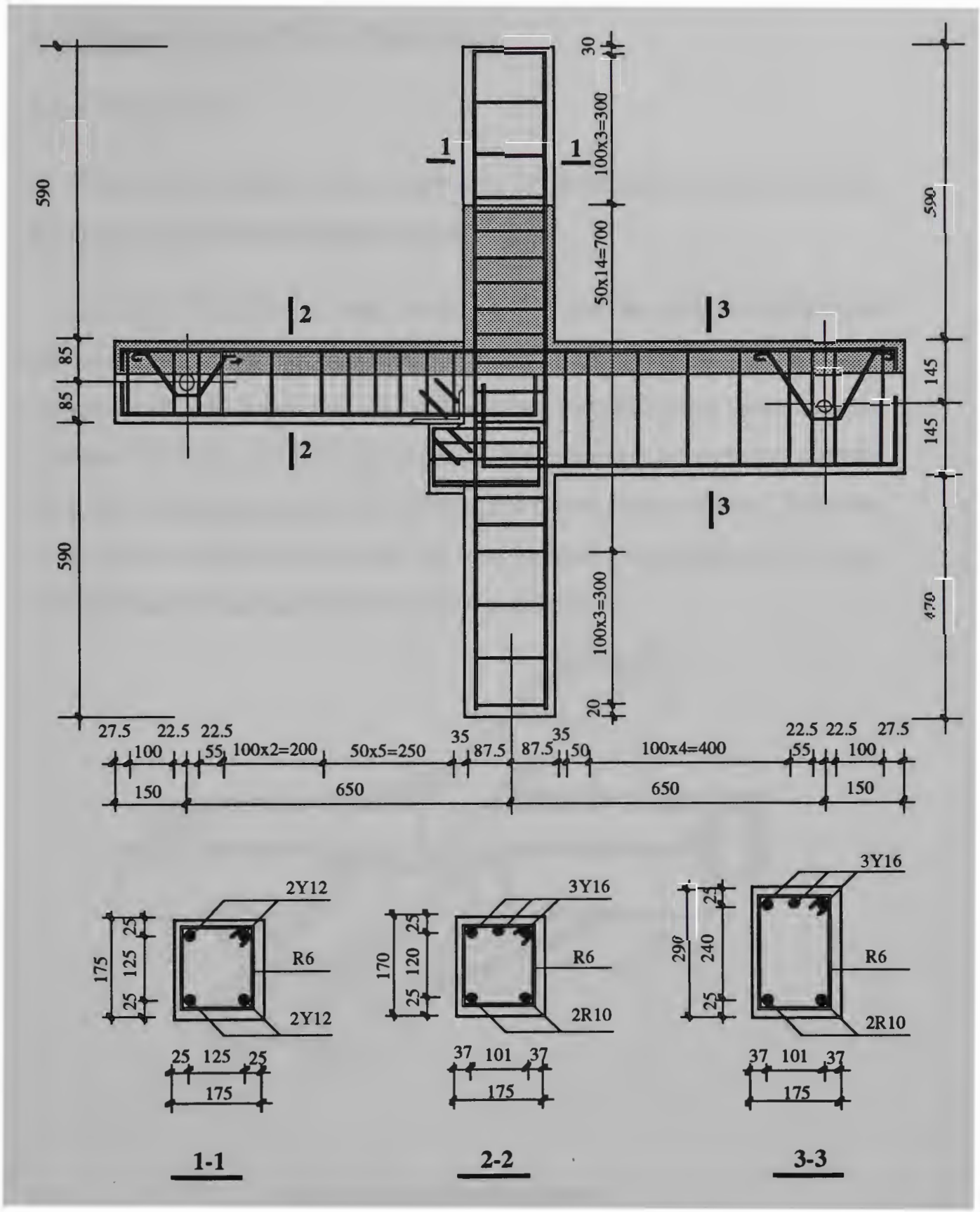

Fig. 3.3.8 Detail of Specimens SPB2 & RPB2

3.4 Preparation of test Specimens

3.4.1 Formwork

Two different kinds of formwork were designed and constructed, namely, horizontal formwork and vertical formwork.

Four sets of horizontal wood forms which could be easily assembled and disassembled after casting, were used for the monolithic specimens and the precast specimens of Type A (see Fig. 3.4.1). The bottom and sides of the formwork are consisted of 18 mm plywood with additional timber board at the corners to keep the form stiff. Bolts were used to hold the sides and bottom pieces together. The forms were painted with thin oil to reduce the bond between the concrete and the wood before placing the fabricated reinforcement cage in the forms.

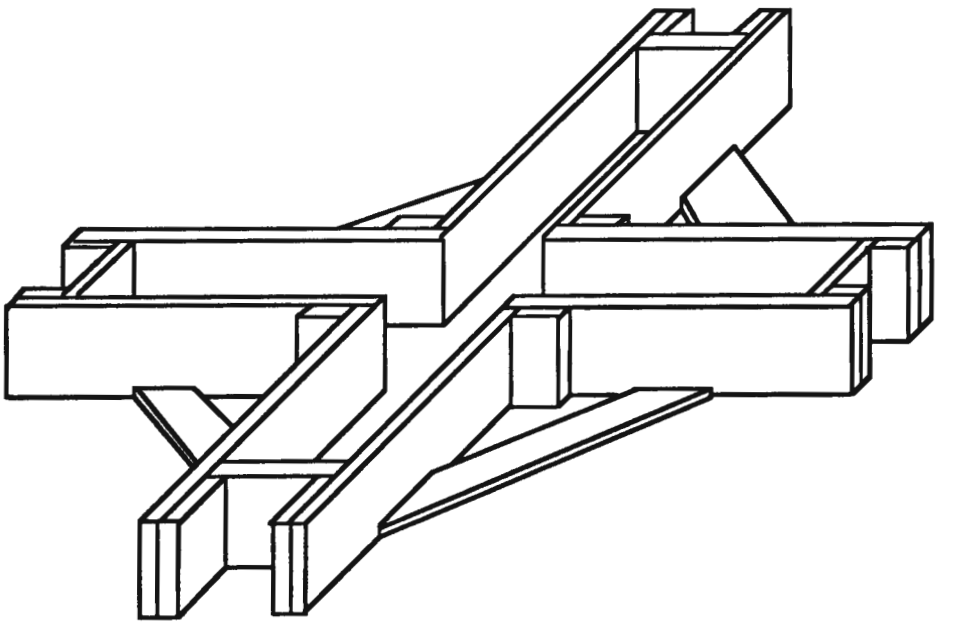

Fig. 3.4.1 Horizontal Formwork

Two sets of vertical plywood formwork were designed and manufactured for the precast specimens Type B (see Fig.3.4.2). It was done such that the upper parts of the steel ties for the specimen could be exposed to the air to allow for the composite

beam to be cast later. There were 2 different parts in the formwork, i.e., one for the lower column, frame beam and corbel and the other for the connecting beam. Plate 3.4.1 shows a pair of formwork and reinforcing cages.

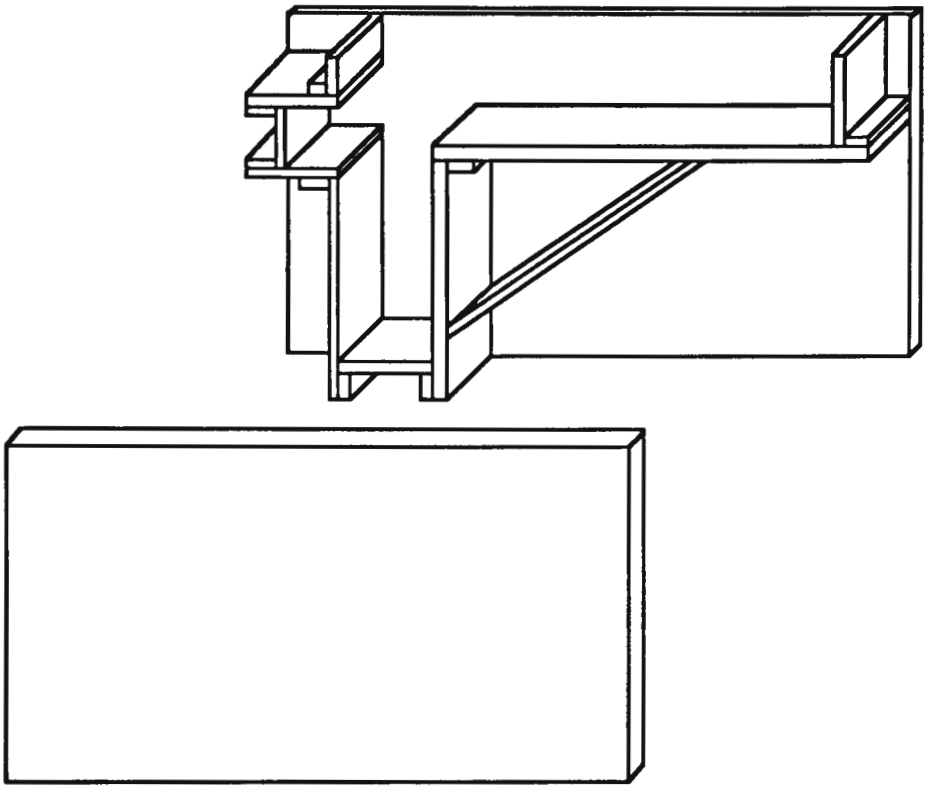

(a) Part A for Lower Column, frame Beam, and Corbel.

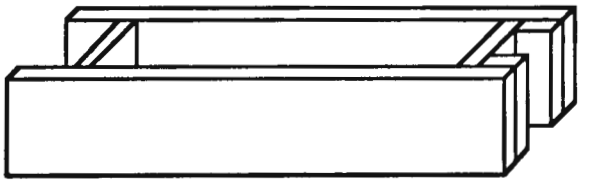

(b) Part B, for Connecting Beam

Fig. 3.4.2 Vertical Formwork

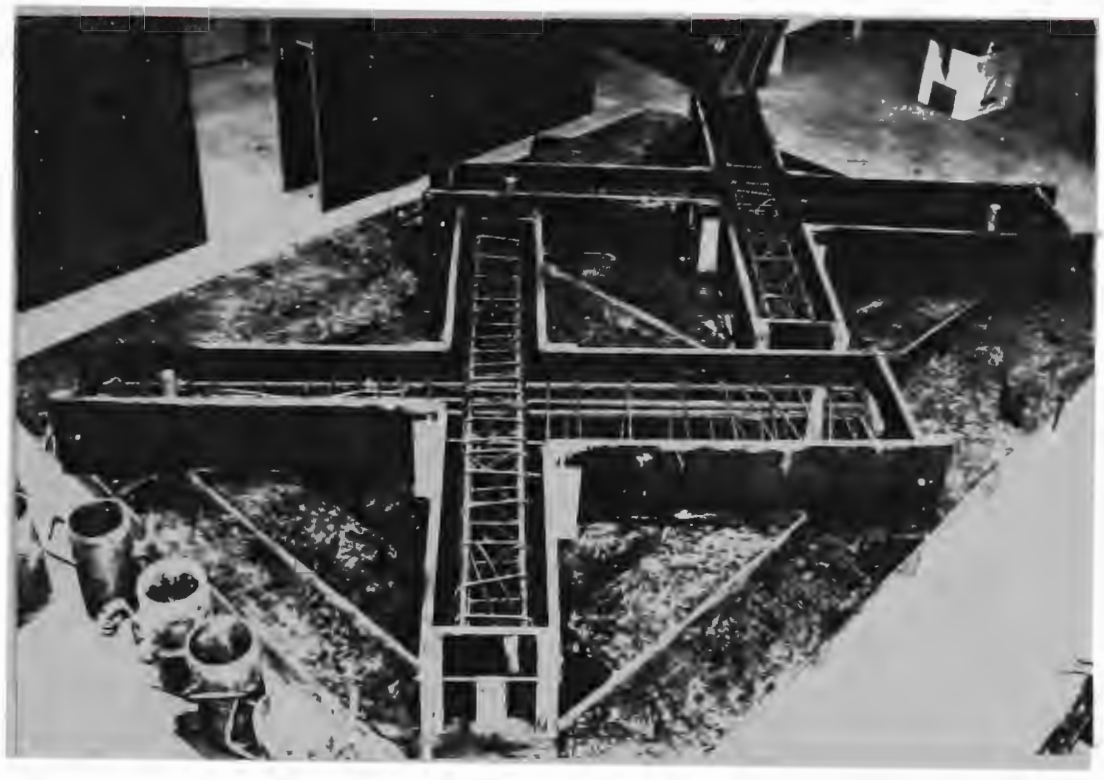

Plate 3.4.1 A Pair of Formwork and Reinforcing Cages

3.4.2 Reinforcement Work

When all the necessary steel bars were cut, bent and made into reinforcing cages according to the design, some high elongation electrical resistance strain gauges were applied to the reinforcing bars. The locations and identifications of the strain gauges in the specimens are given in Fig. 3.4.3.

The procedure of applying the gauges was as follows.

The bars were filed at the location of the gauge to obtain a flat surface about 10 mm by 20 mm. Sandpaper was used to improve the finish of the surface which was then treated with 99% pure alcohol to get a clean surface. The gauges (PL-10-11-120) were laid out on the bars at prescribed gauge locations. Cellophane tape was used to hold the gauges in place. Peeling back one end of the cellophane tape, "supper glue" was applied under the gauge before applying pressure to the gauge. A rubber end of a

wood rod was used to press the gauges in place for 10 seconds. Lead wires were used in which one end was soldered to the strain gauge while the other end was left out of the cage for connecting strain indicator later. The wires, numbered corresponding to those in the strain gauge layout, were fastened with pieces of string to avoid gauge damage during the handling of the bars and placement of concrete. Silicon was then painted over the gauges and wires to provide insulation and moisture proofing.

Reinforcement work was completed after placing reinforcing cage in the form on the bar chairs at suitable locations to provide a consistent concrete cover for the bars.

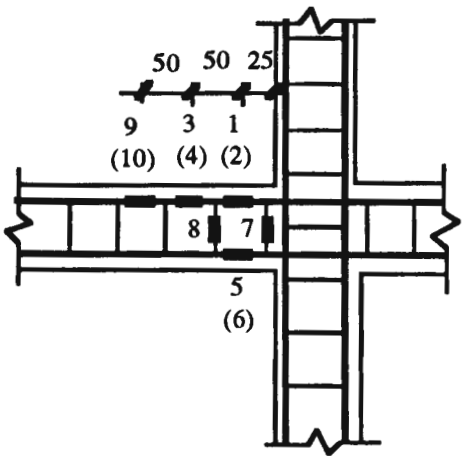

(a) For Monolithic Specimen

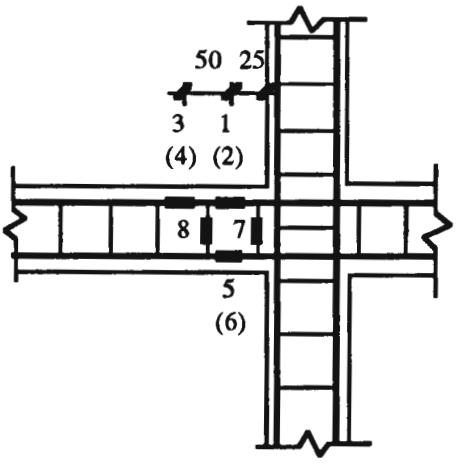

(b) For Precast Specimen of Type A

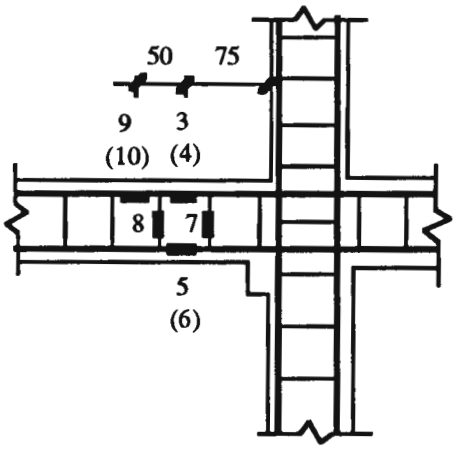

(c) For Precast Specimen of Type B

Fig. 3.4.3 The Locations and Identifications of the Strain Gauges.

3.4.3 Casting and Curing of Concrete

The precast concrete was delivered to the laboratory by ready-mix truck at which time additional water was added to obtain a slump of about 100 mm. The concrete was then shovelled into the forms and compacted with a high frequency vibrator to eliminate voids. The excess concrete was struck off and the surface trowelled to obtain a smooth finish. Several hours after casting, the specimens were covered with damp hessian to provide a moist curing condition. Polyethylene sheets were used over

the hessian to retain moisture. The hessian was kept damp by wetting it twice a day. After seven days, the forms were stripped. The specimens were moist cured similarly for another seven days and then air cured in the laboratory until the time of pouring cast-in-place concrete, which is always more than 28 days after casting. Totally 16 control cylinders were prepared at the same time as the concrete was poured and they were then cured in the same manner. Two cylinders were tested at 7 days after pouring and another two cylinders were tested at 28 days. The rest of the cylinders were tested the same day as the specimens. Plates 3.4.2 to 3.4.5 show two types of precast connections before and after assembling.

Before pouring cast-in-place concrete, the separate parts of specimens PA and PB were aligned and connected carefully (see Yao,1993) and strain gauges were laid at the prescribed locations.

After pouring cast-in-place concrete, the specimens were cured at least 7 days before testing. The method of curing is the same as that of precast concrete.

Before testing, the specimens were painted with white paint; black lines were drawn over the white paint surface of the connection to facilitate identification of the cracks.

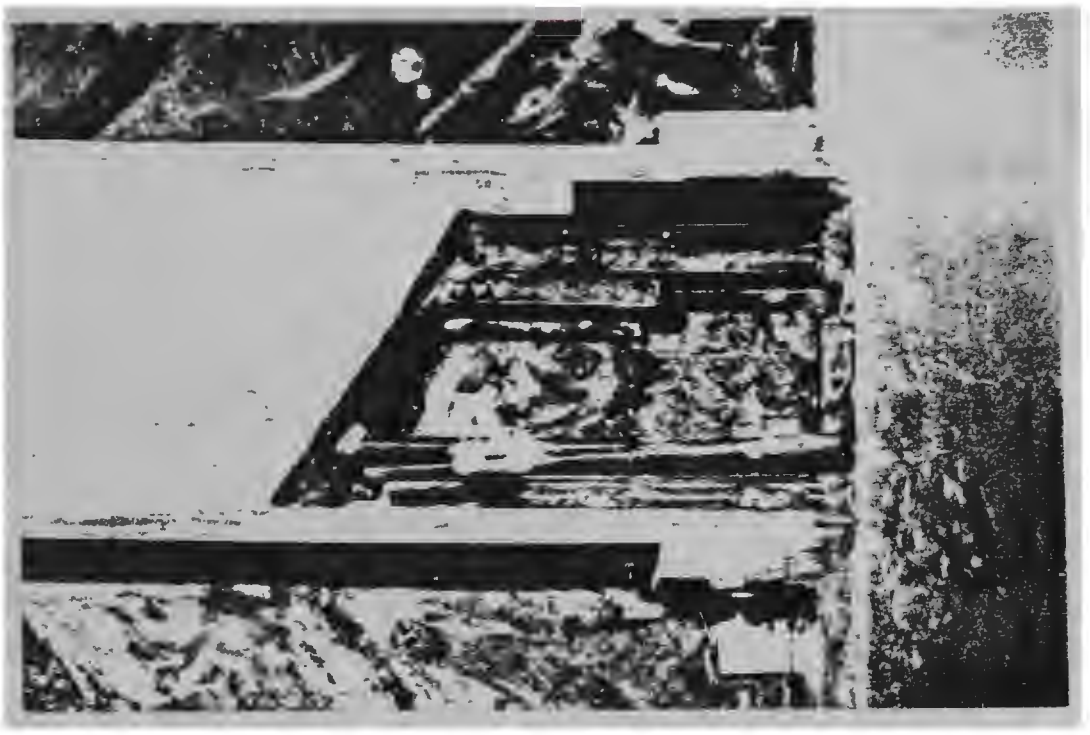

Plate 3.4.2 Connection Type A Before Assembling

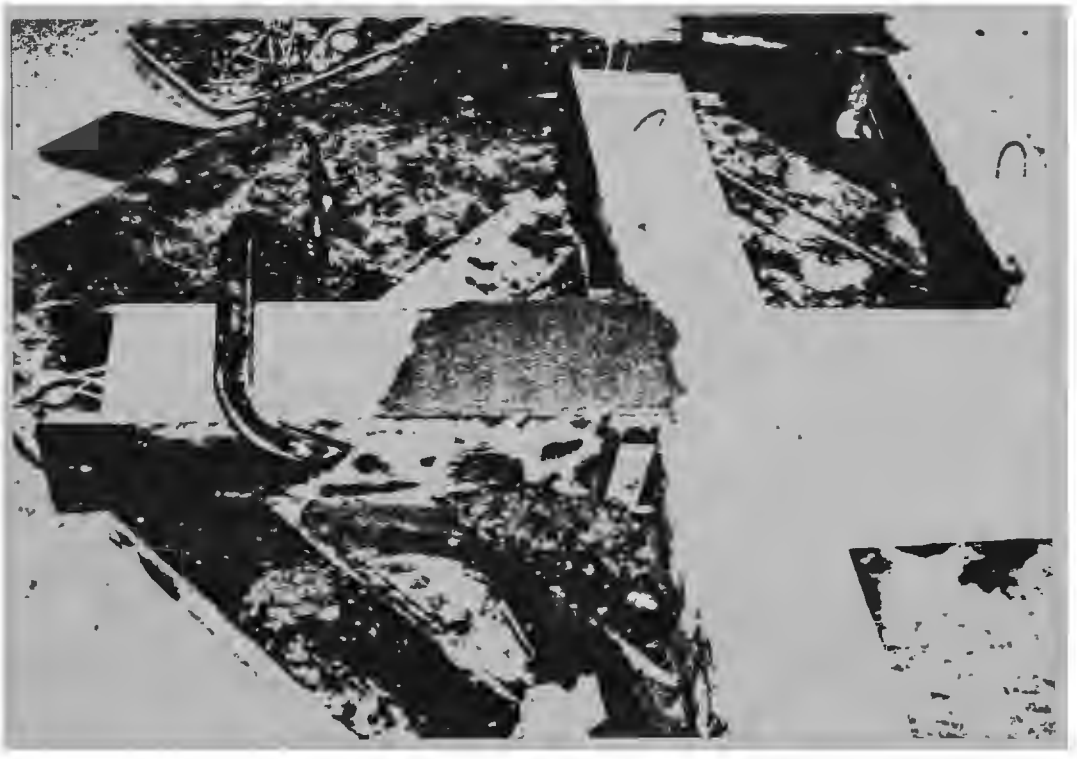

Plate 3.4.3 Connection Type A After Assembling

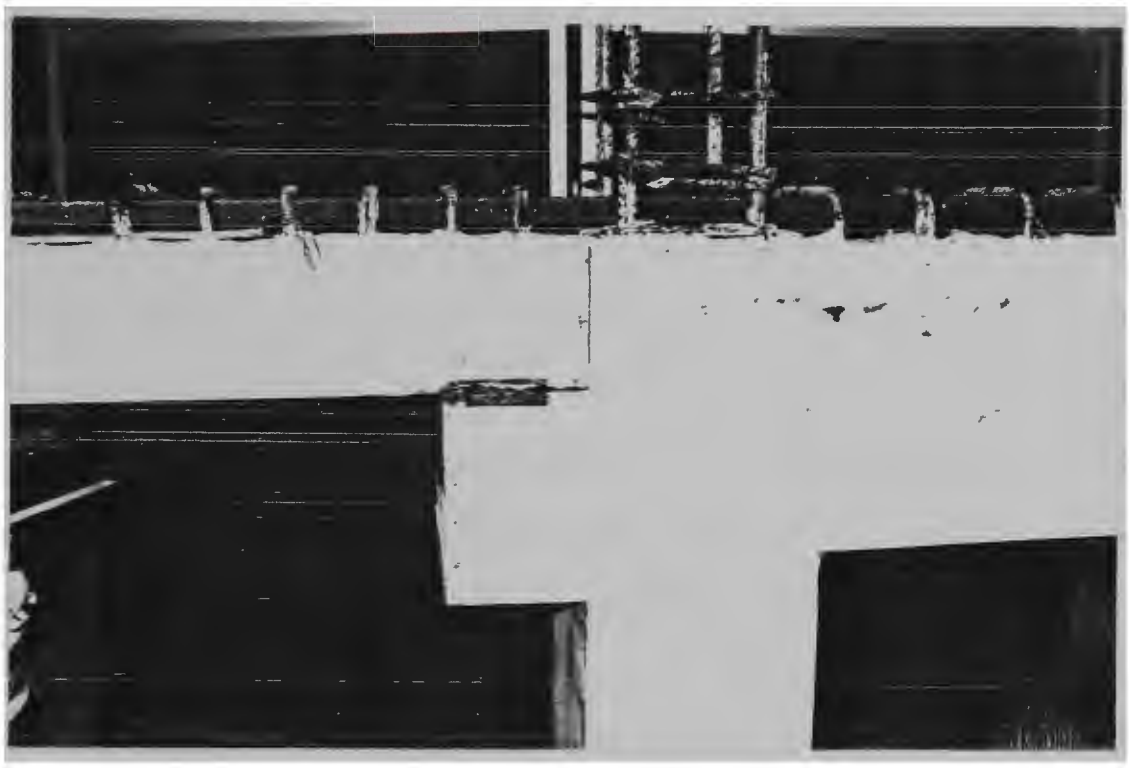

Plate 3.4.4 Connection Type B Before Assembling

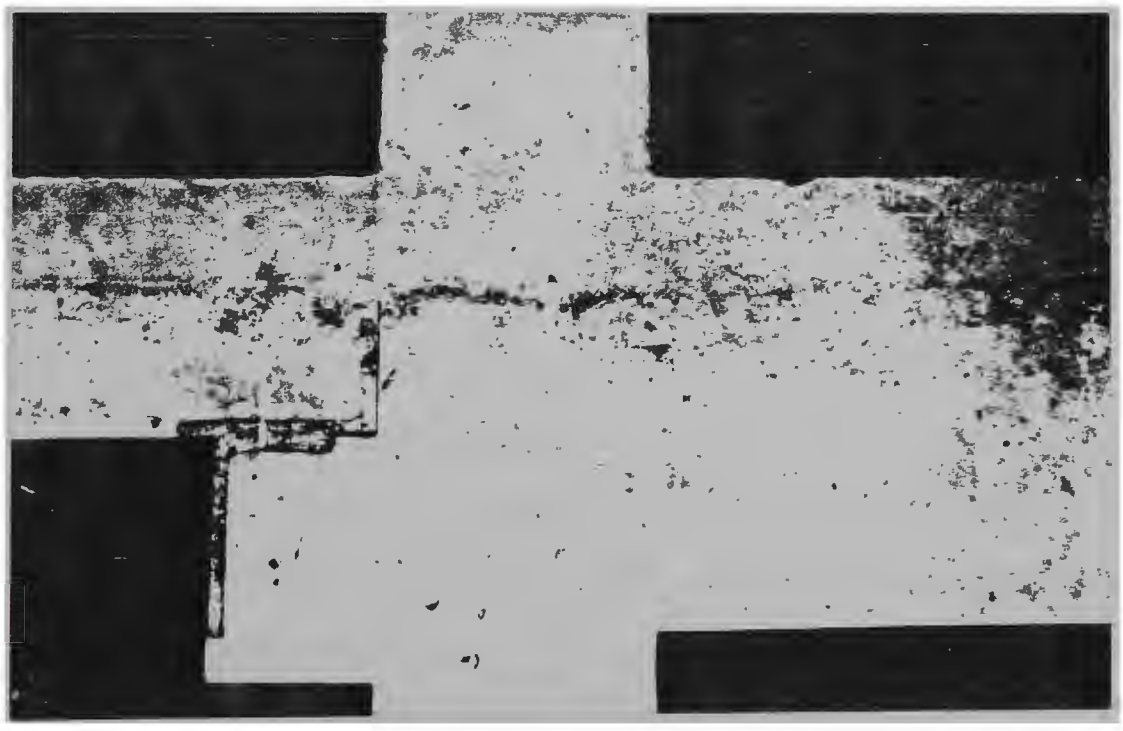

Plate 3.4.5 Connection Type B After Assembling

3.5 Instrumentation

3.5.1 Erection of specimens

A total of twelve beam-column connections were tested at the Civil Engineering Laboratory of the University of Wollongong. The loading frame used to test the specimens is shown in Fig. 3.5.1 and Plate 3.5.1. There were three adjustable steel portal frames anchored to the laboratory strong floor at 650mm spacing. All the specimens were tested in the vertical position as in actual frames. When the specimen was hoisted towards the middle portal loading frame by means of a manual crane, a cap and a saddle was used to restrain the column at top and bottom end respectively. The saddle was fixed to the pedestal of the middle portal loading frame while the cap was fixed to the frame through a jack. The free end of the connecting beam was attached to the jack which was mounted on the loading frame through a saddle and load cell. The saddle was fastened to the beam by a steel pin passing through a steel pipe embedded in the beam. The free end of the frame beam was connected to a cell which was mounted on the loading frame on the right to maintain the balance of the specimen during the test.

3.5.2 Loading and data acquisition

The applied load to the tip of the connecting beam was provided by a Rodgers Hydraulic System (Victor Fluid Power) with a maximum capacity of approximately 1786 kPa (see Plate 3.5.2). The load applied to the specimen was measured by a load cell which was calibrated on a test machine to set and check the loads. This was done by loading machine Hottinger Baldwin MESStechink Darmstadt and Load Checking Instrument HBM Digital Dehnung Semesser DMD, respectively.

Various transducers were used to monitor the applied loads, displacement, deflection, rotation and concrete strains in the specimen. Fig.3.5.1 illustrates the

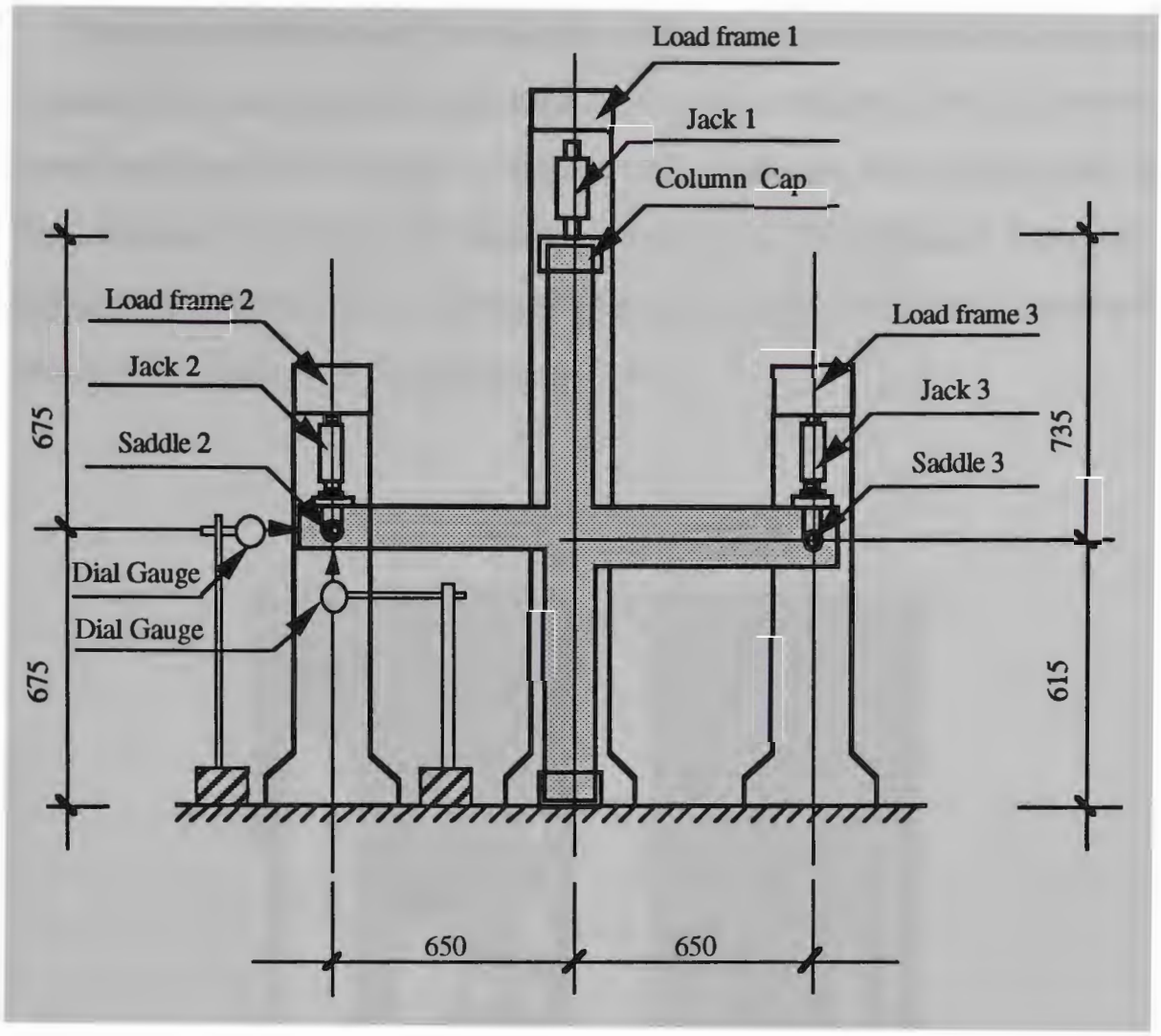

Fig. 3.5.1 Test Set-Up

typical arrangement of instrumentation.

The displacement was measured by means of electrical resistance strain gauges mounted on the top and bottom steel bars as well as on stirrups. Strain gauges were located at identical positions on each specimen such that the measurements could be compared for consistency of results. Gauge locations are indicated in Fig. 3.4.3. All strain gauges in the specimens tested under static loading were connected to a Digital Strainmeter. The strain values and load stages were recorded manually. The strain gauges in the specimens tested under repeated loading were connected to a 3054A Automatic Data Acquisition/Control System (Plate 3.5.3). The strain values and load stages were recorded and printed by the computer automatically.

The vertical deflection of the connection beam directly under the load point was measured by a dial gauge attached to the fixed stand on the floor. For the specimens tested under repeated loading, an additional HP datalogger was used to obtain the load-deflection hysteresis loops instantly (Plate 3.5.4). The horizontal deflections of the beams were measured by Mitutoyo dial gauges mounted on the floor touching the side surface of the end of the connecting beam.

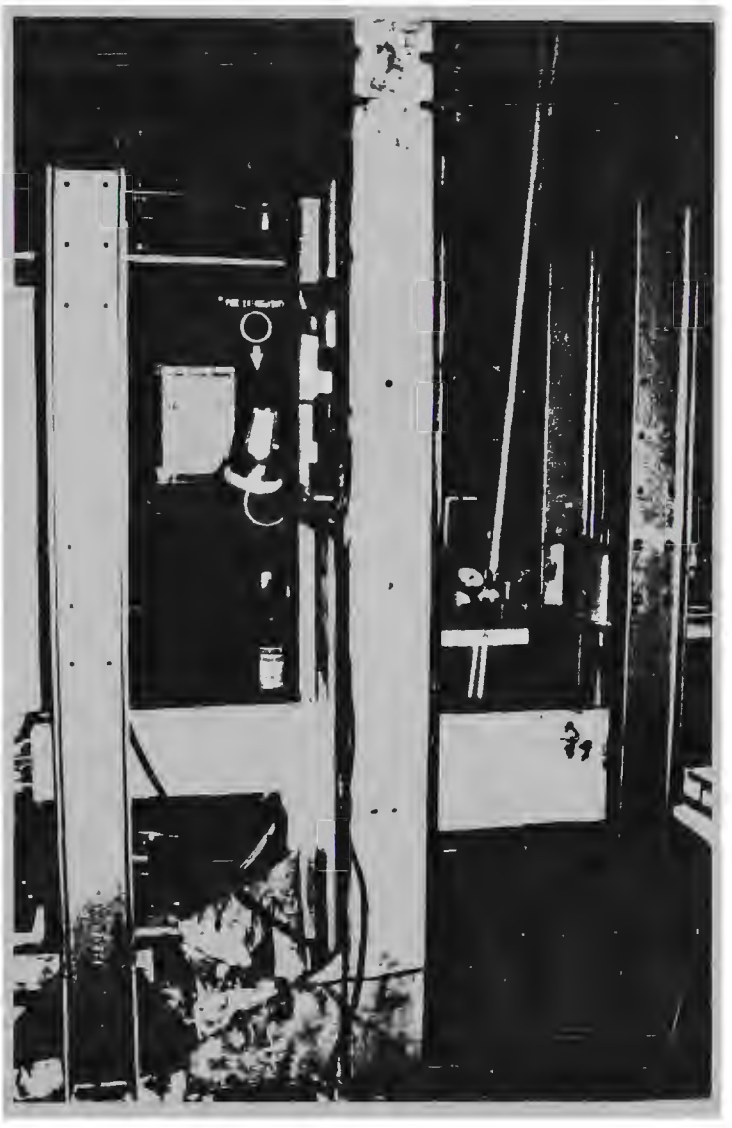

Plate 3.5.1 Loading Rig

Plate 3.5.2 Rogers Hydraulic System and Enerpac Hydraulic System

The concrete strains in tension and compression were measured by a microstrain dial gauges for the specimens tested under static loading. For the specimens tested under repeated loading, the concrete strains were measured by four 60mm long electrical resistance strain gauges attached to the side surface of the connecting beam. They were connected to the Digital strainmeter. The position of the dial gauge and electrical resistance strain gauges are shown in Fig. 3.5.2 and Fig. 3.5.3

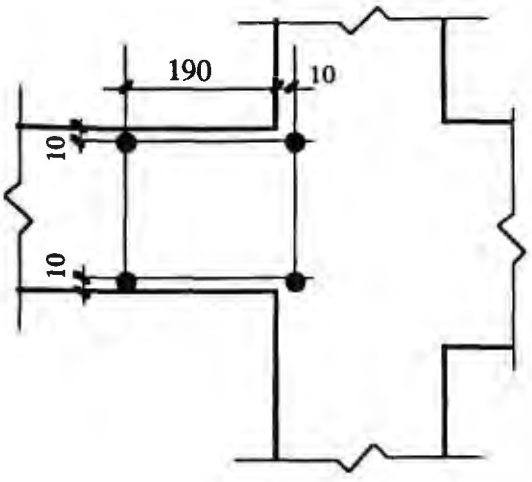

Fig. 3.5.2 Position of Dial Gages for Concrete Strain

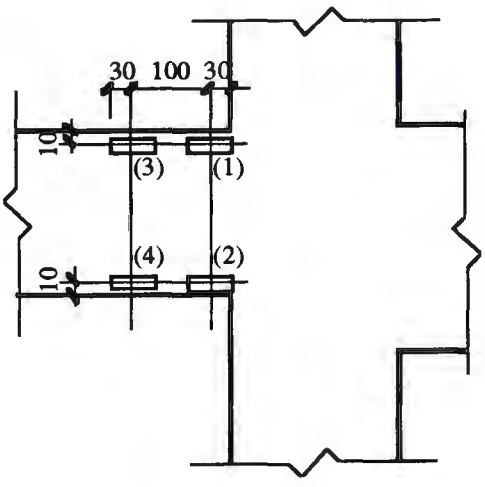

Fig. 3.5.3 Position of Strain Gages for Concrete Strain

Plate 3.5.3 Automatic Data Acquisition / Control System (3054A)

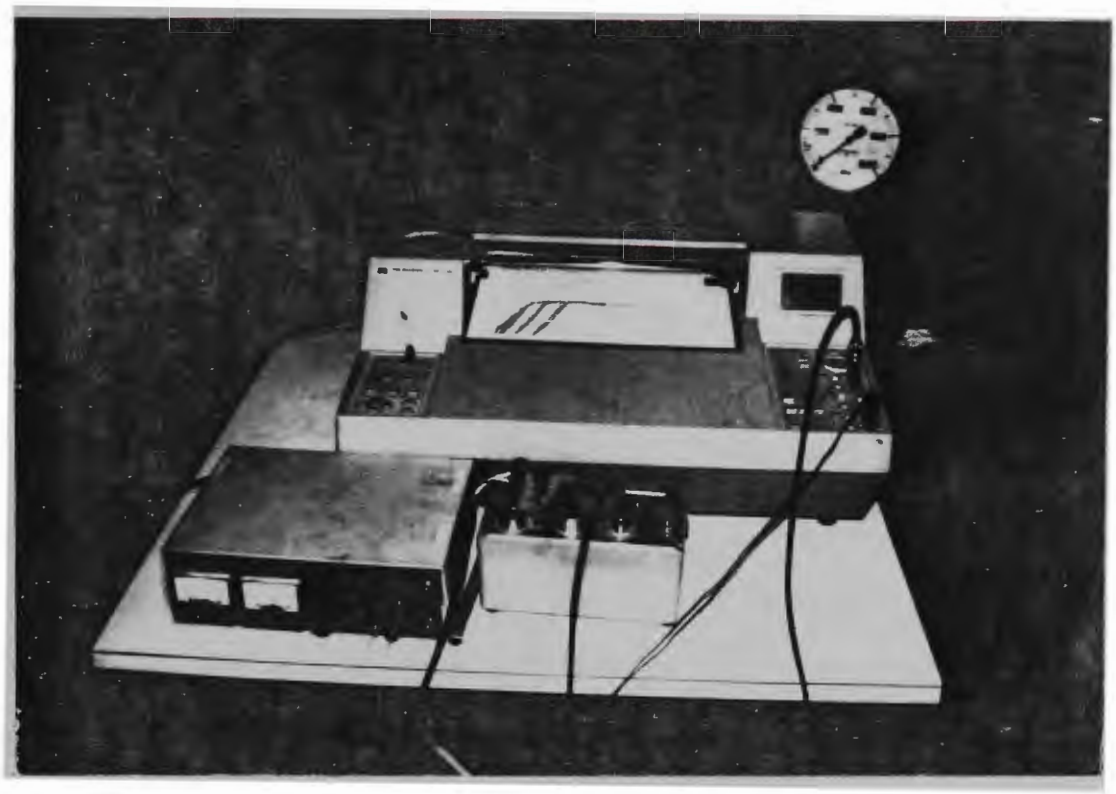

Plate 3.5.4 HP Datalogger

3.6 Experimental Procedure

There were two parts to the experimental program in this study. The first part consisted of testing six specimens under static loading. Load was applied stage by stage until the beam failed. The second part consisted of testing six specimens under repeated loading. Load was controlled by the magnitude of the measured vertical deflection Δ at the tip of the cantilever (see Fig.3.5.1). The vertical-tip deflection was increased in steps of Δ_y where Δ_y is the vertical deflection at first yield.

Six specimens were tested under static loading and another six under repeated loading. Details of each experimental procedure are described in the following sections.

3.6.1 Test procedure for specimens tested under static loading

When a specimen had been positioned in the loading frame and all the instruments

had been connected, an axial load of 150 kN was applied to the column of the specimen. This load was maintained constant throughout the test. Before applying the load to the specimen, all the instruments were checked and adjusted properly. A small load of 1 kN load was applied to make sure that all the instruments were working.

The load was applied to the beam tip step by step. This load increment was calculated based on the ultimate load capacity of each specimen,which depended on the steel ratio and the strength of concrete. Load was increased until the failure of the specimen. When the total applied load is close to the ultimate load, the load increments were reduced to 1 kN. At each load stage, strains of reinforcing bars were measured by the Strainmeter. Strains of concrete were measured by a DEMEC strain gauge meter. The vertical deflection at the load point and the horizontal deflection of the beam was measured by the Mitutoyo dial gauge. All the test data were read and recorded manually. The crack pattern was also inspected at each load stage. Cracks were marked on the surface of the specimens indicating the corresponding load. After testing, the corresponding crack pattern was sketched and photographed. The first yield load was defined as the load at which the strain of the tension reinforcement reached the yield strain of the reinforcing bar. This was obtained from the tension test (see Appendix 3, Table A.3.6).

Failure of a specimen was defined as a marked increase in the deflection at the loading point, accompanied by the appearance of fully developed cracks at the top of the beam and spalling of concrete at the bottom of the beam.

All details of test specimens are presented in Table 3.6.1. In this table, the strength of precast concrete and cast-in-place concrete are the average strengths of all specimens in the group (see Table 3.6.3 and Table 3.6.4). The compressive steel ratio p_c in the connecting beam was calculated as follows:

$$Pc = \frac{fsy'}{fsy}\frac{Asc}{bd}$$
$$= \frac{372}{440} \times \frac{160}{175 \times 137}$$
$$= 5.55 \times 10^{-3}$$

3.6.2 Test procedure for specimens tested under repeated loading

After checking the position of the specimen, and the connections to the instruments, a small load of 1 kN was applied at the beam tip to make sure that all the instruments were working. Then an axial load of 150 kN was applied to the column. The beam tip loading was then applied until the tension steel reinforcement in the beam yielded. At this load stage the deflection at the loading point was recorded and defined as yield deflection Δ_y. The applied loading was then released to zero. This was the first cycle of loading. For the subsequent cycles, the loading was applied in steps, until the vertical deflection reached Δ_y and then released to zero. Tests on these cycles were carried out in a deflection controlled manner, and the loading for each step was selected to obtain the required deflection Δ at the loading point. The loading point deflection was increased in steps corresponding to the deflection ductility ratio $\Delta/\Delta y$.

The procedure was repeated until the failure of the specimen occurred. Failure was defined as the point at which the applied load was less than 80 percent of the load obtained for the first cycle at Δ_y, or the appearance of fully developed cracks at the top of the beam and spalling of the concrete at the bottom of the beam.

A typical load history diagram is shown in Fig 3.6.1. This loading sequence reflects a similarity to the loading of a structure subjected to a moderate earthquake loading.

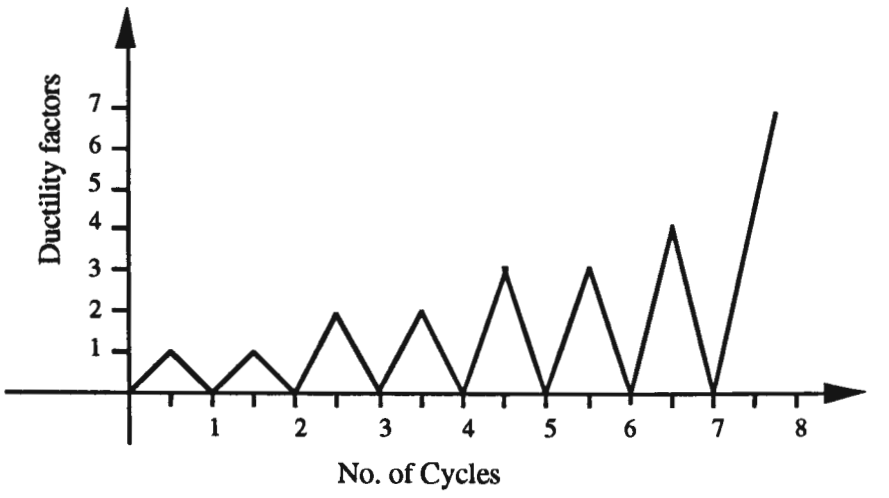

Fig.3.6.1 The Load History

During the testing of the specimen, the load-deflection results were continuously recorded until the specimen failed or until the measured deflection reached such a magnitude that continued recording might have impaired the function of the instrument permanently. An HP datalogger was used to obtain a continuous plot of "load versus deflection" curve of the beam tip. At each load stage, the load was kept constant for a short period of time to permit marking of the crack propagations, taking photos and recording the data. Each crack was marked indicating the corresponding actual load stage.

The location of strain gauges bonded to the reinforcing bar were kept the same as that of specimens tested under static loading (Fig. 3.4.3). They were recorded by the 3054A computer. The location of the strain gauges on the concrete surface are shown in Fig.3.5.3. The strains were recorded by Digital strainmeter.

The details of the test specimens are presented in Table 3.6.2. In this table the strength of precast concrete and cast-in-place concrete are the average strength of all specimens in the group.

Table 3.6.1 Details of Connecting Beam for Specimens Tested Under Static Loading

name of model	type of connc -tion	type of load	type of steel ratio	b (mm)	d (mm)	d_c (mm)	Reinforcement							Concrete	
							top			bottom			space of ties (mm)	strength of precast concrete (MPa)	strength of CIP concrete (MPa)
							Ast (mm^2)	f_{sy} (MPa)	P_t (0/0)	Asc (mm^2)	f_{sy}' (MPa)	P_c (0/00)			
SM1	Mono.	static	1	175	137	31	400	440	1.668	160	372	5.55	50/100	30.26	
SPA1	A	static	1	175	137	31	400	440	1.668	160	372	5.55	50/100	30.26	58.88
SPB1	B	static	1	175	137	31	400	440	1.668	160	372	5.55	50/100	30.26	58.88
SM2	Mono.	static	2	175	137	31	600	440	2.503	160	372	5.55	50/100	30.26	
SPA2	A	static	2	175	137	31	600	440	2.503	160	372	5.55	50/100	30.26	58.88
SPB2	B	static	2	175	137	31	600	440	2.503	160	372	5.55	50/100	30.26	58.88

Table 3.6.2 Details of Connecting Beam for Specimens Tested Under Repeated Loading

name of model	type of connc -tion	type of load	type of steel ratio	b (mm)	d (mm)	d_c (mm)	Reinforcement							Concrete	
							top			bottom			space of ties (mm)	strength of precast concrete (MPa)	strength of CIP concrete (MPa)
							Ast (mm^2)	f_{sy} (MPa)	P_t (0/0)	Asc (mm^2)	f_{sy}' (MPa)	P_c (0/00)			
RM1	Mono.	repeat	1	175	137	31	400	440	1.668	160	372	5.55	50/100	37	
RPA1	A	repeat	1	175	137	31	400	440	1.668	160	372	5.55	50/100	37	67
RPB1	B	repeat	1	175	137	31	400	440	1.668	160	372	5.55	50/100	37	67
RM2	Mono.	repeat	2	175	137	31	600	440	2.503	160	372	5.55	50/100	37	
RPA2	A	repeat	2	175	137	31	600	440	2.503	160	372	5.55	50/100	37	67
RPB2	B	repeat	2	175	137	31	600	440	2.503	160	372	5.55	50/100	37	67

Table 3.6.3 Strength of Precast Concrete

Name of specimen	Date of pouring	Date of testing	Age (days)	Strength (MPa)	Average Strength
SM1	12/8/93	6/10/93	55	30.56	
SPA1	12/8/93	7/10/93	56	28.80	
SPB1	12/8/93	13/10/93	62	30.69	30.26
SM2	12/8/93	13/10/93	62	30.69	
SPA2	12/8/93	12/10/93	61	31.20	
SPB2	12/8/93	8/10/93	57	29.61	
RM1	30/8/93	28/10/93	59	37.24	
RPA1	30/8/93	3/11/93	65	38.96	
RPB1	30/8/93	5/11/93	67	37.56	37
RM2	30/8/93	8/11/93	70	35.46	
RPA2	30/8/93	9/11/93	71	35.33	
RPB2	30/8/93	9/11/93	71	35.01	

Table 3.6.4 Strength of Cast-in-Place Concrete

Name of specimen	Date of pouring	Date of testing	Age (days)	Strength (MPa)	Average Strength
SPA1	22/9/93	7/10/93	15	57.70	
SPB1	22/9/93	13/10/93	21	59.46	58.9
SPA2	22/9/93	12/10/93	20	61.75	
SPB2	22/9/93	8/10/93	16	57.00	
RPA1	5/10/93	3/11/93	29	65.88	
RPB1	5/10/93	5/11/93	31	70.60	67
RPA2	5/10/93	9/11/93	35	68.44	
RPB2	5/10/93	9/11/93	35	63.66	

CHAPTER 4

PRESENTATION AND DISCUSSION OF TEST RESULTS UNDER STATIC LOADING

4.1 Introduction

The performances of six specimens tested under static loading are discussed in this chapter. The steel and concrete strengths are given in the Appendices 3 and 4. The normalised test data are presented in Appendix 1. Because the strains of the compression steel and stirrups in the connecting beams were all well below their yield strains, only the strains of the tension bars were used in the investigation of the strength behaviour of the connections. The analysis of test results were composed of flexural strengths, deformation ductilities and failure modes. From the test data, load-deflection curves for the connecting beam and load-strain curves for the tension bars were drawn and the load stages corresponding to the initial cracking of the beam and the initial yield of the tension bars were determined approximately. Crack patterns were sketched and photographed. Further, comparisons were made between the connecting beam of the monolithic model and the precast models.

4.2 Test Results

4.2.1 Flexural strength

The flexural strength is a very important factor for structural safety. Because the flexural strength were obtained by multiplying the peak beam loading as recorded by the load cell by the span of cantilever connecting beams, the comparison was therefore made with peak beam loading. From the test data, the ultimate loads, P_u, of the connecting beam in precast concrete specimens were all greater than those of the monolithic specimens. This was mainly due to the fact that the strength of the cast-in-place concrete is much greater than the strength of the components. In order to make

the comparison more reasonable, the relative load capacity was introduced. These were obtained as the ratios of the ultimate load, Pu to the corresponding theoretical maximum load, P_{max}. The calculated values of P_{max} were based on an ultimate concrete strain of 0.003 and actual material properties for the steel and concrete which were obtained from the tests carried out previously. The areas of the plain reinforcing bars in compression of the connecting beam were normalised to that of the deformed bars. This was necessary because the compression steel had a yield strength of 371.5 MPa.

The following computations for P_{max} are carried out according to Loo[48], based on the Australia Concrete Structures Code, AS3600-1988[6].

(a) Specimen SM1

b = 175 mm, d = 170 - 33 = 137 mm, d'= 31 mm,

Ast = 2Y16 = 400 mm^2, fsy = 440 MPa,

Asc = 2R10 = 160 mm^2, fsy' = 371.5 MPa,

fc' = 30.26 MPa,

$$P_t = \frac{400}{175x137} = 0.016684$$

$$P_c' = \frac{160x\frac{371.5}{440}}{175x139} = \frac{135}{175x139} = 5.55358x10^{-3}$$

Eq. 3.2 (2) v = 0.85 - 0.007 x (30.26 - 28) = 0.83418

Eq. 3.3 (5)
$$P_B = \frac{0.85f_c'vK_uB}{f_{sy}} = \frac{0.85x30.26x0.83418x\frac{600}{600+440}}{440} = 0.028$$

$$\frac{3}{4}P_B = \frac{3}{4}x0.028 = 0.021$$

But $P_t - P_c' = 0.016684 - 5.55358 \times 10^{-3} = 0.011$

So $Pt\text{-}Pc' < \frac{3}{4}P_B$ (under-reinforced, tension failure)

Eq. 3.5 (3) $$(P_t - P_c')_{limit} = \frac{510x0.83418x30.26x\frac{31}{137}}{(600-440)x440} = 0.0414$$

$P_t - P_c' = 0.011 < (P_t - P_c')_{limit}$

So A_{sc} would not yield at failure.

Eq. 3.5 (12) $$\eta = \frac{0.016684x440 - 600x5.55358x10^{-3}}{1.7x0.83418x30.26} = 0.0934$$

Eq. 3.5 (13) $$\gamma = \frac{600x5.55358x10^{-3}}{0.85x0.83418x30.26} = 0.1553$$

Eq. 3.5 (11) $$K_u = \eta + \sqrt{\eta^2 + \gamma\frac{d_c}{d}} = 0.0934 + \sqrt{0.0934^2 + 0.1553x\frac{31}{137}} = 0.3028$$

$a = vK_ud = 0.83418 \times 0.3028 \times 137 = 34.60$

Eq 3.5 (15)

$$M_{max} = 400x440x(137 - \frac{34.6}{2}) + 600x135x(1 - \frac{31}{0.3028x137})x(\frac{34.6}{2} - 31)$$

$$= 21067200 - 280440$$
$$= 20786760Nmm$$

$$P_{max} = \frac{M_{max}}{L} = \frac{20.78676}{0.5625} = 37kN$$

(b) Specimen SPA1

b = 175 mm, d = 170 - 33 = 137 mm, d'= 31 mm,

A_{st} = 2Y16 = 400 mm^2, f_{sy} = 440 MPa,

A_{sc} = 2R10 = 160 mm^2, f_{sy}' = 371.5 MPa,

f_c' = 30.26 MPa, f_c'' = 58.88 MPa,

$$P_t = \frac{400}{175x137} = 0.016684$$

$$P_c' = \frac{160x\frac{371.5}{440}}{175x139} = \frac{135}{175x139} = 5.55358x10^{-3}$$

Eq. 3.2 (2) v = 0.85 - 0.007 x (58.88 - 28) = 0.6338

Eq. 3.3 (5) $$P_B = \frac{0.85x58.88x0.6338x\frac{600}{600+440}}{440} = 0.0416$$

$$\frac{3}{4}P_B = \frac{3}{4}x0.0416 = 0.0311$$

But $P_t - P_c'$ = 0.016684 - 5.55358 x 10^{-3} = 0.011

So $P_t - P_c' < \frac{3}{4}P_B$ (under-reinforced, tension failure)

Eq. 3.5 (3) $$(P_t - P_c')_{limit} = \frac{510x0.6338x58.88x\frac{31}{137}}{(600-440)x440} = 0.0612$$

$P_t - P_c'$ = 0.011 < $(P_t - P_c')_{limit}$

So A_{sc} would not yield at failure.

Eq. 3.5 (12) $$\eta = \frac{0.016684x440 - 600x5.55358x10^{-3}}{1.7x0.6338x58.88} = 0.0632$$

Eq. 3.5 (13) $\gamma = \frac{600x5.55358x10^{-3}}{0.85x0.6338x58.88} = 0.105$

Eq. 3.5 (11) $K_u = \eta + \sqrt{\eta^2 + \gamma\frac{d_c}{d}} = 0.0632 + \sqrt{0.0632^2 + 0.105x\frac{31}{137}} = 0.2298$

a = vK_ud = 0.6338 x 0.2298 x 137 = 19.954

Eq. 3.5 (15)

$$M_{max} = 400x440x(137 - \frac{19.954}{2}) + 600x135x(1 - \frac{31}{0.2298x137})x(\frac{19.954}{2} - 31)$$

$$= 22356048 - 26103$$

$$= 22329945Nmm$$

$$P_{max} = \frac{M_{max}}{L} = \frac{22.329945}{0.5625} = 39.69kN$$

(c) Specimen SPB1

b = 175 mm, d = 170 - 33 = 137 mm, d'= 31 mm,

Ast = 2Y16 = 400 mm^2, fsy = 440 MPa,

Asc = 2R10 = 160 mm^2, fsy' = 371.5 MPa,

fc' = 30.26 MPa, fc'' = 58.88 MPa,

$$P_t = \frac{400}{175x137} = 0.016684$$

$$P_c' = \frac{160x\frac{371.5}{440}}{175x139} = \frac{135}{175x139} = 5.55358x10^{-3}$$

Eq. 3.2 (2) v = 0.85 - 0.007 x (30.26 - 28) = 0.83418

Eq. 3.3 (5) $$P_B = \frac{0.85 f_c' v K_u B}{f_{sy}} = \frac{0.85x30.26x0.83418x\frac{600}{600+440}}{440} = 0.028$$

$$\frac{3}{4}P_B = \frac{3}{4}x0.028 = 0.021$$

But $P_t - P_c' = 0.016684 - 5.55358 \times 10^{-3} = 0.011$

So $Pt\text{-}Pc' < \frac{3}{4}P_B$ (under-reinforced, tension failure)

Eq. 3.5 (3) $$(P_t - P_c')_{limit} = \frac{510x0.83418x30.26x\frac{31}{137}}{(600-440)x440} = 0.0414$$

$P_t - P_c' = 0.011 < (P_t - P_c')_{limit}$

So A_{SC} would not yield at failure.

Eq. 3.5 (12) $$\eta = \frac{0.016684x440 - 600x5.55358x10^{-3}}{1.7x0.83418x30.26} = 0.0934$$

Eq. 3.5 (13) $$\gamma = \frac{600x5.55358x10^{-3}}{0.85x0.83418x30.26} = 0.1553$$

Eq. 3.5 (11) $$K_u = \eta + \sqrt{\eta^2 + \gamma\frac{d_c}{d}} = 0.0934 + \sqrt{0.0934^2 + 0.1553x\frac{31}{137}} = 0.3028$$

$a = vK_ud = 0.83418 \times 0.3028 \times 137 = 34.60$

Eq. 3.5 (15)

$$M_{max} = 400x440x(137 - \frac{34.6}{2}) + 600x135x(1 - \frac{31}{0.3028x137})x(\frac{34.6}{2} - 31)$$

$$= 21067200 - 280440$$

$$= 20786760Nmm$$

$$P_{max} = \frac{M_{max}}{L} = \frac{20.78676}{0.5125} = 41kN$$

(d) Specimen SM2

b = 175 mm, d = 170 - 33 = 137 mm, d'= 31 mm,

Ast = 3Y16 = 600 mm^2, fsy = 440 MPa,

Asc = 2R10 = 160 mm^2, fsy' = 371.5 MPa,

fc' = 30.26 MPa,

$$P_t = \frac{600}{175x137} = 0.025026$$

$$P_c' = \frac{160x\frac{371.5}{440}}{175x139} = \frac{135}{175x139} = 5.55358x10^{-3}$$

Eq. 3.2 (2) v = 0.85 - 0.007 x (30.26 - 28) = 0.83418

Eq. 3.3 (5) $$P_B = \frac{0.85f_c'vK_uB}{f_{sy}} = \frac{0.85x30.26x0.83418x\frac{600}{600+440}}{440} = 0.028$$

$$\frac{3}{4}P_B = \frac{3}{4}x0.028 = 0.021$$

But $P_t - P_c' = 0.025026 - 5.55358 \times 10^{-3} = 0.0195$

So $P_t - P_c' < \frac{3}{4}P_B$ (under-reinforced, tension failure)

Eq. 3.5 (3) $$(P_t - P_c')_{limit} = \frac{510x0.83418x30.26x\frac{31}{137}}{(600-440)x440} = 0.0414$$

$P_t - P_c' = 0.0195 < (P_t - P_c')_{limit}$

So A_{sc} would not yield at failure.

Eq. 3.5 (12) $$\eta = \frac{0.025026x440 - 600x5.55358x10^{-3}}{1.7x0.83418x30.26} = 0.17895$$

Eq. 3.5 (13) $$\gamma = \frac{600x5.55358x10^{-3}}{0.85x0.83418x30.26} = 0.1553$$

Eq. 3.5 (11)

$$K_u = \eta + \sqrt{\eta^2 + \gamma\frac{d_c}{d}} = 0.17895 + \sqrt{0.017895^2 + 0.1553x\frac{31}{137}} = 0.4381$$

$a = vK_ud = 0.83418 \times 0.4381 \times 137 = 50.07$

Eq. 3.5 (11)

$$M_{max} = 600x440x(137 - \frac{50.07}{2}) + 600x135x(1 - \frac{31}{0.4381x137})x(\frac{50.07}{2} - 31)$$

$$= 29558760 - 233612$$

$$= 29325148Nmm$$

$$P_{max} = \frac{M_{max}}{L} = \frac{29.325148}{0.5625} = 52.14kN$$

(e) Specimen SPA2

b = 175 mm, d = 170 - 33 = 137 mm, d'= 31 mm,

Ast = 3Y16 = 600 mm^2, fsy = 440 MPa,

Asc = 2R10 = 160 mm^2, fsy' = 371.5 MPa,

fc' = 30.26 MPa, fc" = 58.88 MPa,

$$P_t = \frac{600}{175x137} = 0.025026$$

$$P_c' = \frac{160x\frac{371.5}{440}}{175x139} = \frac{135}{175x139} = 5.55358x10^{-3}$$

Eq. 3.2 (2) $v = 0.85 - 0.007 \times (58.88 - 28) = 0.6338$

Eq. 3.3 (5) $$P_B = \frac{0.85x58.88x0.6338x\frac{600}{600+440}}{440} = 0.0416$$

$$\frac{3}{4}P_B = \frac{3}{4}x0.0416 = 0.0311$$

But $P_t - P_c' = 0.025026 - 5.55358 \times 10^{-3} = 0.0195$

So $P_t - P_c' < \frac{3}{4}P_B$ (under-reinforced, tension failure)

Eq. 3.5 (3) $$(P_t - P_c')_{limit} = \frac{510x0.6338x58.88x\frac{31}{137}}{(600-440)x440} = 0.0612$$

$P_t - P_c' = 0.0195 < (P_t - P_c')_{limit}$

So A_{sc} would not yield at failure.

Eq. 3.5 (12) $$\eta = \frac{0.025026x440 - 600x5.55358x10^{-3}}{1.7x0.6338x58.88} = 0.12105$$

Eq. 3.5 (13) $$\gamma = \frac{600x5.55358x10^{-3}}{0.85x0.6338x58.88} = 0.105$$

Eq. 3.5 (11) $$K_u = \eta + \sqrt{\eta^2 + \gamma\frac{d_c}{d}} = 0.12105 + \sqrt{0.12105^2 + 0.105x\frac{31}{137}} = 0.317$$

$a = vK_ud = 0.6338 \times 0.317 \times 137 = 27.525$

Eq. 3.5 (15)

$$M_{max} = 600x440x(137 - \frac{27.525}{2}) + 600x135x(1 - \frac{31}{0.317x137})x(\frac{27.525}{2} - 31)$$

$$= 32534700 - 399591$$

$$= 32135109Nmm$$

$$P_{max} = \frac{M_{max}}{L} = \frac{32.135109}{0.5625} = 57.13kN$$

(f) Specimen SPB2

b = 175 mm, d = 170 - 33 = 137 mm, d'= 31 mm,

Ast = 3Y16 = 600 mm^2, fsy = 440 MPa,

Asc = 2R10 = 160 mm^2, fsy' = 371.5 MPa,

fc' = 30.26 MPa, fc" = 58.88 MPa,

$$P_t = \frac{600}{175x137} = 0.025026$$

$$P_c' = \frac{160x\frac{371.5}{440}}{175x139} = \frac{135}{175x139} = 5.55358x10^{-3}$$

Eq. 3.2 (2) v = 0.85 - 0.007 x (30.26 - 28) = 0.83418

Eq. 3.3 (5) $$P_B = \frac{0.85f_c'vK_uB}{f_{sy}} = \frac{0.85x30.26x0.83418x\frac{600}{600+440}}{440} = 0.028$$

$$\frac{3}{4}P_B = \frac{3}{4}x0.028 = 0.021$$

But $P_t - P_c' = 0.025026 - 5.55358 \times 10^{-3} = 0.0195$

So $Pt\text{-}Pc' < \frac{3}{4} P_B$ (under-reinforced, tension failure)

Eq. 3.5 (3) $$(P_t - P_c')_{limit} = \frac{510x0.83418x30.26x\frac{31}{137}}{(600-440)x440} = 0.0414$$

$P_t - P_c' = 0.0195 < (P_t - P_c')_{limit}$

So A_{sc} would not yield at failure.

Eq. 3.5 (12) $$\eta = \frac{0.025026x440 - 600x5.55358x10^{-3}}{1.7x0.83418x30.26} = 0.17895$$

Eq. 3.5 (13) $$\gamma = \frac{600x5.55358x10^{-3}}{0.85x0.83418x30.26} = 0.1553$$

Eq. 3.5 (11)

$$K_u = \eta + \sqrt{\eta^2 + \gamma\frac{d_c}{d}} = 0.17895 + \sqrt{0.017895^2 + 0.1553x\frac{31}{137}} = 0.4381$$

$a = vK_ud = 0.83418 \times 0.4381 \times 137 = 50.07$

Eq. 3.5 (15)

$$M_{max} = 600x440x(137 - \frac{50.07}{2}) + 600x135x(1 - \frac{31}{0.4381x137})x(\frac{50.07}{2} - 31)$$

$$= 29558760 - 233612$$

$$= 29325148Nmm$$

$$P_{max} = \frac{M_{max}}{L} = \frac{29.325148}{0.5125} = 57.22kN$$

The calculated and measured ultimate loads for connecting beams are given in Table 4.2.1.

Table 4.2.1 Comparison of the load capacity

Name of Specimen	*Compressive strength of concrete(MPa)	Calculated ultimate load P_{max} (kN)	measured ultimate load P_u (kN)	P_u / P_{max}
SM1	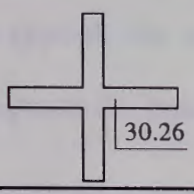	37	39	1.05
SPA1	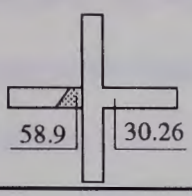	40	49	1.23
SPB1	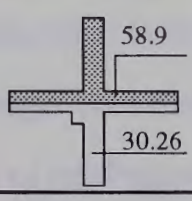	41	52	1.15
SM2	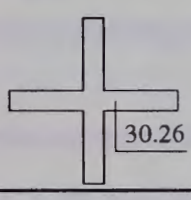	52	52	1.00
SPA2	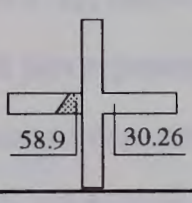	57	64	1.12
SPB2	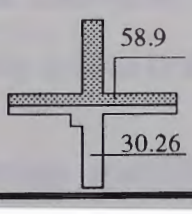	57	66	1.14

* Represents strengths obtained from cylinders at the time of specimen tested

From Table 4.2.1, it is clearly seen that the load capacities of precast concrete connecting beams were all greater than those of their monolithic counterparts. The reasons for this are as follows.

· for connection type A, the welding of the reinforcing bars can both strengthen the steel cage and improve the load carrying capacity of the connecting beam;

· for connection type B, the higher strength of the cast-in-place concrete in the tension area can also improve the load carrying capacity of the connecting beams, which was ignored in calculation;

· for all specimens, either monolithic models or precast models, their practical ultimate loads were all larger than their theoretical maximum loads. This is because of the strain hardening of reinforcing bars in the connection. If strain hardening effects are included, the predicted strength agrees well with the ultimate strength.

The load-strain curves of the tension steel bars in the connecting beams are shown in Fig.A.1.7 to A.1.12, based on the normalised load-strain test data for each of the specimens. Each plot represents the behaviour of one particular gauge on the various models. These curves demonstrate that the strain behaviour of the tension bars during the tests and the load-strain curve of the tension steel used in precast concrete specimens are very similar to those in the monolithic specimens.

4.2.2 Deformation ductility

A significant consideration that may have to be added to load capacity is the deformation ductility. It is important to ensure that in the extreme event of a structure being loaded to failure, it will behave in a ductile manner. This means ensuring that the structure will not fail in a brittle fashion without warning but will be capable of large deformations at near-maximum load carrying capacity. The large deflection at near-maximum load give ample warning of failure, and by maintaining load carrying

capacity, total collapse may be prevented and lives saved. Also, the ductile behaviour of members enables the redistribution of bending moments (Park & Paulay)[56].

The ductility is usually expressed as the ratio of the maximum deflection at near-maximum load , Δ_u, to the deflection at the initial yield, Δ_y (Pillai & Kirk)[64]. On the basis of the definition above, the deflection ductility of all the specimens can be calculated approximately and are presented in Table 4.2.2. The initial yield deflection Δ_y was determined by two methods. In the first method, the deflection at which the maximum strain in the tensile steel reaches the yield strain given by the load-strain curve of the reinforcement is taken as Δ_y. In the second Method, Δ_y is taken as the deflection at which a small increment of load causes a substantial increase in deflection. It was seen that both methods give almost the same value for Δ_y.

From Table 4.2.2, it is clear that:

· All the precast models, SPA1, SPB1 and SPA2, SPB2, possessed greater ductility than their monolithic counterpart SM1 and SM2. This means that both these two types of precast connections can be considered to have adequate ductilities. This also verifies the safety of application of the precast concrete connections for use in building frames.

· Use of high reinforcement ratios in connecting beams reduces the ductility. This shows the importance of limiting the steel ratio under p_{all} and of avoiding the use of high steel ratios in practice.

From the load-deflection test data of each specimen, the load-deflection curves can be drawn (according to Park & Paulay, 1975) as shown in Appendix 1. A combined plot is also provided for further comparison (Fig.4.2.1). Each model had the same precast concrete strength of 30.26 MPa and each of the three models had the same steel content, 2Y16 and 3Y16 respectively. The only difference was the connection details.

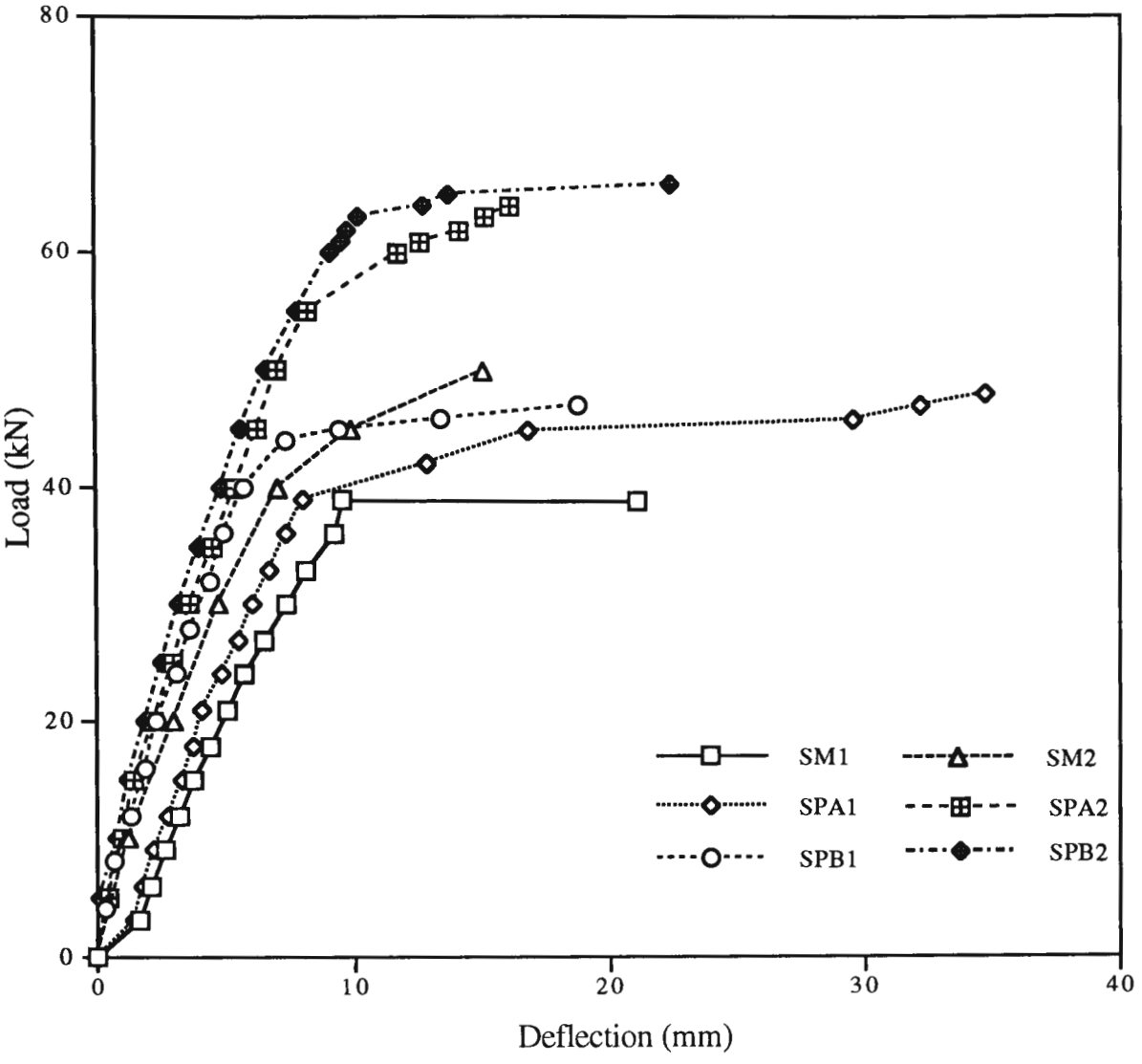

Fig.4.2.1 Load-deflection Curves for specimens under static load

Table 4.2.2 Ductility Capacity of Specimens Tested Under Static Loading

Name of Specimen	*Compressive strength of concrete(MPa)	first yield deflection Δ_y (mm)	Ultimate deflection Δ_u (mm)	Ductility Δ_u/Δ_y
SM1	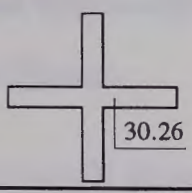	8.07	21.06	2.61
SPA1	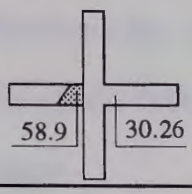	8.03	34.71	4.32
SPB1	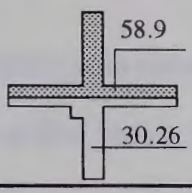	5.74	18.71	3.26
SM2	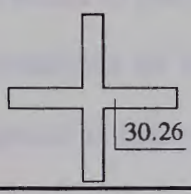	7.05	15.02	2.13
SPA2	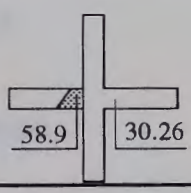	8.20	28.20	3.44
SPB2	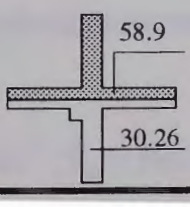	9.10	22.38	2.46

* Represents strengths obtained from cylinders at the time of specimen tested

From the plots in Fig. 4.2.2, some important results are obtained as follows:

(1) The load-deflection curves of precast models are very similar to those of the monolithic models. This indicates that the load-deflection behaviour of the precast models was at least the same as that of the monolithic models. There was no premature failure occurring in any of the precast connections.

(2) The ultimate load capacities of all the precast models, SPA1, SPB1 and SPA2, SPB2, are much higher than those of their corresponding monolithic models SM1 and SM2. The main reasons have been discussed in Section 4.2.1. These show that both kinds of connections had enough strength and load carrying capacity for use in precast reinforced concrete frames.

(3) Because stiffness is in direct proportion to the angle between the tangent to the curve and the deflection axis, it can be seen that both the precast connections had higher stiffness, especially before yielding. They also had larger ductility than the monolithic connections.

Ductility of a member is usually expressed as the ratio of the ultimate deformation to the deformation at first yield. Sometimes, ductility is defined as the ratio of ultimate rotation of the end beam to yield rotation. The larger the ratio, the better the ductile behaviour. The rotations of the end-beam of each specimen and their rotation ductilities are computed as follows.

(a) Specimen SM1

Ultimate deflection $\Delta_u = 21.06$ mm

Ultimate longitudinal movement $\Delta_{Hu} = 3.84$ mm

Ultimate rotation $\theta_u = \tan^{-1}\frac{\Delta_u}{\Delta_{Hu}} = \tan^{-1}\frac{21.06}{562.5+3.84} = 2.13$

Yield deflection $\Delta_y = 8.07$ mm

Yield longitudinal movement $\Delta_{Hy} = 1.49$ mm

Yield rotation $\theta_y = \tan^{-1}\frac{\Delta_y}{\Delta_{Hy}} = \tan^{-1}\frac{8.07}{562.5+1.49} = 0.082$

$$Rotation\ \ Ductility = \frac{\theta_u}{\theta_y} = 2.60$$

(b) Specimen SPA1

Ultimate deflection $\Delta_u = 34.71$ mm

Ultimate longitudinal movement $\Delta_{Hu} = 4.46$ mm

Ultimate rotation $\theta_u = \tan^{-1}\frac{\Delta_u}{\Delta_{Hu}} = \tan^{-1}\frac{34.71}{562.5+4.46} = 3.503$

Yield deflection $\Delta_y = 8.03$ mm

Yield longitudinal movement $\Delta_{Hy} = 1.77$ mm

Yield rotation $\theta_y = \tan^{-1}\frac{\Delta_y}{\Delta_{Hy}} = \tan^{-1}\frac{8.03}{562.5+1.77} = 0.815$

$$Rotation\ \ Ductility = \frac{\theta_u}{\theta_y} = 4.30$$

(c) Specimen SPB1

Ultimate deflection $\Delta_u = 18.71$ mm

Ultimate longitudinal movement $\Delta_{Hu} = 4.01$ mm

Ultimate rotation $\theta_u = \tan^{-1}\frac{\Delta_u}{\Delta_{Hu}} = \tan^{-1}\frac{18.71}{562.5+4.01} = 1.89$

Yield deflection $\Delta_y = 5.74$ mm

Yield longitudinal movement $\Delta_{Hy} = 0.89$ mm

Yield rotation $\theta_y = \tan^{-1}\frac{\Delta_y}{\Delta_{Hy}} = \tan^{-1}\frac{5.74}{562.5+0.89} = 0.584$

Rotation Ductility $= \frac{\theta_u}{\theta_y} = 3.24$

(d) Specimen SM2

Ultimate deflection $\Delta_u = 15.02$ mm

Ultimate longitudinal movement $\Delta_{Hu} = 2.11$ mm

Ultimate rotation $\theta_u = \tan^{-1}\frac{\Delta_u}{\Delta_{Hu}} = \tan^{-1}\frac{15.02}{562.5+2.11} = 1.524$

Yield deflection $\Delta_y = 7.05$ mm

Yield longitudinal movement $\Delta_{Hy} = 1.56$ mm

Yield rotation $\theta_y = \tan^{-1}\frac{\Delta_y}{\Delta_{Hy}} = \tan^{-1}\frac{7.05}{562.5+1.56} = 0.716$

Rotation Ductility $= \frac{\theta_u}{\theta_y} = 2.13$

(e) Specimen SPA2

Ultimate deflection $\Delta_u = 28.2$ mm

Ultimate longitudinal movement $\Delta_{Hu} = 3.77$ mm

Ultimate rotation $\theta_u = \tan^{-1}\frac{\Delta_u}{\Delta_{Hu}} = \tan^{-1}\frac{28.20}{562.5+3.77} = 2.85$

Yield deflection $\Delta_y = 8.2$ mm

Yield longitudinal movement $\Delta_{Hy} = 1.45$ mm

Yield rotation $\theta_y = \tan^{-1}\frac{\Delta_y}{\Delta_{Hy}} = \tan^{-1}\frac{8.20}{562.5+1.45} = 0.833$

Rotation Ductility $= \frac{\theta_u}{\theta_y} = 3.42$

(f) Specimen SPB2

Ultimate deflection $\Delta_u = 22.38$ mm

Ultimate longitudinal movement $\Delta_{Hu} = 3.83$ mm

Ultimate rotation $\theta_u = \tan^{-1}\frac{\Delta_u}{\Delta_{Hu}} = \tan^{-1}\frac{22.38}{562.5+3.83} = 2.263$

Yield deflection $\Delta_y = 9.1$ mm

Yield longitudinal movement $\Delta_{Hy} = 1.77$ mm

Yield rotation $\theta_y = \tan^{-1}\frac{\Delta_y}{\Delta_{Hy}} = \tan^{-1}\frac{9.10}{562.5+1.77} = 0.924$

Rotation Ductility $= \frac{\theta_u}{\theta_y} = 2.45$

All the results of specimens tested under static loading are summarised in table 4.2.3.

Table 4.2.3 Summary of Test Results of specimens tested under static loading

Name	F_c' (MPa)	P_y (kN)	P_u (kN)	P_{max} (kN)	$\frac{p_u}{p_{max}}$	Δ_y (mm)	Δ_u (mm)	$\frac{\Delta_u}{\Delta_y}$	θ_y (°)	θ_u (°)	$\frac{\theta_u}{\theta_y}$
SM1	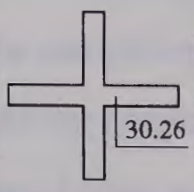	33	39	37	1.05	8.07	21.06	2.61	0.82	2.13	2.60
SPA1	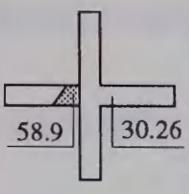	39	49	40	1.23	8.03	34.71	4.32	0.815	3.503	4.30
SPB1	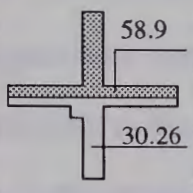	40	52	41	1.15	5.74	18.71	3.26	0.584	1.89	3.24
SM2	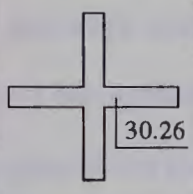	40	52	52	1.00	7.05	15.02	2.13	0.716	1.524	2.13
SPA2	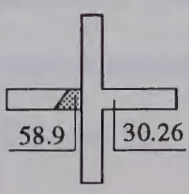	55	64	57	1.12	8.20	28.20	3.44	0.833	2.85	3.42
SPB2	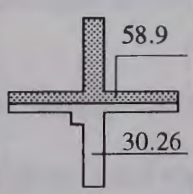	60	66	57	1.14	9.10	22.38	2.46	0.924	2.263	2.45

Note: P_y --yield load

P_u--theoretical ultimate load

P_{max}--measured ultimate load

Δ_y--yield deflection

Δ_u--ultimate deflection

θ_y--yield rotation

θ_u--ultimate rotation

4.2.3 Crack behaviour and failure modes of connections

During the test, crack patterns were inspected and marked on the surface of specimen indicating the corresponding load. After testing, crack patterns were sketched and photographed, as shown in Plates 4.2.1 to 4.2.6 and Figs. 4.2.2 to 4.2.7. All the specimens were failed in tension as expected in the design stage. No premature failure occurred in the precast connections. The detailed description, comparisons and analyses of the failure modes are given as follows.

(a) Specimen SM1

SM1 was the monolithic connection with 2Y16 as tension bars. The specimen had a 5% higher load carrying capacity compared to its theoretical value. The first crack appeared close to the column face at a very early load stage, P_b=6 kN. This load was 15.4 % of the ultimate load. When applied load P_b was increased to 38 % P_u, the second and third cracks appeared approximately parallel to the first one. With the increase of the applied load, more cracks appeared and were well distributed along the tension zone of the concrete. Tension failure occurred with a principal crack occurring at the beam root. This was accompanied by spalling of concrete at the underside root of the beam as deformation became excessive. The crack pattern of SM1 is shown in Plate 4.2.1 and Fig. 4.2.2.

(b) Specimen SPA1

SPA1 was the precast connection with Type A configuration. The specimen had a 23 % higher load carrying capacity compared to its theoretical value. When the applied load was P_b=9 kN, 18 % of its ultimate load, the first crack appeared at the root section of the connecting beam. This was the weakest section because of the largest moment and interface of the precast and cast-in-place concrete. When the applied load P_b reached 24.5 % of the ultimate load, the second and third cracks

appeared. Along with the progressive growing of the first crack, the second crack grew rapidly and continued till it reached the bottom of the beam. The specimen experienced a tensile failure with two principal failure cracks occurring at and near the root of the connecting beam, accompanied by spalling of the concrete at the bottom root of the connecting beam.

The crack pattern of specimen SPA1 is shown in Plate 4.2.2 and Fig. 4.2.3.

(c) Specimen SPB1

Specimen SPB1 was the precast connection with Type B configuration. The specimen had 15 % higher load carrying capacity compared to its theoretical value. When the applied load P_b was P_b=8 kN, 15.4% of its ultimate load, the first two cracks appeared at the edge and the middle portion of the corbel. These were the weakest sections because of the influence of the corbel. With the increase of the applied load, more cracks appeared and were well distributed all over the edge of the corbel. When P_b=12 kN, 23.1 % of its ultimate load, the third crack appeared. When P_b=24 kN, 46.2 % P_u, a longitudinal shear crack between the precast and cast-in-place concrete appeared near the loading point. This was mainly due to insufficient treatment before casting cast-in-place concrete such as roughening and wetting the interface. Tension failure occurred with the principal crack at the edge of the corbel accompanied by a small amount of spalling in the concrete at the bottom of the connecting beam near the edge of the corbel.

The crack pattern of specimen SPB1 is shown in Plate 4.2.3 and Fig. 4.2.4.

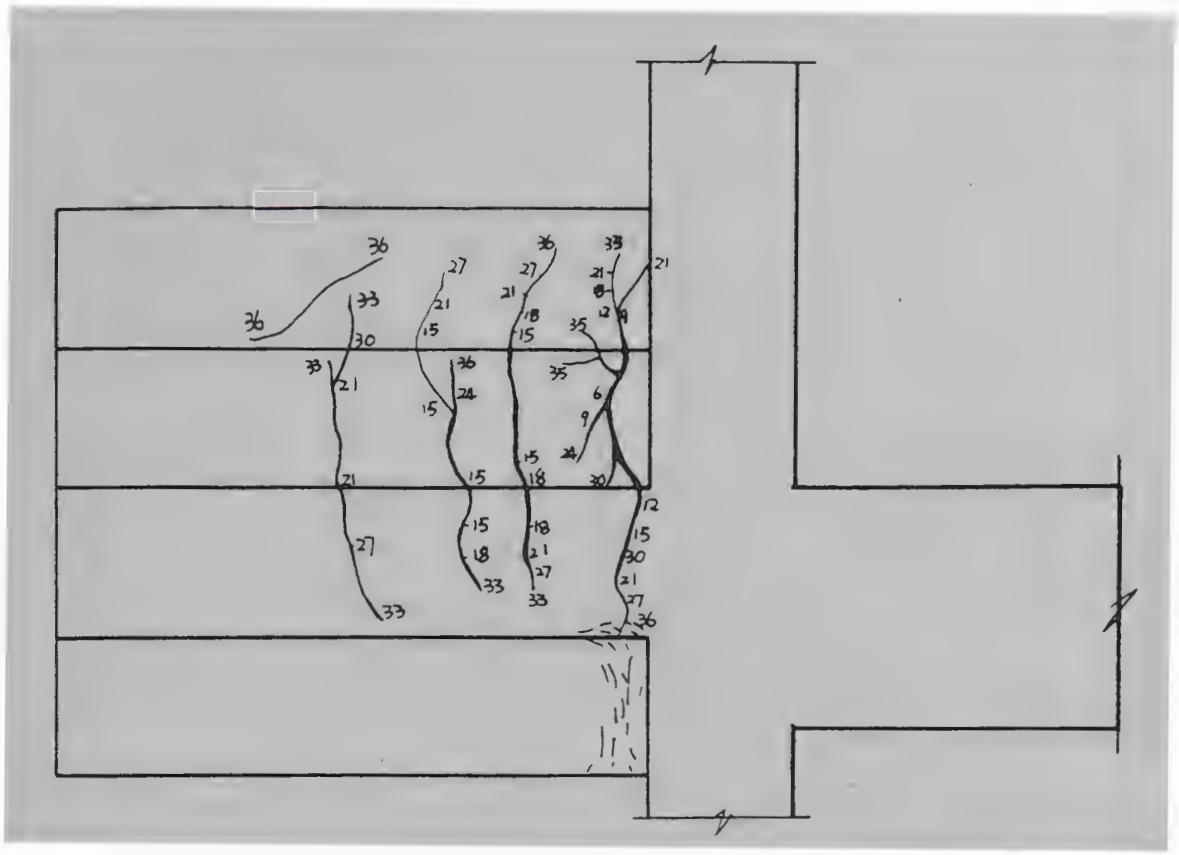

Fig. 4.2.2 Crack Pattern for Specimen SM1

Plate 4.2.1 Crack Pattern for Specimen SM1

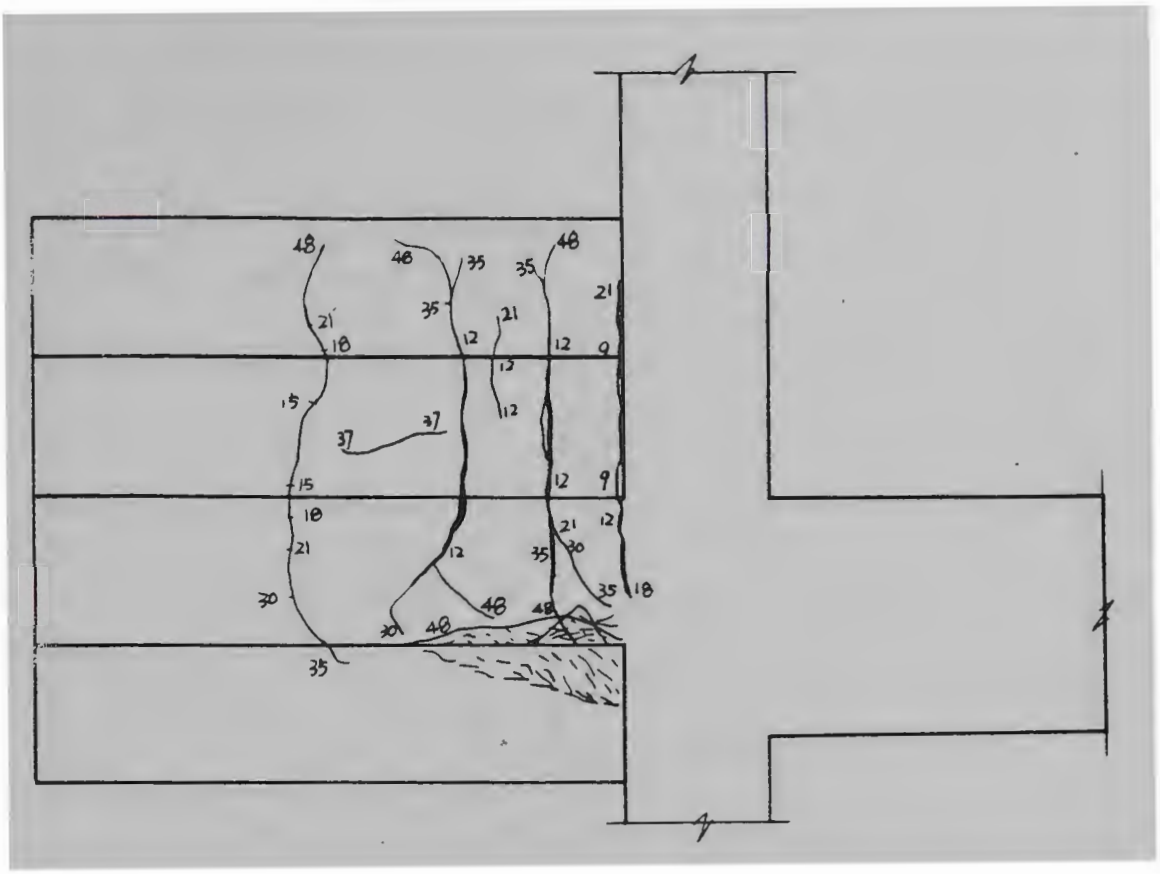

Fig. 4.2.3 Crack Pattern for Specimen SPA1

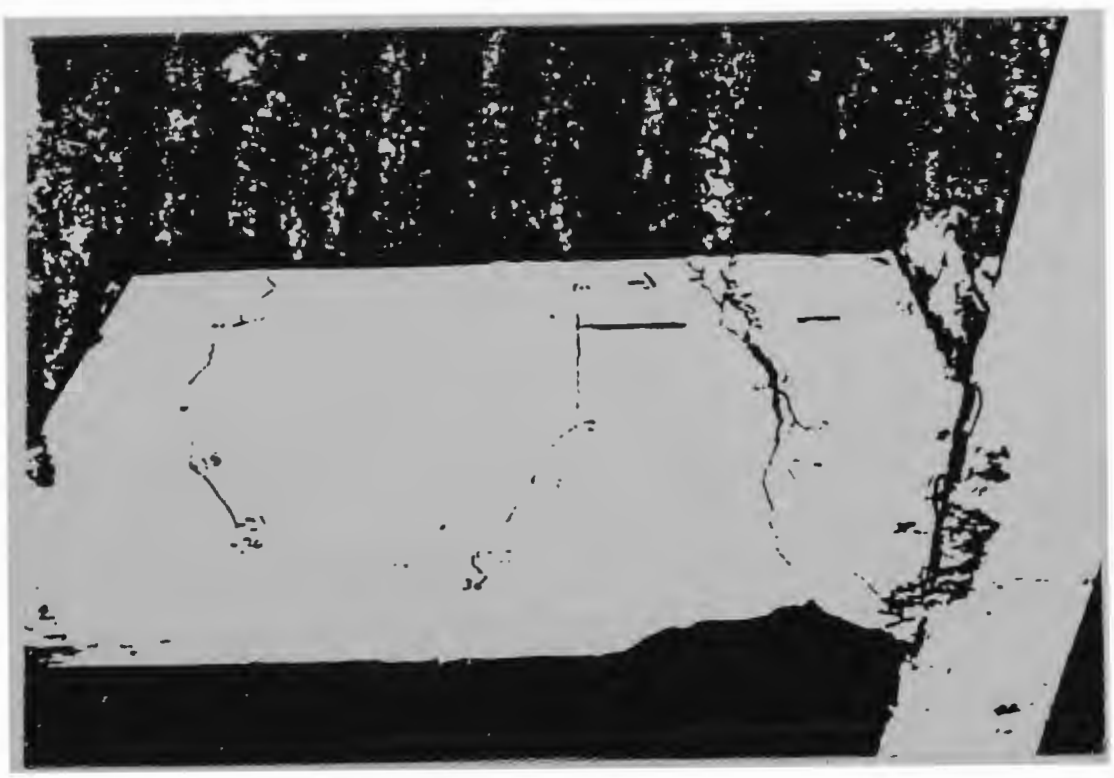

Plate 4.2.2 Crack Pattern for Specimen SPA1

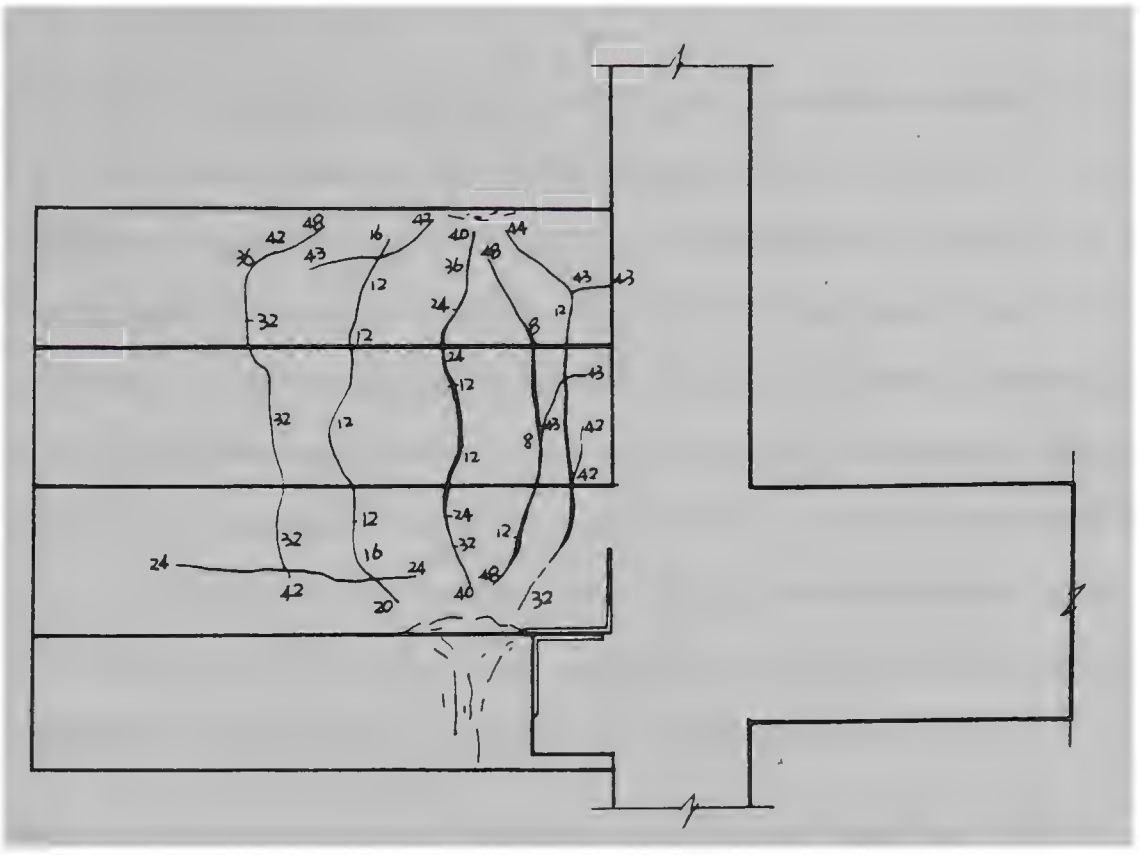

Fig. 4.2.4 Crack Pattern for Specimen SPB1

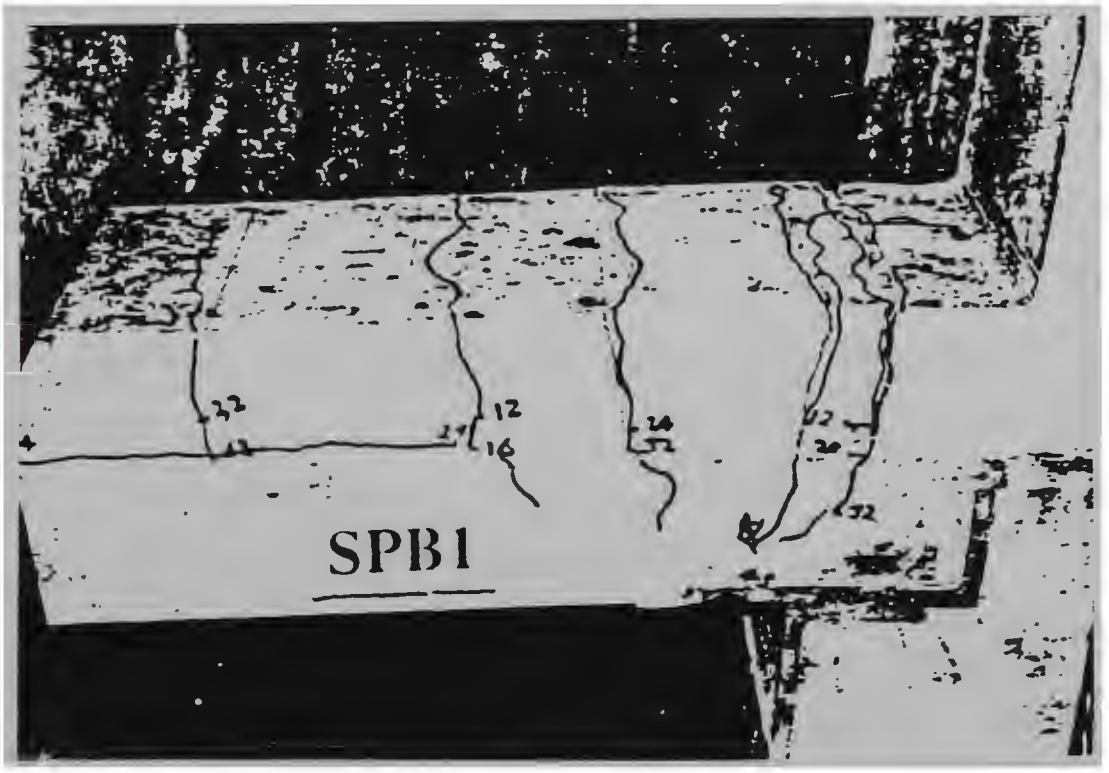

Plate 4.2.3 Crack Pattern for Specimen SPB1

(d) Specimen SM2

SM2 was the monolithic connection with a higher steel ratio compared to SM1. The ultimate load was just the same as the theoretical value, P_u=52 kN. The first crack appeared at the load P_b=10 kN, 20 % of its ultimate load, at the root of the connecting beam. When applied load P_b=20 kN, 40 % of its ultimate load, a second crack appeared. With the increase of the applied loads, more cracks appeared and were well distributed along the tension zone of the concrete. At around the ultimate load stage, there was a great deal of " random " cracking on the top surface of the beam and energy seemed to be dissipated well. The specimen was observed to fail in tension with the principal failure crack occurring at the root of connecting beam accompanied by some spalling of the concrete at bottom of the beam root.

The crack pattern of specimen SM2 is shown in Plate 4.2.4 and Fig. 4.2.5.

(e) Specimen SPA2

SPA2 was the Type A precast connection with 3Y16 as tension bars. The specimen had a 12 % higher load carrying capacity compared to its theoretical value. The first crack appeared at the face of column when the applied load reached 15 % of its ultimate load. When the applied load reached 31.3 % of its ultimate load, a second crack appeared. Like specimen SPA1, this second crack grew rapidly and continued till it reached the bottom of the beam. This became the second principal crack. The mode of failure was identical to that of specimen SPA1 with two principal failure cracks occurring at the connecting beam near the root of the cantilever. This was accompanied by spalling of the concrete at bottom of the beam.

The crack pattern of specimen SPA2 is presented in Plate 4.2.5 and Fig. 4.2.6.

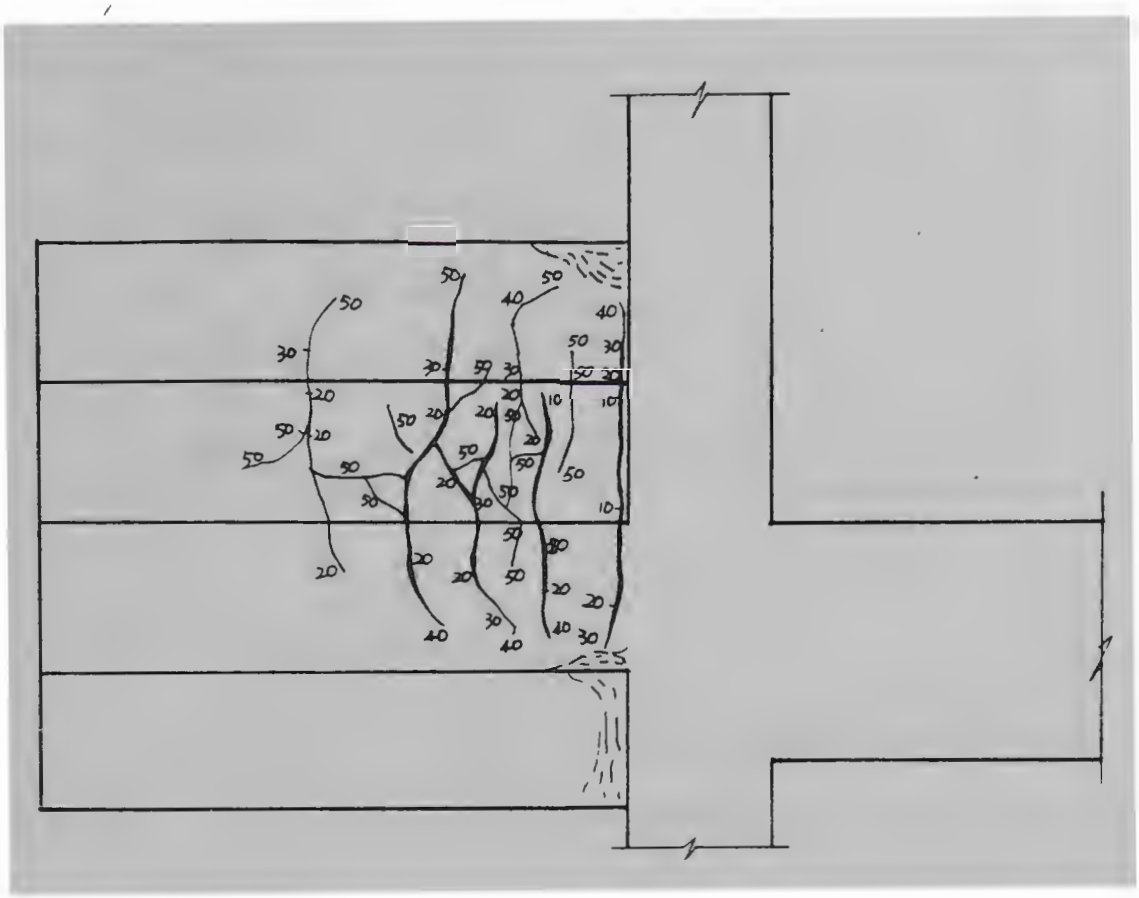

Fig. 4.2.5 Crack Pattern for Specimen SM2

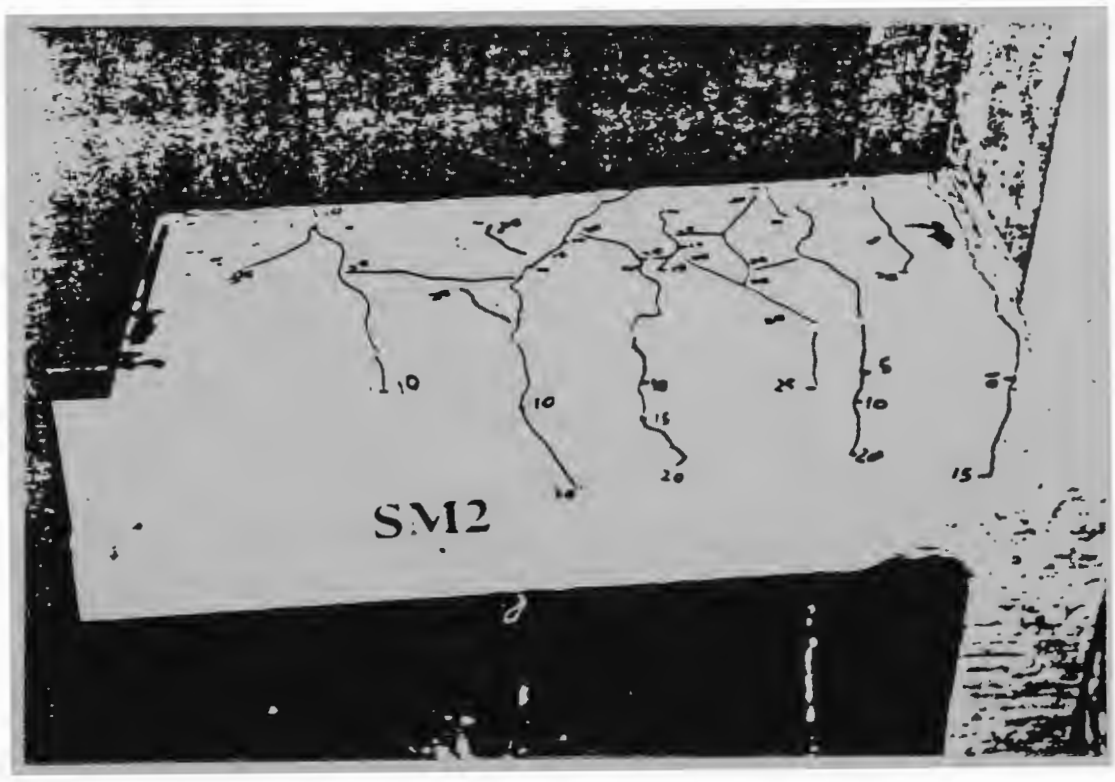

Plate 4.2.4 Crack Pattern for Specimen SM2

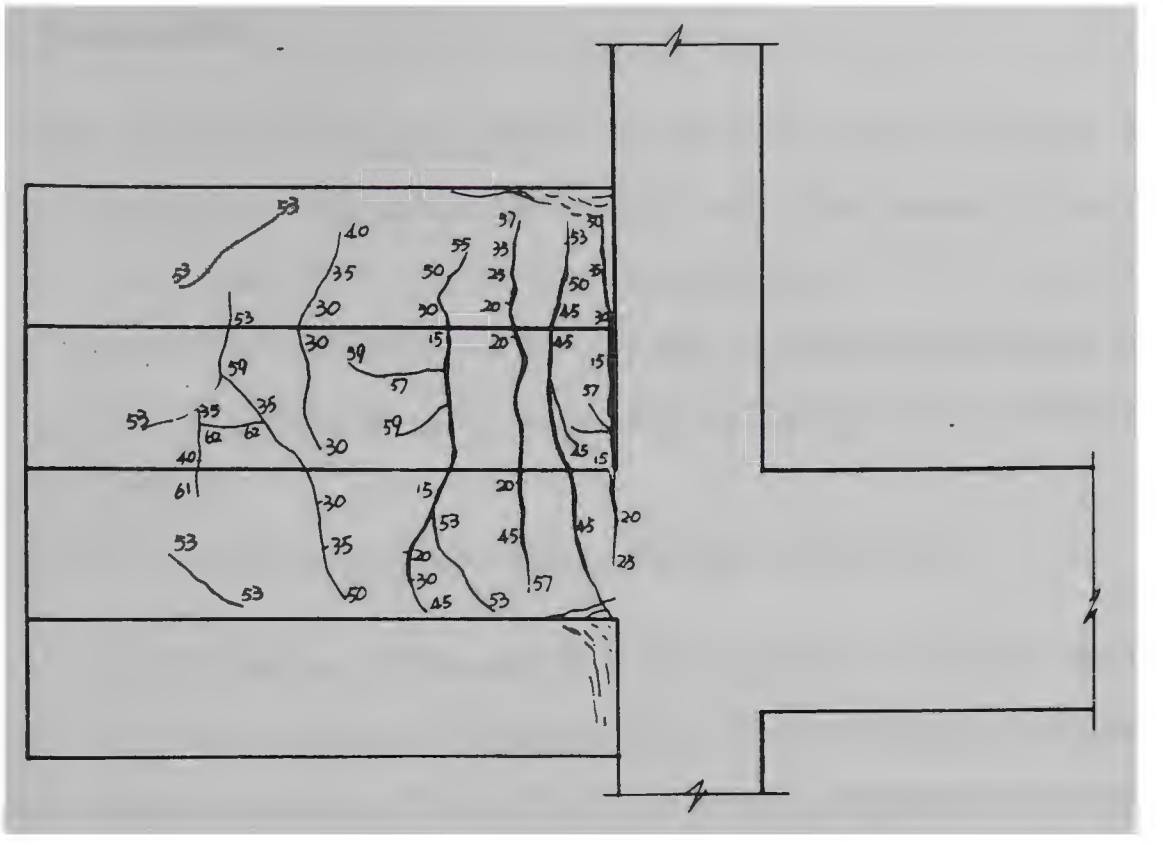

Fig. 4.2.6 Crack Pattern for Specimen SPA2

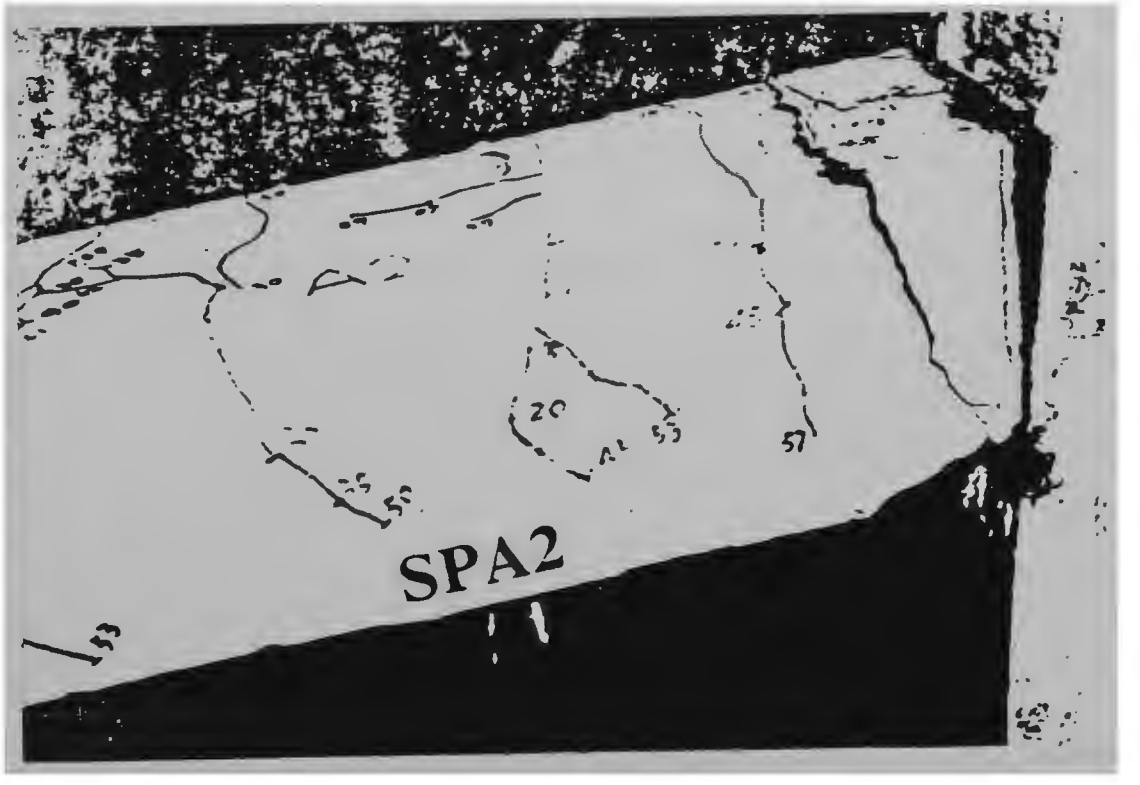

Plate 4.2.5. Crack Pattern for Specimen SPA2

(f) Specimen SPB2

SPB2 was the second Type B precast connection with a higher steel ratio. The ultimate load was 14 % higher than the theoretical value. The first crack appeared at 22.7 % of the ultimate load while a second crack appeared at 30 % of the ultimate load. The second crack developed in the early stages of loading and continued to be the principal crack as the first crack. The specimen experienced a tension failure like specimen SPB1.

The crack pattern of SPB2 is presented in Plate 4.2.6 and Fig 4.2.7.

For easy comparison, all the crack patterns are presented in the same diagram shown in Fig. 4.2.8. The loads corresponding to the first and the second cracks for each specimen are given in Table 4.2.4. The diagram indicates that the crack development and crack pattens at failure are all largely identical. Table 4.2.4 indicates that the first cracking load of the precast models are all larger than their monolithic counterparts, but the second cracking load was smaller than those of the monolithic models. However, the tests still indicate that these two types of precast concrete beam-column connections are considered to have adequate strength, rigidity and ductility.

Table 4.2.4 load value of first & second cracking for specimens tested under static loading

specimen	first crack load P_1 (kN)	P_1/P_u (%)	second crack load P_2 (kN)	P_2/P_u (%)
SM1	6	15.4	15	38.5
SPA1	9	18.0	12	24.5
SPB1	8	15.4	12	23.1
SM2	10	20.0	20	40.0
SPA2	15	23.4	20	31.3
SPB2	15	22.7	20	30.0

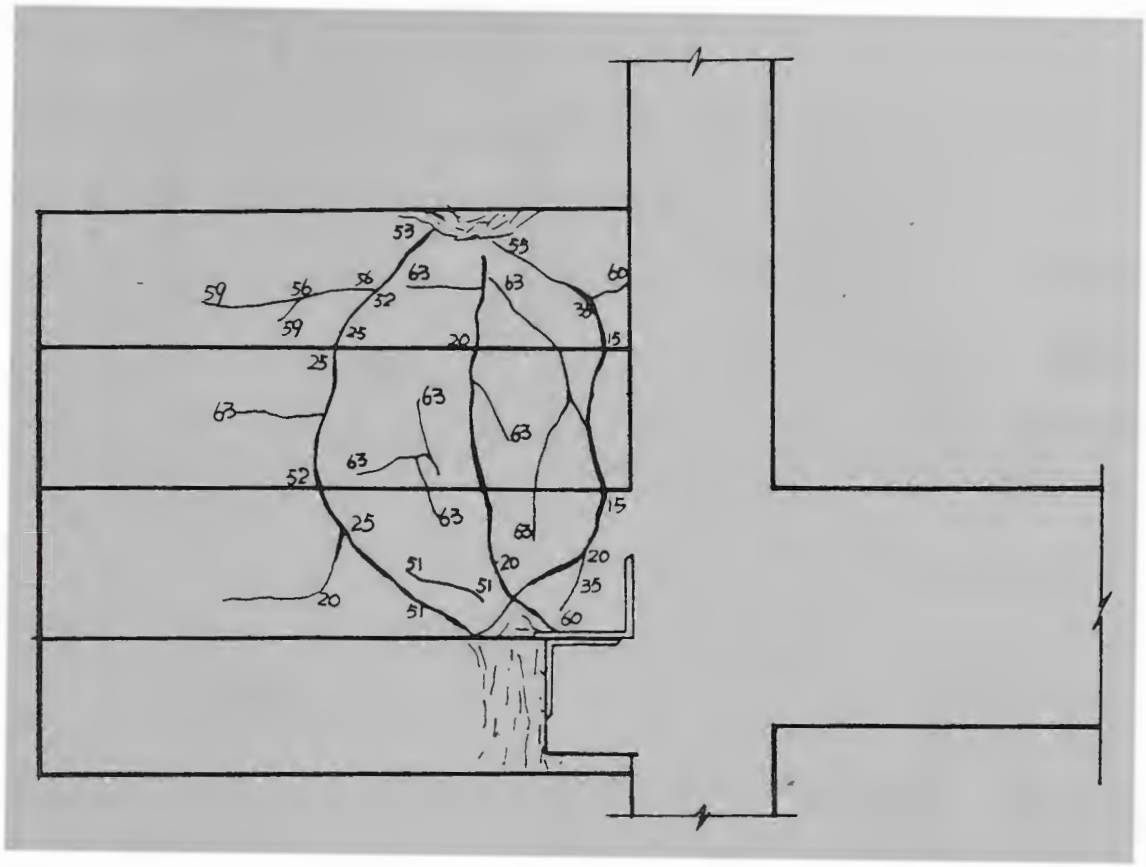

Fig. 4.2.7 Crack Pattern for Specimen SPB2

Plate 4.2.6 Crack Pattern for Specimen SPB2

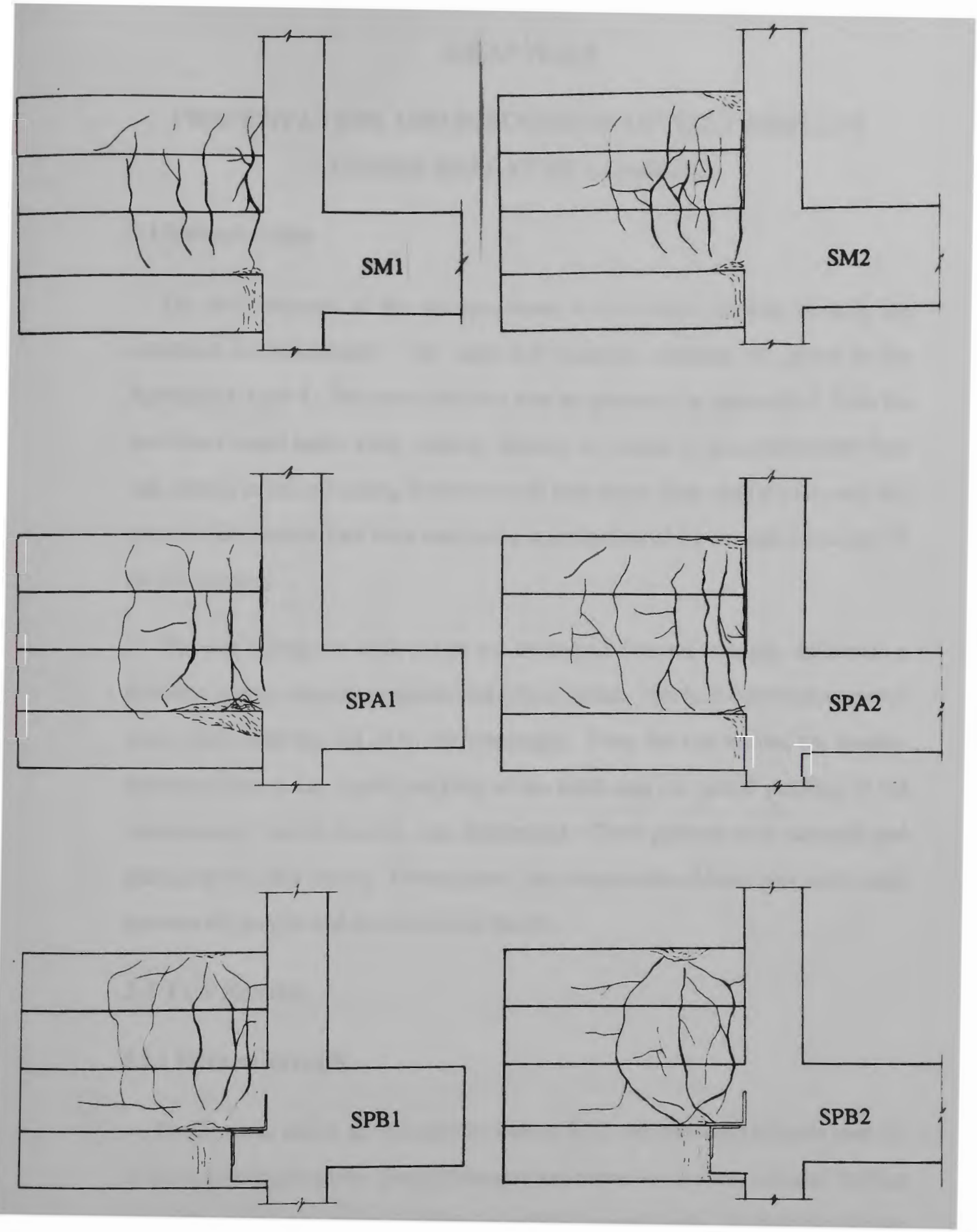

Fig. 4.2.8 Crack Pattern for All Specimen Tested Under Static Loading

CHAPTER 5

PRESENTATION AND DISCUSSION OF TEST RESULTS UNDER REPEATED LOADING

5.1 Introduction

The performances of the six specimens tested under repeated loading are discussed in this chapter. The steel and concrete strengths are given in the Appendices 3 and 4. The normalised test data are presented in Appendix 2. Like the specimens tested under static loading, because the strains in the compression bars and stirrups in the connecting beams were all well below their yield strains, only the strains of the tension bars were used in the investigation of the strength behaviour of the connections.

The test results are analysed in the context of flexural strength, deformation ductility, energy absorbing capacity and failure modes. The load-deformation curves were drawn with the aid of an HP datalogger. From the test results, the loading corresponding to the initial cracking of the beam and the initial yielding of the reinforcement bars in tension were determined. Crack patterns were sketched and photographed after testing. Further more, the comparisons of behaviour were made between the precast and the monolithic models.

5.2 Test Results

5.2.1 Flexural strength

For the same reason as discussed in Section 4.2.1, the measured ultimate load, P_u of the connecting beam for precast concrete specimens tested under repeated loading were all greater than those for their monolithic counterparts. In order to further study the load carrying capacity, the theoretical maximum load P_{max} for each

specimen was calculated based on an ultimate concrete strain of 0.003, and the actual steel and concrete properties .

(a) Specimen SM1

b = 175 mm, d = 170 - 33 = 137 mm, d'= 31 mm,

A_{st} = 2Y16 = 400 mm^2, f_{sy} = 440 MPa,

A_{sc} = 2R10 = 160 mm^2, f_{sy}' = 371.5 MPa,

f_c' = 37 MPa,

$$P_t = \frac{400}{175x137} = 0.016684$$

$$P_c' = \frac{160x\frac{371.5}{440}}{175x139} = \frac{135}{175x139} = 5.55358x10^{-3}$$

Eq. 3.2 (2) v = 0.85 - 0.007 x (37 - 28) = 0.787

Eq. 3.3 (5) $$P_B = \frac{0.85f_c' vK_u B}{f_{sy}} = \frac{0.85x37x0.787x\frac{600}{600+440}}{440} = 0.032$$

$$\frac{3}{4}P_B = \frac{3}{4}x0.032 = 0.024$$

But $P_t - P_c' = 0.016684 - 5.55358 \times 10^{-3} = 0.011$

So $P_t - P_c' < \frac{3}{4}P_B$ (under-reinforced, tension failure)

Eq. 3.5 (3) $$(P_t - P_c')_{limit} = \frac{510x0.787x37x\frac{31}{137}}{(600-440)x440} = 0.0477$$

$P_t - P_c' = 0.011 < (P_t - P_c')_{limit}$

So A_{sc} would not yield at failure.

Eq. 3.5 (12) $$\eta = \frac{0.016684x440 - 600x5.55358x10^{-3}}{1.7x0.787x37} = 0.081$$

Eq. 3.5 (13) $$\gamma = \frac{600x5.55358x10^{-3}}{0.85x0.787x37} = 0.1345$$

Eq. 3.5 (11) $$K_u = \eta + \sqrt{\eta^2 + \gamma\frac{d_c}{d}} = 0.081 + \sqrt{0.081^2 + 0.1345x\frac{31}{137}} = 0.273$$

$a = vK_ud = 0.787 \times 0.273 \times 137 = 29.43$

Eq. 3.5 (15)

$$M_{max} = 400x440x(137 - \frac{29.43}{2}) + 600x135x(1 - \frac{31}{0.273x137})x(\frac{29.43}{2} - 31)$$

$$= 21522160 - 225755$$
$$= 21296405Nmm$$

$$P_{max} = \frac{M_u}{L} = \frac{21.2964}{0.5625} = 37.86kN$$

(b) Specimen SPA1

$b = 175$ mm, $d = 170 - 33 = 137$ mm, $d' = 31$ mm,

$A_{st} = 2Y16 = 400$ mm^2, $f_{sy} = 440$ MPa,

$A_{sc} = 2R10 = 160$ mm^2, $f_{sy}' = 371.5$ MPa,

$f_c' = 37$ MPa, $f_c'' = 67$ MPa,

$$P_t = \frac{400}{175x137} = 0.016684$$

$$P_c' = \frac{160x\frac{371.5}{440}}{175x139} = \frac{135}{175x139} = 5.55358x10^{-3}$$

Eq. 3.2 (2) $v = 0.85 - 0.007 \times (67 - 28) = 0.577$

Eq. 3.3 (5) $$P_B = \frac{0.85f_c' vK_u B}{f_{sy}} = \frac{0.85x67x0.577x\frac{600}{600+440}}{440} = 0.043$$

$$\frac{3}{4}P_B = \frac{3}{4}x0.043 = 0.032$$

But $P_t - P_c' = 0.016684 - 5.55358 \times 10^{-3} = 0.011$

So $P_t - P_c' < \frac{3}{4}P_B$ (under-reinforced, tension failure)

Eq. 3.5 (3) $$(P_t - P_c')_{limit} = \frac{510x0.577x67x\frac{31}{137}}{(600-440)x440} = 0.063$$

$P_t - P_c' = 0.011 < (P_t - P_c')_{limit}$

So A_{sc} would not yield at failure.

Eq. 3.5 (12) $$\eta = \frac{0.016684x440 - 600x5.55358x10^{-3}}{1.7x0.577x67} = 0.061$$

Eq. 3.5 (13) $$\gamma = \frac{600x5.55358x10^{-3}}{0.85x0.577x67} = 0.10133$$

Eq. 3.5 (11) $$K_u = \eta + \sqrt{\eta^2 + \gamma\frac{d_c}{d}} = 0.061 + \sqrt{0.061^2 + 0.10133x\frac{31}{137}} = 0.224$$

$a = vK_u d = 0.577 \times 0.224 \times 137 = 17.71$

Eq. 3.5 (15)

$$M_{max} = 400x440x(137 - \frac{17.71}{2}) + 600x135x(1 - \frac{31}{0.224x137})x(\frac{17.71}{2} - 31)$$

$$= 22553520 + 18237$$

$$= 22571757 Nmm$$

$$Pmax = \frac{M_u}{L} = \frac{22.571757}{0.5625} = 40.13kN$$

(c) Specimen SPB1

b = 175 mm, d = 170 - 33 = 137 mm, d'= 31 mm,

A_{st} = 2Y16 = 400 mm^2, f_{sy} = 440 MPa,

A_{sc} = 2R10 = 160 mm^2, f_{sy}' = 371.5 MPa,

f_c' = 37 MPa, f_c'' = 67 MPa,

$$P_t = \frac{400}{175x137} = 0.016684$$

$$P_c' = \frac{160x\frac{371.5}{440}}{175x139} = \frac{135}{175x139} = 5.55358x10^{-3}$$

Eq. 3.2 (2) v = 0.85 - 0.007 x (37 - 28) = 0.787

Eq. 3.3 (5) $$P_B = \frac{0.85f_c' vK_uB}{f_{sy}} = \frac{0.85x37x0.787x\frac{600}{600+440}}{440} = 0.032$$

$$\frac{3}{4}P_B = \frac{3}{4}x0.032 = 0.024$$

But $P_t - P_c' = 0.016684 - 5.55358 \times 10^{-3} = 0.011$

So $P_t - P_c' < \frac{3}{4} P_B$ (under-reinforced, tension failure)

Eq. 3.5 (3) $$(P_t - P_c')_{limit} = \frac{510x0.787x37x\frac{31}{137}}{(600-440)x440} = 0.0477$$

$P_t - P_c' = 0.011 < (P_t - P_c')_{limit}$

So A_{sc} would not yield at failure.

Eq. 3.5 (12) $$\eta = \frac{0.016684x440 - 600x5.55358x10^{-3}}{1.7x0.787x37} = 0.081$$

Eq. 3.5 (13) $$\gamma = \frac{600x5.55358x10^{-3}}{0.85x0.787x37} = 0.1345$$

Eq. 3.5 (11) $$K_u = \eta + \sqrt{\eta^2 + \gamma\frac{d_c}{d}} = 0.081 + \sqrt{0.081^2 + 0.1345x\frac{31}{137}} = 0.273$$

$a = vK_ud = 0.787 \times 0.273 \times 137 = 29.43$

Eq. 3.5 (15)

$$M_{max} = 400x440x(137 - \frac{29.43}{2}) + 600x135x(1 - \frac{31}{0.273x137})x(\frac{29.43}{2} - 31)$$

$$= 21522160 - 225755$$
$$= 21296405Nmm$$

$$P_{max} = \frac{M_u}{L} = \frac{21.2964}{0.5125} = 41.55kN$$

(d) Specimen SM2

b = 175 mm, d = 170 - 33 = 137 mm, d'= 31 mm,

A_{st} = 3Y16 = 600 mm^2, f_{sy} = 440 MPa,

A_{sc} = 2R10 = 160 mm^2, f_{sy}' = 371.5 MPa,

$f_c' = 37$ MPa,

$$P_t = \frac{600}{175x137} = 0.025026$$

$$P_c' = \frac{160x\frac{371.5}{440}}{175x139} = \frac{135}{175x139} = 5.55358x10^{-3}$$

Eq. 3.2 (2) $v = 0.85 - 0.007 \text{ x } (37 - 28) = 0.787$

Eq. 3.3 (5) $$P_B = \frac{0.85f_c' vK_u B}{f_{sy}} = \frac{0.85x37x0.787x\frac{600}{600+440}}{440} = 0.032$$

$$\frac{3}{4}P_B = \frac{3}{4}x0.032 = 0.024$$

But $P_t - P_c' = 0.025026 - 5.55358 \text{ x } 10^{-3} = 0.0195$

So $P_t - P_c' < \frac{3}{4}P_B$ (under-reinforced, tension failure)

Eq. 3.5 (3) $$(P_t - P_c')_{limit} = \frac{510x0.787x37x\frac{31}{137}}{(600-440)x440} = 0.0477$$

$P_t - P_c' = 0.0195 < (P_t - P_c')_{limit}$

So A_{sc} would not yield at failure.

Eq. 3.5 (12) $$\eta = \frac{0.025026x440 - 600x5.55358x10^{-3}}{1.7x0.787x37} = 0.1552$$

Eq. 3.5 (13) $$\gamma = \frac{600x5.55358x10^{-3}}{0.85x0.787x37} = 0.1345$$

Eq. 3.5 (11) $$K_u = \eta + \sqrt{\eta^2 + \gamma\frac{d_c}{d}} = 0.1552 + \sqrt{0.1552^2 + 0.1345x\frac{31}{137}} = 0.3887$$

$a = vK_u d = 0.3887 \times 0.787 \times 137 = 41.91$

Eq. 3.5 (15)

$$M_{max} = 600x440x(137 - \frac{41.91}{2}) + 600x135x(1 - \frac{31}{0.3887x137})x(\frac{41.97}{2} - 31)$$

$$= 30635880 - 339991$$

$$= 30295889 Nmm$$

$$P_{max} = \frac{M_u}{L} = \frac{30.296}{0.5625} = 53.86 kN$$

(e) Specimen SPA2

b = 175 mm, d = 170 - 33 = 137 mm, d'= 31 mm,

A_{st} = 3Y16 = 600 mm^2, f_{sy} = 440 MPa,

A_{sc} = 2R10 = 160 mm^2, f_{sy}' = 371.5 MPa,

f_c' = 37 MPa, f_c'' = 67 MPa,

$$P_t = \frac{600}{175x137} = 0.025026$$

$$P_c' = \frac{160x\frac{371.5}{440}}{175x139} = \frac{135}{175x139} = 5.55358x10^{-3}$$

Eq. 3.2 (2) $v = 0.85 - 0.007 \times (67 - 28) = 0.577$

Eq. 3.3 (5) $$P_B = \frac{0.85f_c' vK_u B}{f_{sy}} = \frac{0.85x67x0.577x\frac{600}{600+440}}{440} = 0.043$$

$$\frac{3}{4}P_B = \frac{3}{4}x0.043 = 0.032$$

But $P_t - P_c' = 0.025026 - 5.55358 \times 10^{-3} = 0.0195$

So $P_t - P_c' < \frac{3}{4} P_B$ (under-reinforced, tension failure)

Eq. 3.5 (3) $$(P_t - P_c')_{limit} = \frac{510x0.577x67x\frac{31}{137}}{(600-440)x440} = 0.063$$

$P_t - P_c' = 0.0195 < (P_t - P_c')_{limit}$

So A_{sc} would not yield at failure.

Eq. 3.5 (12) $$\eta = \frac{0.025026x440 - 600x5.55358x10^{-3}}{1.7x0.577x67} = 0.1169$$

Eq. 3.5 (13) $$\gamma = \frac{600x5.55358x10^{-3}}{0.85x0.577x67} = 0.10133$$

Eq. 3.5 (11) $$K_u = \eta + \sqrt{\eta^2 + \gamma\frac{d_c}{d}} = 0.1169 + \sqrt{0.1169^2 + 0.10133x\frac{31}{137}} = 0.308$$

$a = vK_ud = 0.308x\ 0.577\ x\ 137 = 24.35$

Eq. 3.5 (15)

$$M_{max} = 600x440x(137 - \frac{24.35}{2}) + 600x135x(1 - \frac{31}{0.308x137})x(\frac{24.35}{2} - 31)$$

$$= 32953800 - 404587$$
$$= 32549213Nmm$$

$$P_{max} = \frac{M_u}{L} = \frac{32.55}{0.5625} = 57.86kN$$

(f) Specimen SPB2

b = 175 mm, d = 170 - 33 = 137 mm, d'= 31 mm,

A_{st} = 3Y16 = 600 mm^2, f_{sy} = 440 MPa,

A_{sc} = 2R10 = 160 mm^2, f_{sy}' = 371.5 MPa,

f_c' = 37 MPa, f_c'' = 67 MPa,

$$P_t = \frac{600}{175x137} = 0.025026$$

$$P_c' = \frac{160x\frac{371.5}{440}}{175x139} = \frac{135}{175x139} = 5.55358x10^{-3}$$

Eq. 3.2 (2) $v = 0.85 - 0.007 \times (37 - 28) = 0.787$

Eq. 3.3 (5) $$P_B = \frac{0.85f_c' vK_uB}{f_{sy}} = \frac{0.85x37x0.787x\frac{600}{600+440}}{440} = 0.032$$

$$\frac{3}{4}P_B = \frac{3}{4}x0.032 = 0.024$$

But $P_t - P_c' = 0.025026 - 5.55358 \times 10^{-3} = 0.0195$

So $P_t - P_c' < \frac{3}{4}P_B$ (under-reinforced, tension failure)

Eq. 3.5 (3) $$(P_t - P_c')_{limit} = \frac{510x0.787x37x\frac{31}{137}}{(600-440)x440} = 0.0477$$

$P_t - P_c' = 0.0195 < (P_t - P_c')_{limit}$

So A_{sc} would not yield at failure.

Eq. 3.5 (12) $$\eta = \frac{0.025026x440 - 600x5.55358x10^{-3}}{1.7x0.787x37} = 0.1552$$

Eq. 3.5 (13) $$\gamma = \frac{600x5.55358x10^{-3}}{0.85x0.787x37} = 0.1345$$

Eq. 3.5 (11) $$K_u = \eta + \sqrt{\eta^2 + \gamma \frac{d_c}{d}} = 0.1552 + \sqrt{0.1552^2 + 0.1345x\frac{31}{137}} = 0.3887$$

$$a = vK_ud = 0.3887 \times 0.787 \times 137 = 41.91$$

Eq. 3.5 (15)

$$M_{max} = 600x440x(137 - \frac{41.91}{2}) + 600x135x(1 - \frac{31}{0.3887x137})x(\frac{41.97}{2} - 31)$$

$$= 30635880 - 339991$$

$$= 30295889Nmm$$

$$Pmax = \frac{M_u}{L} = \frac{30.296}{0.5125} = 59.114kN$$

The calculated and measured ultimate loads of the connecting beams are presented in Table 5.2.1.

Upon looking at the results of comparison in Table 5.2.1, it is clear that the ratios of the ultimate load to the theoretical maximum load for precast models are all larger than those for the corresponding monolithic models. This means that the precast models are stronger than their monolithic counterparts.

Reinforced concrete moment resisting frame-structures situated in areas of earthquake activity must be capable of having large deformation ductility without degradation of the load carrying capacity. In order to study the change of load carrying capacity throughout the test, two load carrying capacity factors, v_1 and v_2, were introduced. Factor v_1 is defined as the ratio of the maximum load applied to the specimen at each cycle, to the maximum load applied to the specimen at the first yield cycle. Factor v_2 is defined as the ratio of the maximum load applied to the specimen at each cycle, to the theoretical maximum load P_{max} throughout the test. The larger the values of v_1 and v_2, the lesser is the degradation of load-carrying capacity. The values of v_1 and v_2 for all specimens at different cycles are given in

Table 5.2.2 and Table 5.2.3, respectively. Because the deflection at each cycle for specimen SM1 was controlled by relative deflection considering the residual deflection, the absolute deflection at the second cycle was $1.3\Delta_y$, and those at third and fourth cycles were $2.6\Delta_y$ and $3.4\ \Delta_y$ respectively. In order to compare these specimens at the same conditions, normalised values of v_1 and v_2 are calculated. These are presented as the bracketed figures in Table 5.2.2 and Table 5.2.3 . They are chosen at deflection ductility of 1, 2, 3 respectively.

Table 5.2.2 and Table 5.2.3 show that the precast specimens experienced more cycles than their monolithic counterparts. The values of v_1 and v_2 for the precast specimens are all generally larger than those of monolithic specimens. This mean that the precast specimens experienced no more degradation in load carrying capacity than the monolithic models. This further indicates that these two types of precast reinforced concrete beam-column connections are stronger or at least have the same strength as their monolithic counterparts, when subjected to moderate earthquake type loading.

Table 5.2.1 Load capacity of specimens tested under repeated loading

Name of Specimen	*Compressive strength of concrete (MPa)	Calculated ultimate load P_{max} (kN)	measured ultimate load P_u (kN)	P_u / P_{max}
RM1	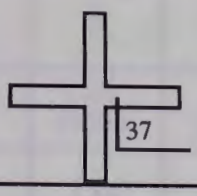	37.9	41	1.08
RPA1	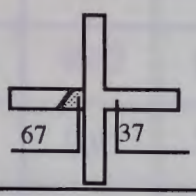	40.1	47	1.18
RPB1	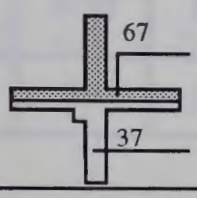	41.6	48	1.15
RM2	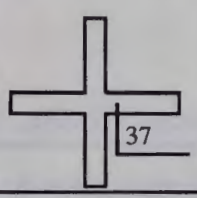	53.86	59	1.10
RPA2	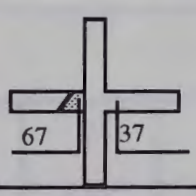	57.9	68	1.18
RPB2	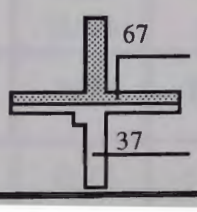	59.1	70	1.18

* Represents strengths obtained from cylinders at the time of specimen tested

Table 5.2.2 Load capacity factor v_1 for specimens tested under repeated loading

Ratio of maximum load at each cycle to that of first yield cycle								
Name of Model	cycle No.							
	1	2	3	4	5	6	7	8
RM1	1	1.23 (0.91)	1.60 (1.40)	1.64 (1.62)	1.64			
RPA1	1	1.00	1.40	1.40	1.56	1.33	1.45	
RPB1	1	0.62	1.84	1.76	1.88	1.84	1.92	
RM2	1	0.97	1.48	1.35	1.46	1.23		
RPA2	1	0.99	1.44	1.29	1.40	1.47	1.51	
RPB2	1	0.97	1.59	1.18	1.59	1.45	1.43	1.39

Table 5.2.3 Load capacity factor v_2 for specimens tested under repeated loading

Ratio of maximum load at each cycle to theoretical ultimate load								
Name of Models	cycle No.							
	1	2	3	4	5	6	7	8
RM1	0.66	0.81 (0.60)	1.06 (0.93)	1.09 (1.07)	1.08			
RPA1	0.74	0.77	1.05	1.06	1.18	1.00	1.09	
RPB1	0.60	0.37	1.11	1.06	1.13	1.11	1.16	
RM2	0.74	0.72	1.10	1.01	1.09	0.91		
RPA2	0.78	0.77	1.12	1.00	1.09	1.14	1.18	
RPB2	0.74	0.72	1.18	0.88	1.18	1.08	1.07	1.03

5.2.2 Deformation ductility

In the event of a moderate earthquake, the structure must survive several cycles of repeated loading without significant strength and stiffness degradation to maintain the integrity of the structure. The capacity of the structure to deform beyond yield or elastic limit with minimum loss of strength and stiffness depends upon the ductility of their members, which is defined as the ratio of the maximum deformation developed in a member to its yield deformation. The deflection ductility is defined as the ratio of the maximum load-point deflection attained at any cycle to the first yield deflection. The deflection ductilities for all the specimens are given in Table 5.2.4. Although the ultimate deflection ductility of RM1 was larger than the precast specimens RPA1 and RPB1, RM1 experienced less cycles than its precast counterparts RPA1 and RPB1. So the comparisons are not on the same basis. Ignoring specimens of RM1, RPA1 and RPB2, and comparing specimens RM2, RPA2 and RPB2, it is clear that both types of precast specimen attain larger ultimate deflection ductility values. They are 5.85 and 6.16 respectively without strength degradation, while RM2 only attained a value of 5.74 but with a 9 % strength degradation compared to its theoretical maximum load (see Table 5.2.3).

Table 5.2.4 Displacement ductilities for specimens tested under repeated loading

Ratio of maximum displacement at each cycle to that of first yield cycle								
Name of Model	cycle No.							
	1	2	3	4	5	6	7	8
RM1	1	1.3	2.6	3.4	7.7			
RPA1	1	1	2	2	3	3	6.32	
RPB1	1	1	2	2	3	3	7.0	
RM2	1	1	2	2	3	5.74		
RPA2	1	1	2	2	3	3	5.85	
RPB2	1	1	2	2	3	3	4	6.16

Some more comparisons are made as follows.

(1) Comparing the specimens RPA1 and RPB1, which survived the seventh loading cycle, RPB1 produced a larger deflection ductility with larger factors of v_1 and v_2. This means that Type B precast connections are more ductile and stronger than Type A.

(2) Comparing the specimens RPA2 and RPB2, RPB2 survived more load cycles with larger ductility factors than RPA2. This also shows that Type B precast connections are stronger in the event of a moderate earthquake.

(3) Comparing the results of the two different steel ratio groups, it is found that the use of higher steel ratios reduces the deflection ductility.

The load-deflection diagrams for each specimen were drawn by the HP datalogger and are shown in Fig. 5.2.1 through 5.2.6.

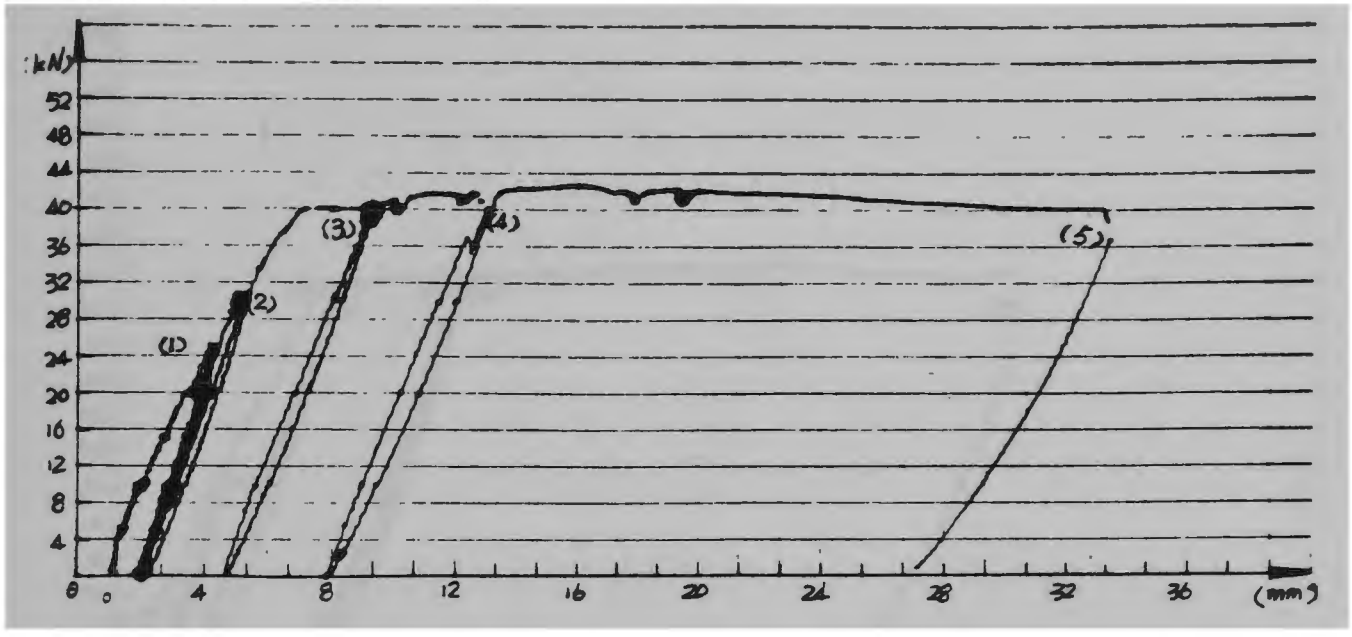

Fig.5.2.1 Load-Deflection Curve for Specimen RM1

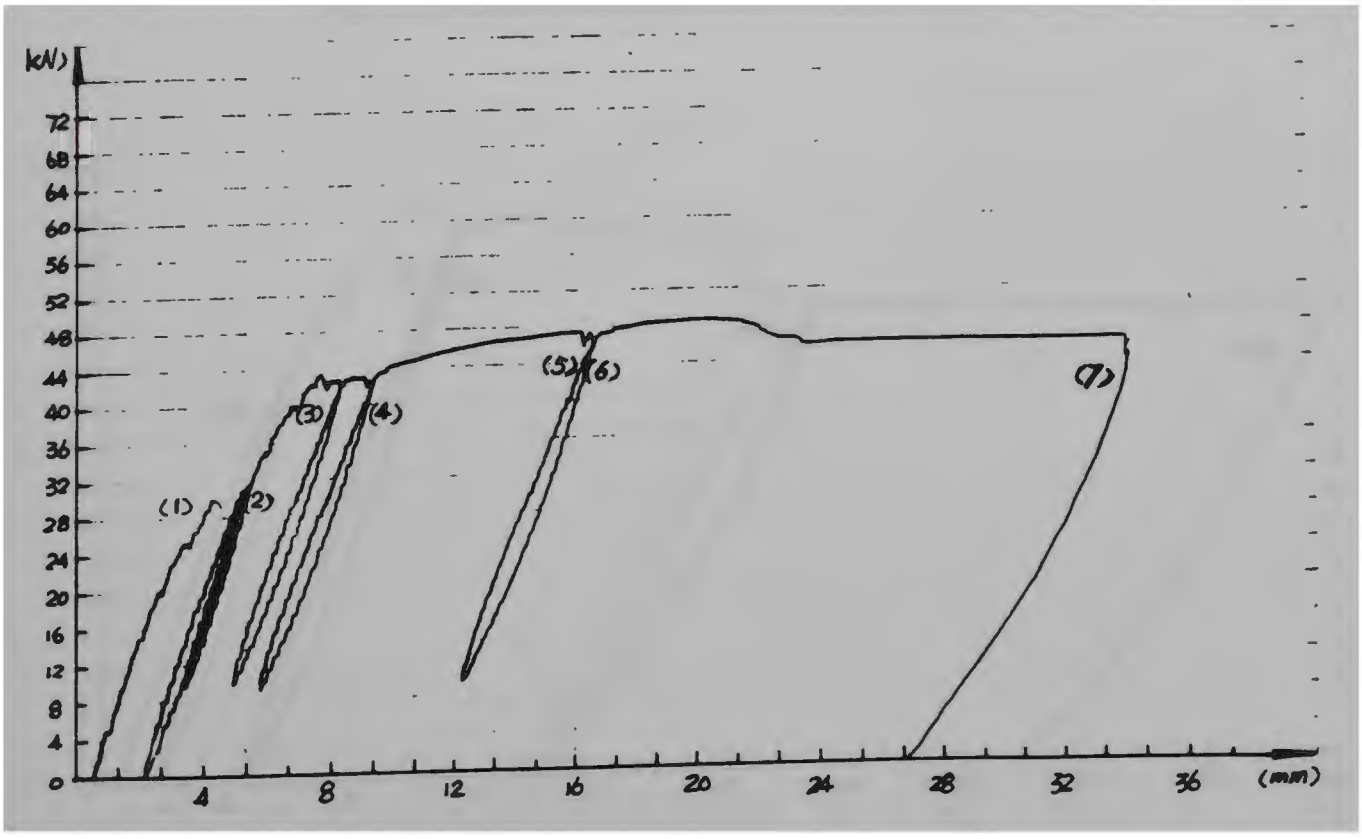

Fig. 5.2.2 Load-Deflection Curve for Specimen RPA1

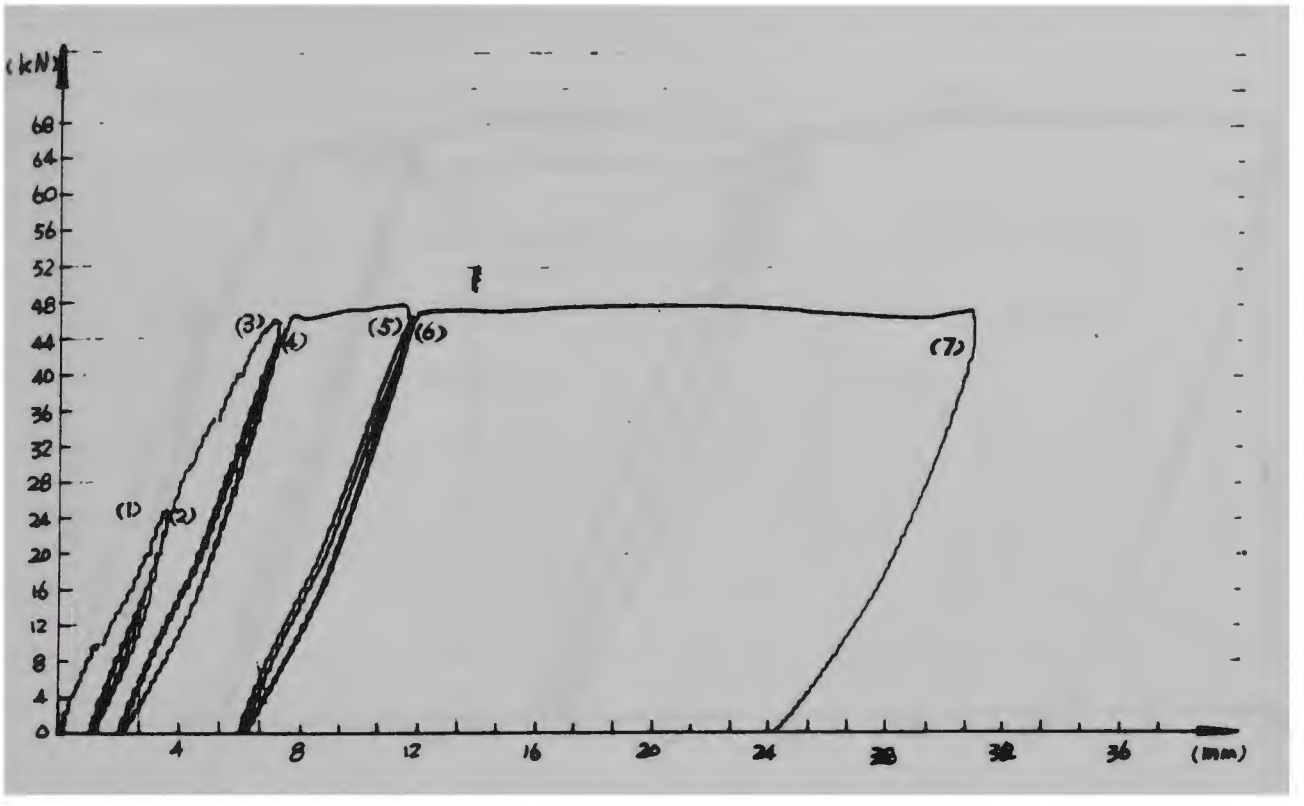

Fig. 5.2.3 Load-Deflection Curve for Specimen RPB1

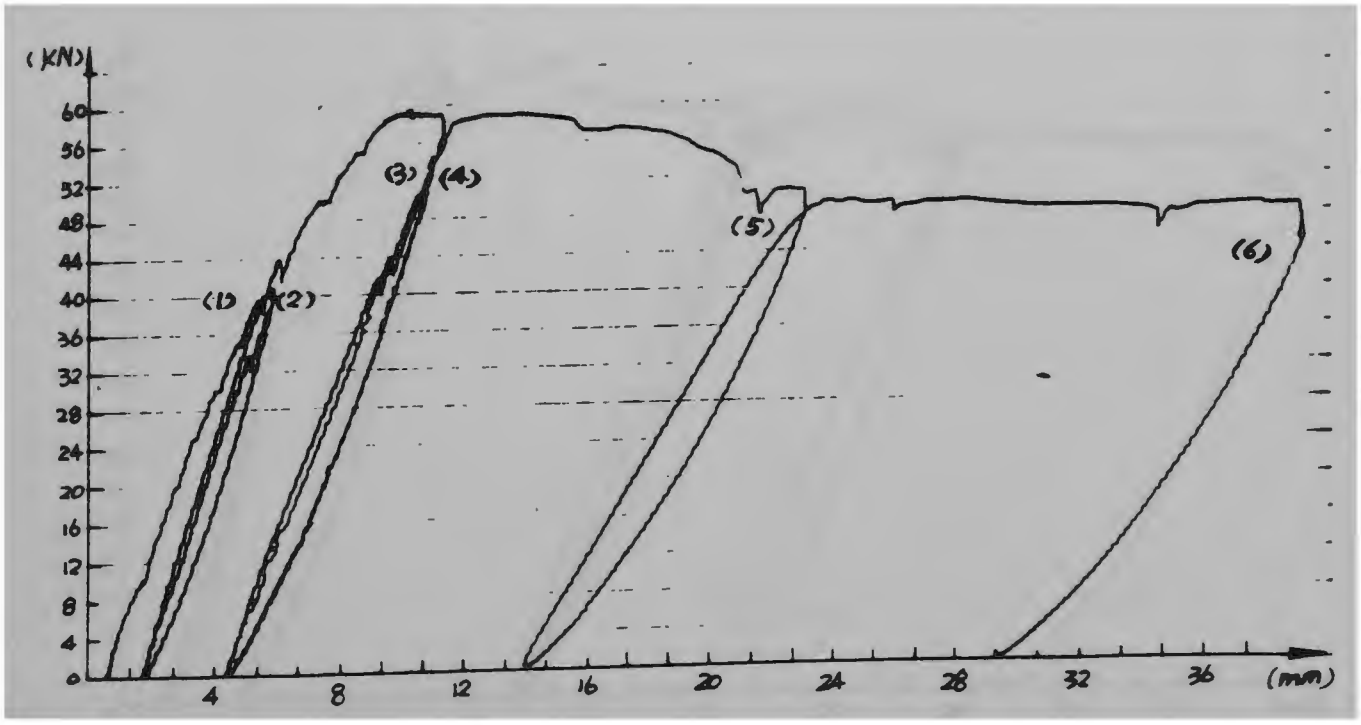

Fig. 5.2.4 Load-Deflection Curve for Specimen RM2

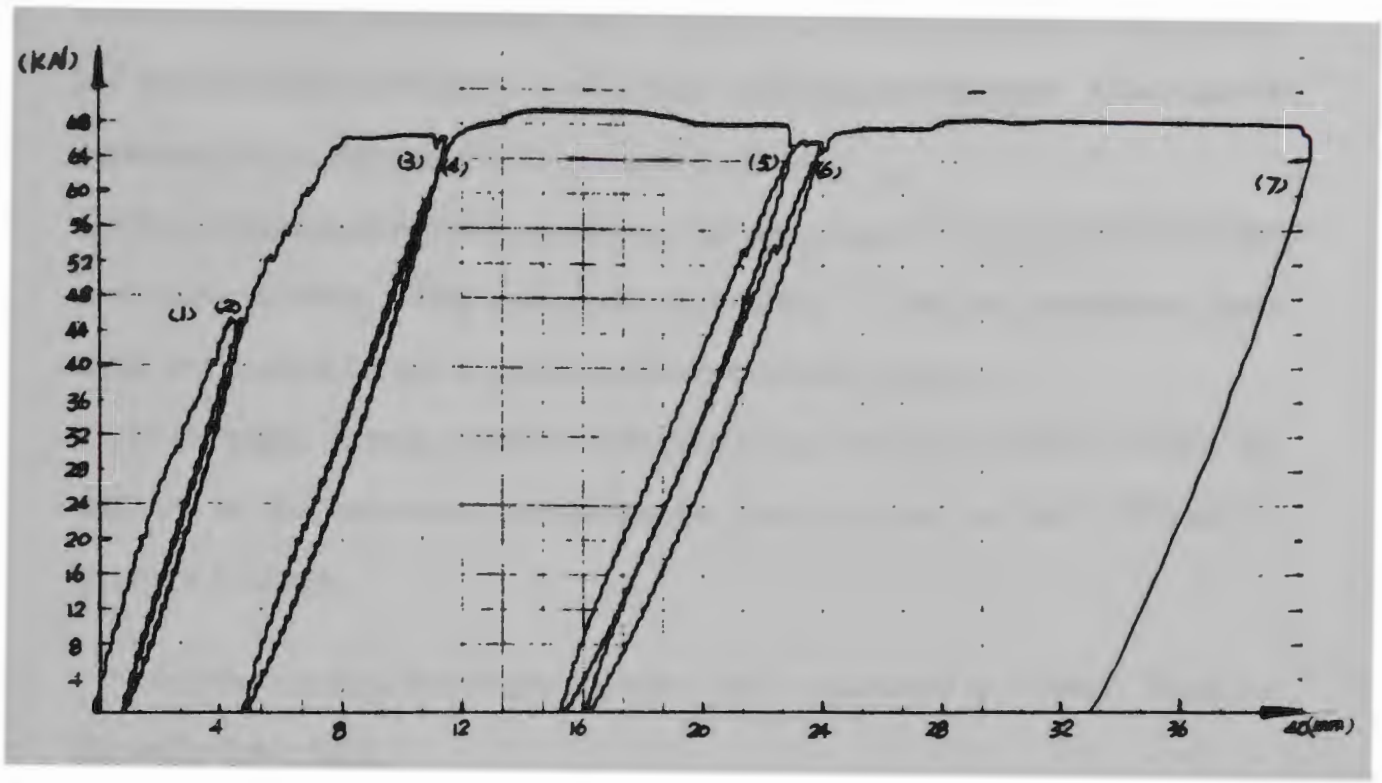

Fig. 5.2.5 Load-Deflection Curve for Specimen RPA2

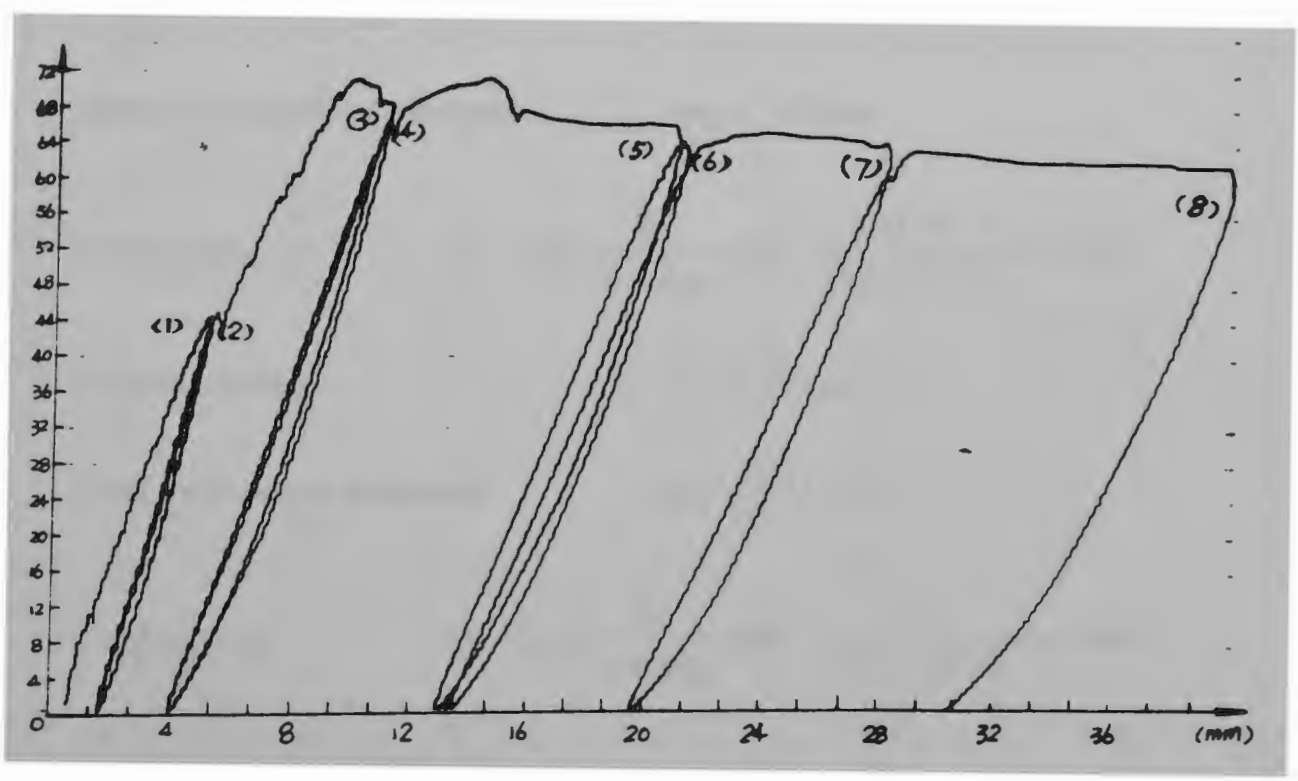

Fig. 5.2.6 Load-Deflection Curve for Specimen RPB2

From these diagrams, more results were obtained as follows:

(1) The load-deflection curves of precast models are very similar to those of the monolithic model. This indicates that both types of precast connections have at least the same load-deflection behaviour as their monolithic counterparts. There was no premature failure occurring in the precast connections.

(2) The ultimate load carrying capacities of all the precast models are higher than the monolithic models. This means that both kinds of precast connections have sufficient strength for use in precast reinforced concrete frames.

(3) Even though there is a residual deflection at the end of each cycle of loading, the stiffness of the connection on subsequent loading is not seriously affected by previous loadings.

From the test data, the rotation ductility can be calculated as follows. These are shown in Table 5.2.6.

(a) Specimen RM1

Ultimate deflection $\Delta_u = 33.70$ mm

Ultimate longitudinal movement $\Delta_{Hu} = 7.67$ mm

Ultimate rotation $$\theta_u = \tan^{-1}\frac{\Delta_u}{L+\Delta_{Hu}} = \tan^{-1}\frac{33.70}{562.5+7.67} = 3.383$$

Yield deflection $\Delta_y = 4.37$ mm

Yield longitudinal movement $\Delta_{Hy} = 0.74$ mm

Yield rotation $$\theta_y = \tan^{-1}\frac{\Delta_y}{L+\Delta_{Hy}} = \tan^{-1}\frac{4.37}{562.5+0.74} = 0.4445$$

Rotation Ductility $= \frac{\theta_u}{\theta_y} = 7.61$

(b) Specimen RPA1

Ultimate deflection $\Delta_u = 34.33$ mm

Ultimate longitudinal movement $\Delta_{Hu} = 8.01$ mm

Ultimate rotation $\theta_u = \tan^{-1}\frac{\Delta_u}{L+\Delta_{Hu}} = \tan^{-1}\frac{34.33}{562.5+8.01} = 3.44$

Yield deflection $\Delta_y = 5.43$ mm

Yield longitudinal movement $\Delta_{Hy} = 1.61$ mm

Yield rotation $\theta_y = \tan^{-1}\frac{\Delta_y}{L+\Delta_{Hy}} = \tan^{-1}\frac{5.43}{562.5+1.61} = 0.551$

Rotation Ductility $= \frac{\theta_u}{\theta_y} = 6.25$

(c) Specimen RPB1

Ultimate deflection $\Delta_u = 30.79$ mm

Ultimate longitudinal movement $\Delta_{Hu} = 9.5$ mm

Ultimate rotation $\theta_u = \tan^{-1}\frac{\Delta_u}{L+\Delta_{Hu}} = \tan^{-1}\frac{30.79}{562.5+9.5} = 3.08$

Yield deflection $\Delta_y = 4.4$ mm

Yield longitudinal movement $\Delta_{Hy} = 1.0$ mm

Yield rotation $\theta_y = \tan^{-1}\frac{\Delta_y}{L+\Delta_{Hy}} = \tan^{-1}\frac{4.4}{562.5+1.0} = 0.447$

Rotation Ductility $= \frac{\theta_u}{\theta_y} = 6.89$

(d) Specimen SM2

Ultimate deflection $\Delta_u = 38.06$ mm

Ultimate longitudinal movement $\Delta_{Hu} = 6.49$ mm

Ultimate rotation $\theta_u = \tan^{-1}\frac{\Delta_u}{L+\Delta_{Hu}} = \tan^{-1}\frac{38.06}{562.5+6.49} = 3.827$

Yield deflection $\Delta_y = 6.63$ mm

Yield longitudinal movement $D_{Hy} = 1.52$ mm

Yield rotation $\theta_y = \tan^{-1}\frac{\Delta_y}{L+\Delta_{Hy}} = \tan^{-1}\frac{6.63}{562.5+1.52} = 0.673$

Rotation Ductility $= \frac{\theta_u}{\theta_y} = 5.69$

(e) Specimen SPA2

Ultimate deflection $\Delta_u = 41.15$ mm

Ultimate longitudinal movement $\Delta_{Hu} = 12.31$ mm

Ultimate rotation $\theta_u = \tan^{-1}\frac{\Delta_u}{L+\Delta_{Hu}} = \tan^{-1}\frac{41.15}{562.5+12.31} = 4.095$

Yield deflection $\Delta_y = 7.04$ mm

Yield longitudinal movement $\Delta_{Hy} = 2.81$ mm

Yield rotation $\theta_y = \tan^{-1}\frac{\Delta_y}{L+\Delta_{Hy}} = \tan^{-1}\frac{7.04}{562.5+2.81} = 0.713$

Rotation Ductility $= \frac{\theta_u}{\theta_y} = 5.74$

(f) Specimen RPB2

Ultimate deflection $\Delta_u = 40.66$ mm

Ultimate longitudinal movement $\Delta_{Hu} = 8.62$ mm

Ultimate rotation $\theta_u = \tan^{-1}\frac{\Delta_u}{L+\Delta_{Hu}} = \tan^{-1}\frac{40.66}{562.5+8.62} = 4.072$

Yield deflection $\Delta_y = 6.60$ mm

Yield longitudinal movement $\Delta_{Hy} = 0.94$ mm

Yield rotation $\theta_y = \tan^{-1}\frac{\Delta_y}{L+\Delta_{Hy}} = \tan^{-1}\frac{6.60}{562.5+0.94} = 0.671$

Rotation Ductility $= \frac{\theta_u}{\theta_y} = 6.07$

5.2.3 Energy dissipation

Perhaps the most important aspect of structural performance under the seismic type of loading is the ability of dissipating energy. The energy-dissipating capacities of beam-column connections are a function of the area under the load-deformation curve and indicate the degree of effectiveness of the connection to withstand earthquake loading. For all the specimens, the energy dissipated in each cycle was

calculated and presented in Table 5.2.5 The energy dissipated per cycle is defined as the area enclosed by the load-deflection plot. When the specimen has yielded, the deflection increases even with a constant load. This means that if the load is not released immediately, there is an increase of energy dissipation. Therefore, the value of energy dissipation in each cycle given in Table 5.2.5 cannot be used for any comparison. But, the values of cumulative energy dissipated is very useful. The larger the values, the more earthquake loading the connection can withstand. The monolithic model RM1 survived only five cycles while its precast counterparts RPA1 and RPB1 survived seven complete cycles. The cumulative energy dissipated by RPA1 and RPB1 was approximately 16 % and 8 % higher than that of RM1 respectively. Similarly, monolithic model RM2 survived six cycles while precast models RPA2 and RPB2 survived seven and eight cycles respectively. RPA2 and RPB2 had 35 % and 21 % higher energy dissipating capacity than that of RM2. This indicates that the precast concrete connections of Type A and Type B have adequate capacity to absorb energy when they withstand moderate earthquake type loading.

All the results of the specimens tested under repeated loading are summarised in Table 5.2.6.

Table 5.2.5 Energy dissipations for specimens tested under repeated loading

Name of Model	Energy dissipation during each cycle								Cumulative energy dissipation (kN-mm)
	Cycle No.								
	1	2	3	4	5	6	7	8	
RM1	45	34	319	389	2045				2832
RPA1	107	25	198	131	751	46	2017		3275
RPB1	48	9	160	26	513	55	2249		3061
RM2	85	51	514	108	1670	2026			4455
RPA2	128	39	781	77	1895	258	2873		6053
RPB2	108	30	561	116	1718	185	1118	1574	5411

Table 5.2.6 Summary of Test Results for specimens tested under repeated loading

Name	F_c' (MPa)	P_y (kN)	P_u (kN)	P_{max} (kN)	$\frac{P_u}{P_{max}}$	Δ_y (mm)	Δ_u (mm)	$\frac{\Delta_u}{\Delta_y}$	θ_y (°)	θ_u (°)	$\frac{\theta_u}{\theta_y}$	energy dissip. (kN-mm)
RM1	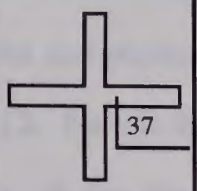	25	41	37.86	1.08	4.37	33.7	7.7	0.44	3.38	7.61	2832
RPA1	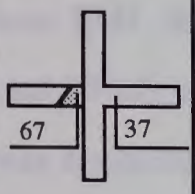	30	47.2	40.13	1.18	5.43	34.33	6.32	0.55	3.44	6.25	3275
RPB1	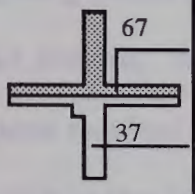	25	48	41.55	1.16	4.4	30.79	7.0	0.45	3.08	6.89	3061
RM2	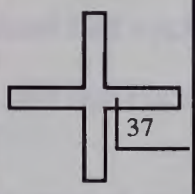	40	59	53.86	1.1	6.63	38.06	5.74	0.67	3.83	5.69	4455
RPA2	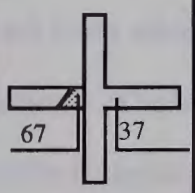	45	68	57.86	1.18	7.04	41.15	5.85	0.71	4.10	5.74	6053
RPB2	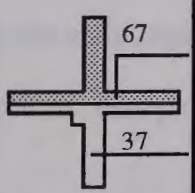	44	70	59.11	1.18	6.6	40.66	6.16	0.67	4.07	6.07	5411

Note: P_y --yield load
P_u-theoretical ultimate load
P_{max}--measured ultimate load
Δ_y--yield deflection
Δ_u--ultimate deflection
θ_y--yield rotation
θ_u--ultimate rotation

5.2.4 Crack behaviour and failure modes of connections

During the test, crack patterns were inspected and marked on the surface of the specimen indicating the corresponding load. After testing, crack patterns were sketched and photographed. These are shown in plates 5.2.1 to 5.2.6 and Fig. 5.2.7 to 5.2.12. For all the specimens, the primary damage during the test occurred in the vicinity of the weakest section. These include the beam-column interface for specimens RM1, RM2 and RPA1, RPA2 or the edge of the corbel for specimens RPB1 and RPB2. All of these damages can be attributed to flexural action. As the beam was displaced downward during the first half cycle of loading, flexural cracks propagating about two-thirds of the depth of the beam were observed first at the weakest section. Additional downward displacement of the beam for most of the specimens resulted in inclined cracks forming at the end of the flexural cracks and continuing to the level of the bottom reinforcement. Unloading of the beam during the second half cycle of loading resulted in the cracks narrowing but at zero load, the cracks still remained open due to yielding of the top reinforcement.

The second and subsequent cycles of loading at the same displacement level produced little additional cracking. Cracks opened and narrowed during repeated load action. The subsequent cycles of loading at the higher displacement level produced a little more cracking and the existing cracks became wider.

All the specimens failed in tension as expected in the design stage. The detailed descriptions, comparison and analyses are given as follows.

(a) Specimen RM1

RM1 was the monolithic connection with a lower steel ratio. The specimen had a 8% higher load carrying capacity compared to its theoretical value. The first crack appeared in the portion of the beam adjacent to the beam-column interface, when the

applied load was P_b = 10 kN, 24 % of its ultimate load. When the applied load P_b reached 37 % of its ultimate load, the second and subsequent cracks appeared. As the beam was displaced downward during the third cycle, some small transverse cracks along the vertical cracks in the beam were observed. At the last cycle, an inclined crack appeared near the beam-column connection. The specimens failed in tension with some spalling of concrete at the bottom of the connecting beam root.

The crack pattern of specimen SM1 is shown in Plate 5.2.1 and Fig. 5.2.7.

(b) Specimen RPA1

RPA1 was the Type A precast connection with a lower steel ratio. The specimen had a 18 % higher load carrying capacity compared to the theoretical value. The first series of cracks appeared in the portion of the beam near the beam-column interface when the applied load (P_b = 15 kN) was 32 % of its ultimate load. When the applied load was, P_b = 25 kN, 53 % of its ultimate load, the second series of cracks appeared approximately parallel to the first series of cracks. The subsequent cycles of loading at the higher displacement level produced no new cracks but made existing cracks become longer and wider. At the last cycle, a small amount of inclined cracks were observed. Tension failure occurred with a principal crack occurring at the beam root. This was accompanied by spalling of concrete at the underside of the beam as deformation became excessive.

The crack pattern of RPA1 is shown in Plate 5.2.2 and Fig. 5.2.8.

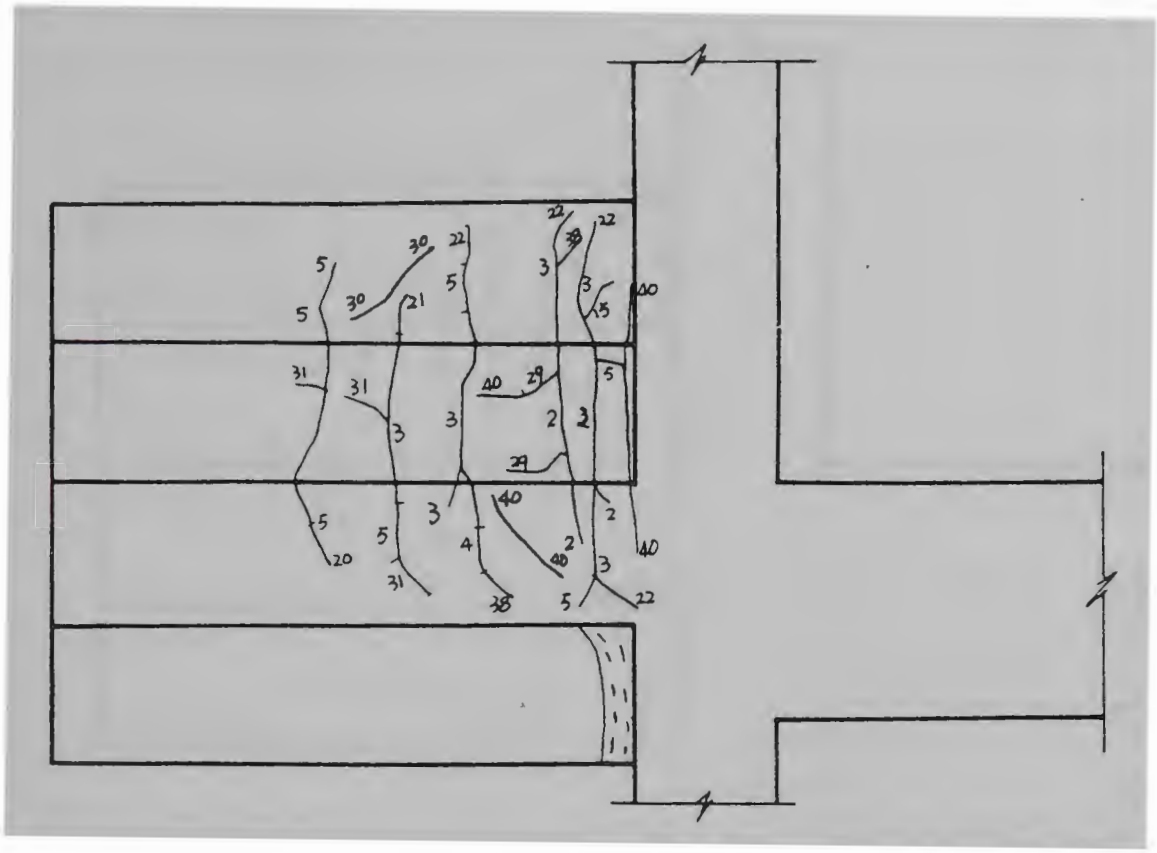

Fig. 5.2.7 Crack Pattern for Specimen RM1

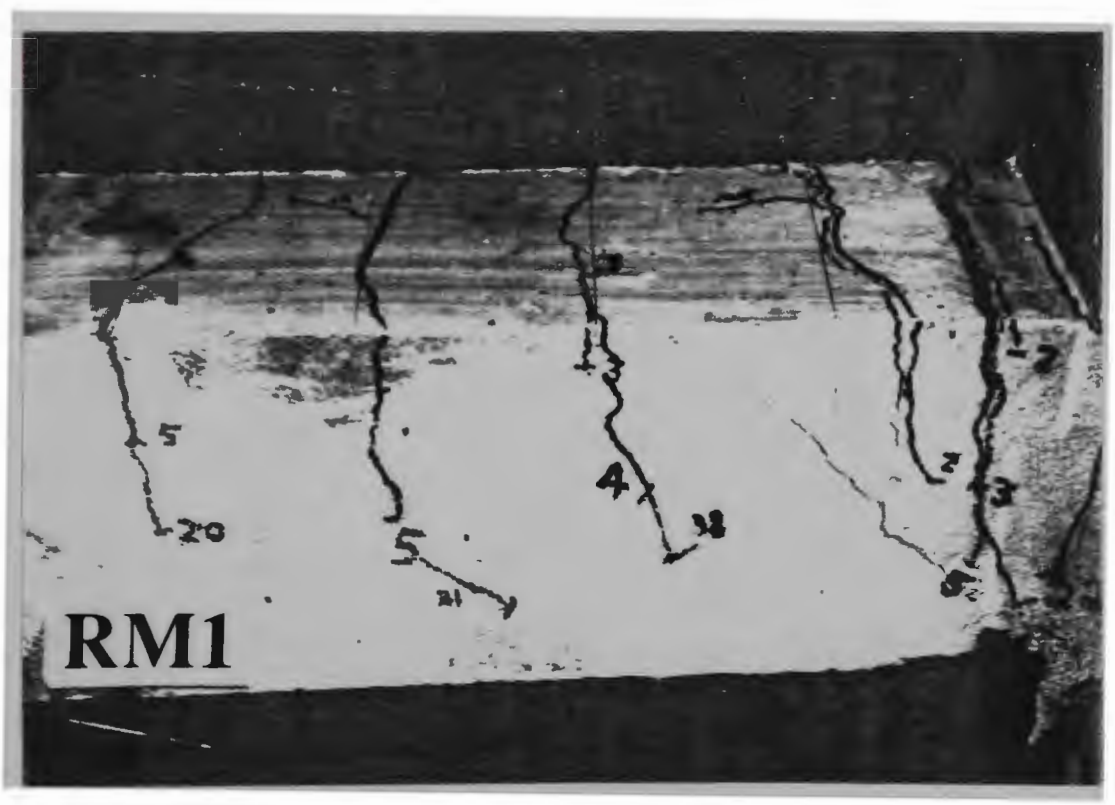

Plate 5.2.1 Crack Pattern for Specimen RM1

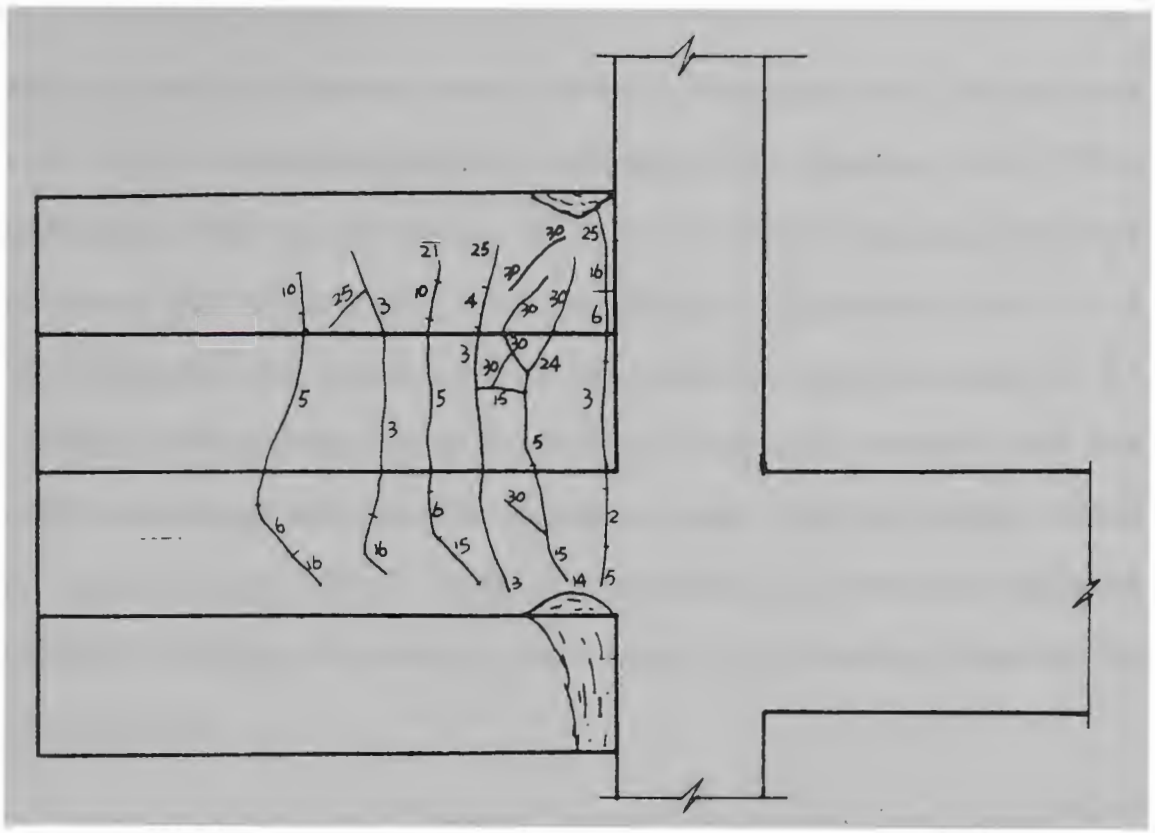

Fig. 5.2.8 Crack Pattern for Specimen RPA1

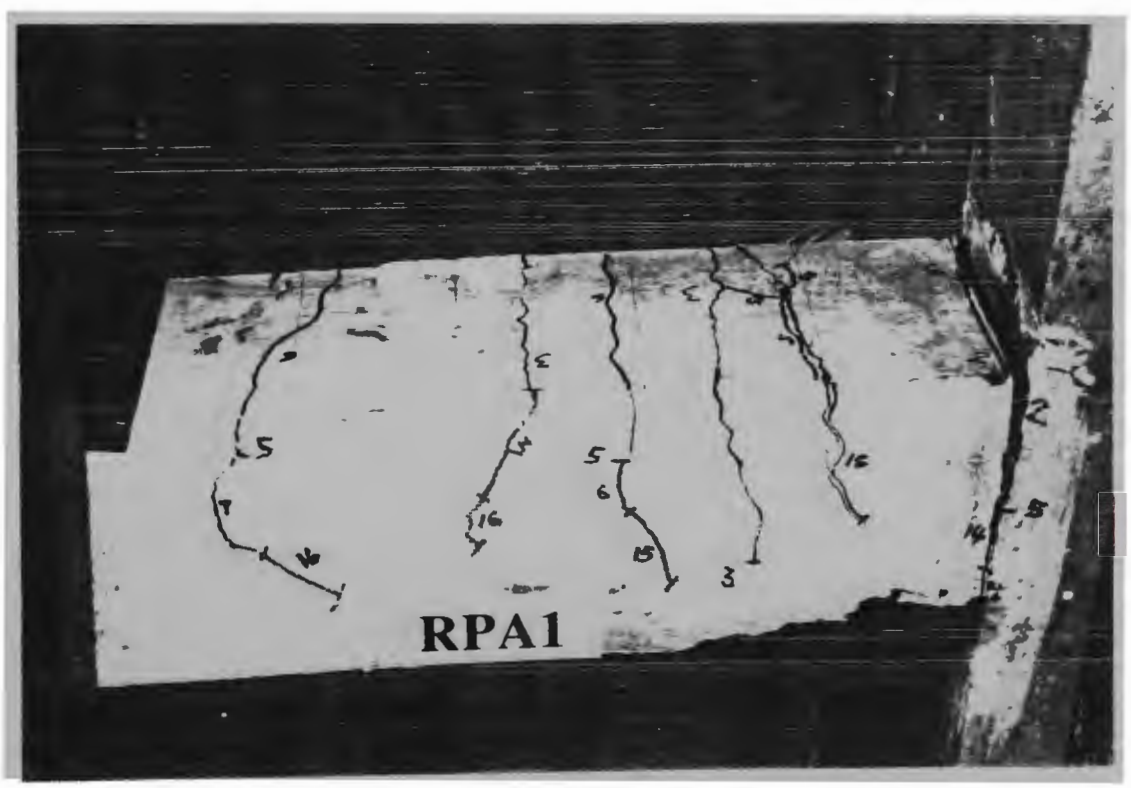

Plate 5.2.2 Crack Pattern for Specimen RPA1

(c) Specimen RPB1

RPB1 was the Type B precast connection with a lower steel ratio. The specimen had a 16 % higher load carrying capacity compared to the theoretical value. When the applied load was P_b = 10 kN, i.e. 20 % of its ultimate load, the first crack appeared at the edge of the corbel. When the applied load P_b reached 20 kN, i.e. 42 % of its ultimate load, the second crack was observed at the root of the beam. At the third cycle of loading at the higher displacement level, a new vertical crack was observed accompanied with some fine transverse cracks along the existing vertical cracks. At the last cycle, tension failure occurred with the crack becoming wider and accompanied by spalling of concrete at the bottom of the connecting beam near the edge of the corbel.

The crack pattern of specimen RPB1 is shown in Plate 5.2.3 and Fig. 5.2.9.

(d) Specimen RM2

RM2 was the monolithic connection with a higher steel ratio. The specimen had a 10 % higher load carrying capacity compared to the theoretical value. The first series of cracks were observed when the applied load was 10 kN, i.e. 17 % of its ultimate load. The second series of cracks appeared when the load reached 20 kN, i.e. 34 % of its ultimate load. At the second and subsequent cycles, some small transverse cracks appeared and some inclined cracks were observed. These inclined cracks grew very rapidly and continued till it reached the bottom of the beam. Tension failure occurred with a principal vertical crack at the end of the beam and a principal inclined crack occurred at last cycle near the beam end. This was accompanied by some spalling of the concrete at the bottom of the connecting beam root.

The crack pattern of specimen RM2 is shown in plate 5.2.4 and Fig. 5.2.10.

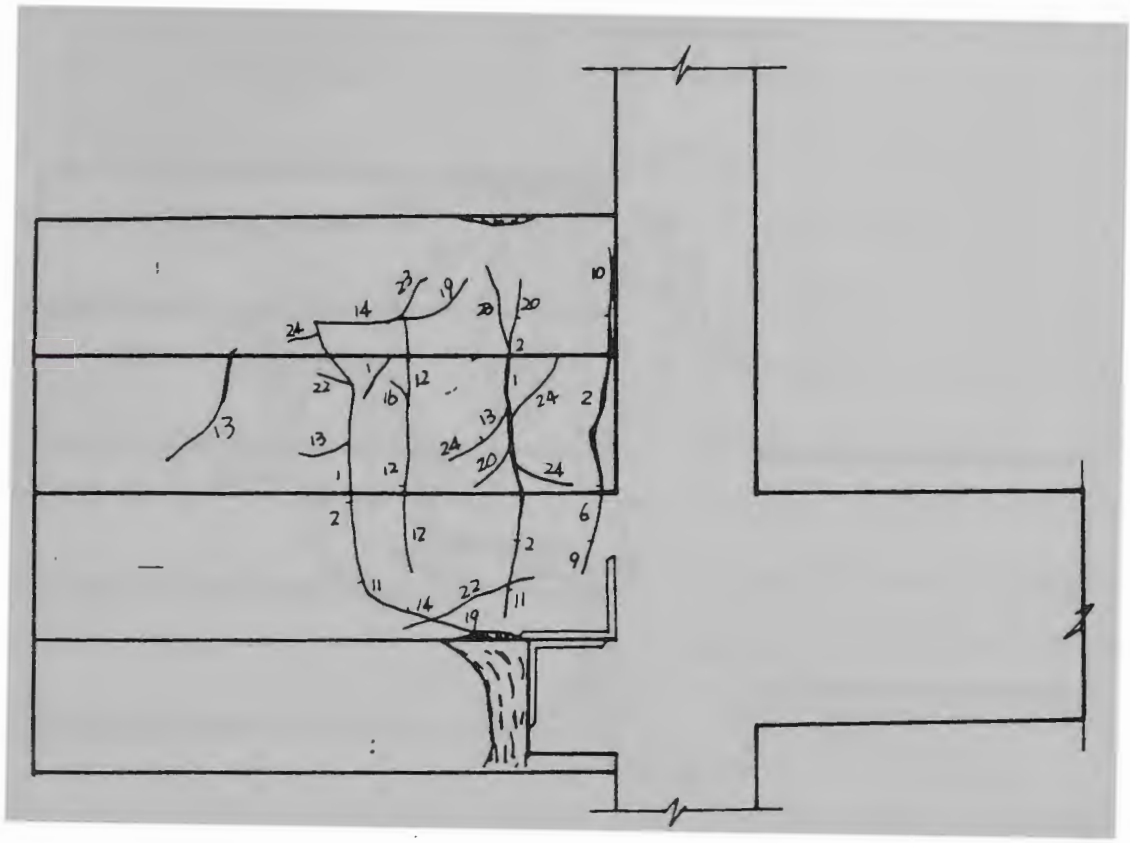

Fig. 5.2.9 Crack Pattern for Specimen RPB1

Plate 5.2.3 Crack Pattern for Specimen RPB1

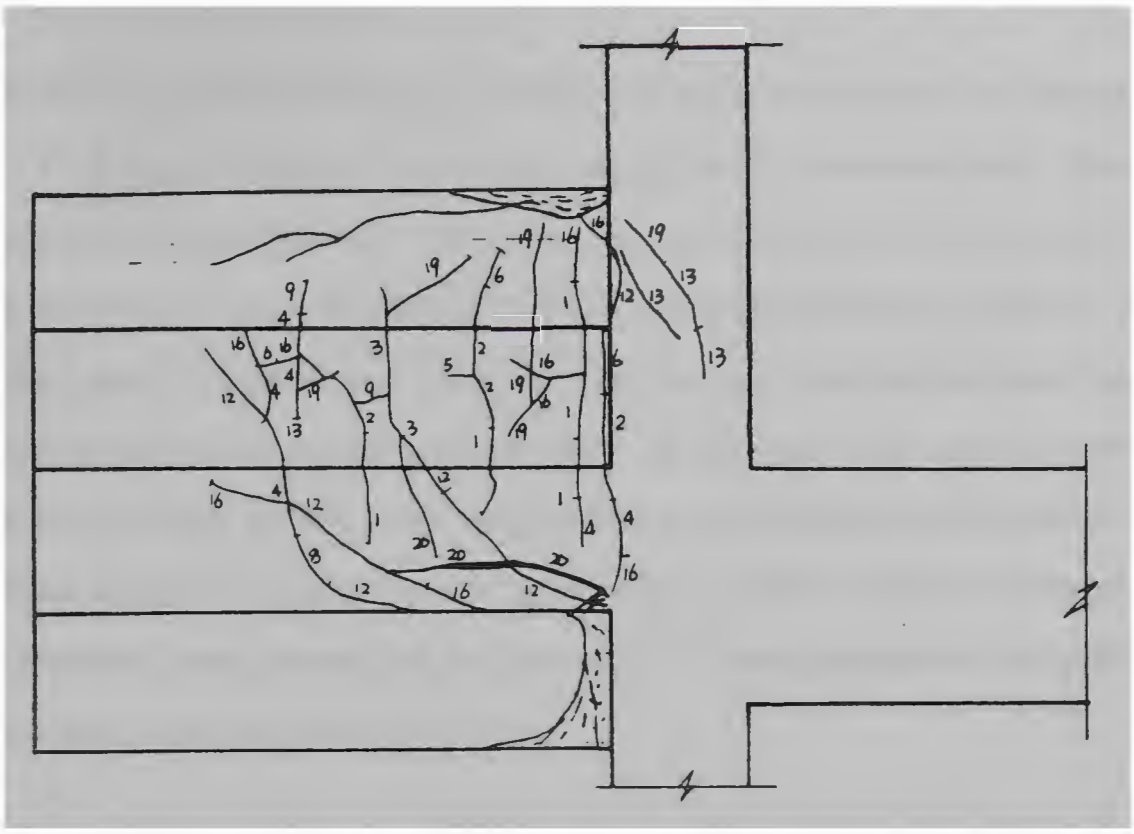

Fig. 5.2.10 Crack Pattern for Specimen RM2

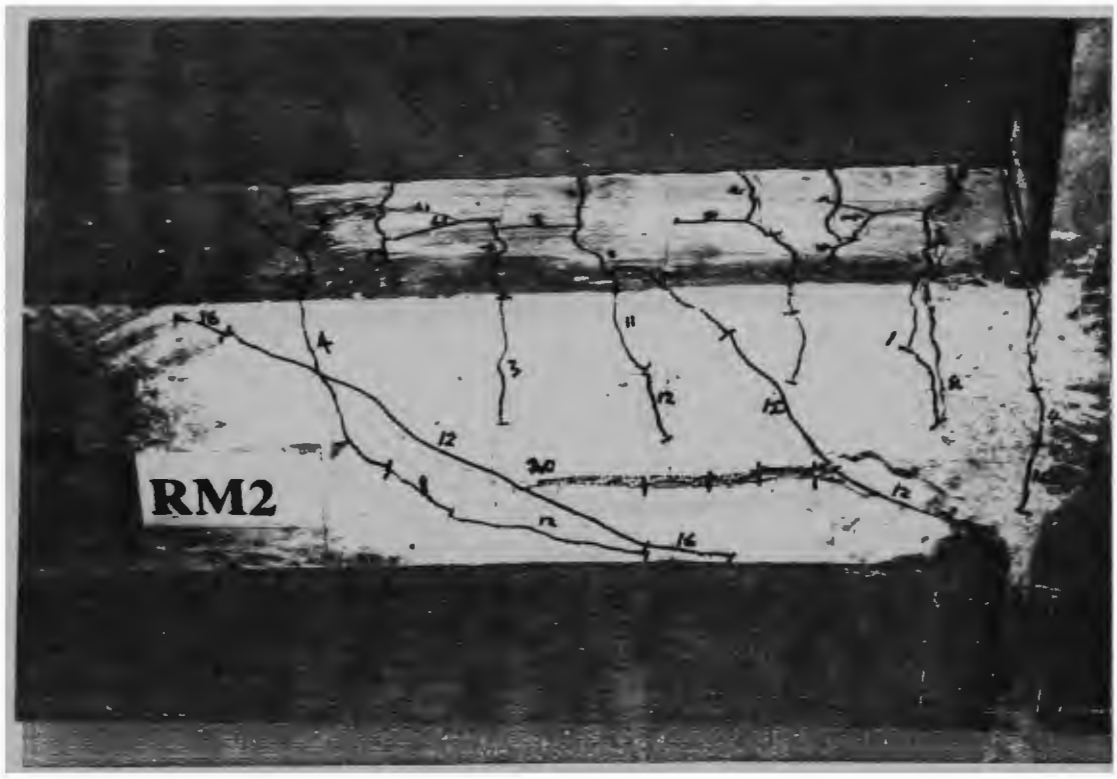

Plate 5.2.4 Crack Pattern for Specimen RM2

(e) Specimen RPA2

RPA2 was the Type A precast connection with a higher steel ratio. The specimen had a 18 % higher load carrying capacity compared to the theoretical value. When the applied load was 10 kN, or 15 % of its ultimate load, the first series of cracks were observed and when the applied load was increased, more cracks appeared. At the third cycle, a new vertical crack occurred near the beam root and grew very quickly to become the second principal crack. At this cycle, some inclined cracks were observed near the load point where there was a hole provided in the section to facilitate loading, and hence the section weakened. Tension failure occurred with two principal cracks occurring at the beam root. This was accompanied by spalling of concrete at the underside of the beam.

The crack pattern of specimen RPA2 is shown in Plate 5.2.5 and Fig. 5.2.11.

(f) Specimen RPB2

RPB2 was the Type B precast connection with a higher steel ratio. The specimen had a 18 % higher load carrying capacity compared to the theoretical value. The first crack was observed near the edge of the corbel when the applied load was 10 kN, or 14 % of its ultimate load. Vertical cracks were observed in the first cycle, but no new vertical cracks were formed until the fifth cycle during which a new vertical crack occurred at the edge of the corbel. During the second and the fourth cycles, only elongation of the existing crack was observed. With additional cycles, some inclined cracks occurred near the load point. A great number of " random " cracks occurred on the top surface of the beam near the ultimate load. The specimen was observed to fail in tension with the principal failure crack occurring near the corbel. This was again accompanied by some spalling of concrete at the bottom of the beam.

The crack pattern of specimen RPB2 was shown in Plate 5.2.6 and Fig. 5.2.12.

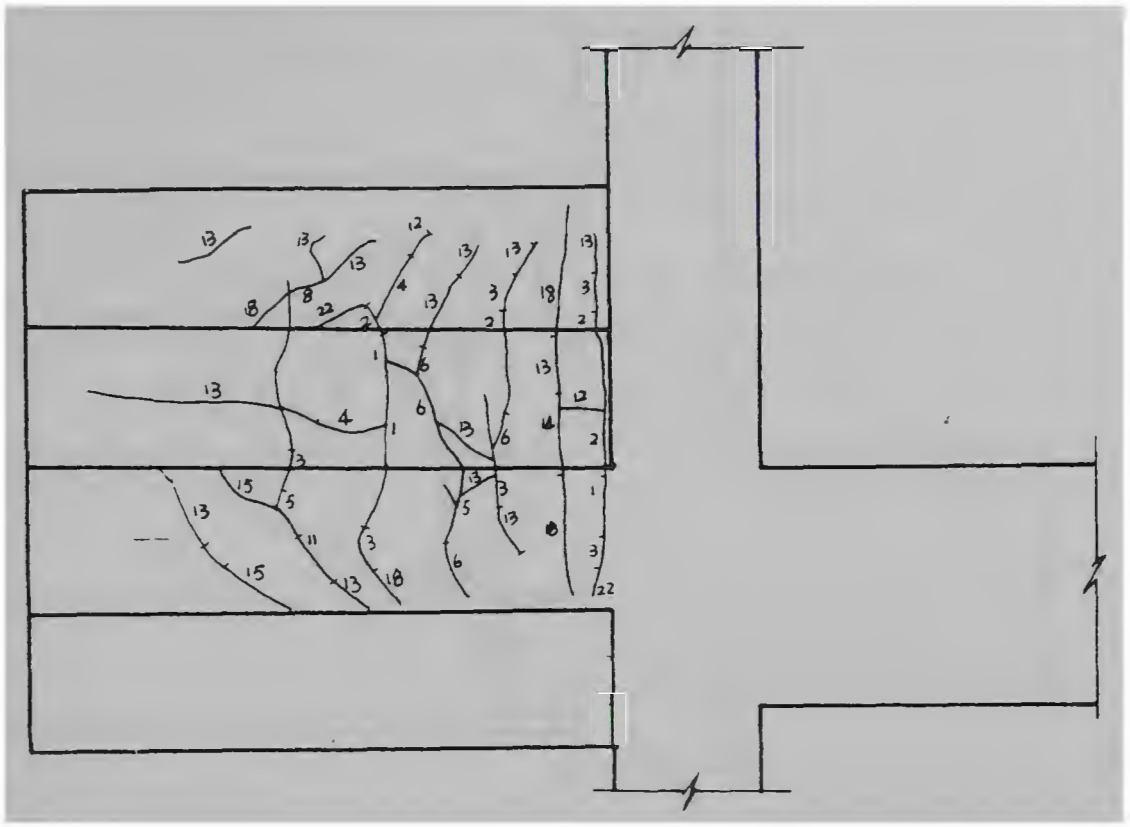

Fig. 5.2.11 Crack Pattern for Specimen RPA2

Plate 5.2.5 Crack Pattern for Specimen RPA2

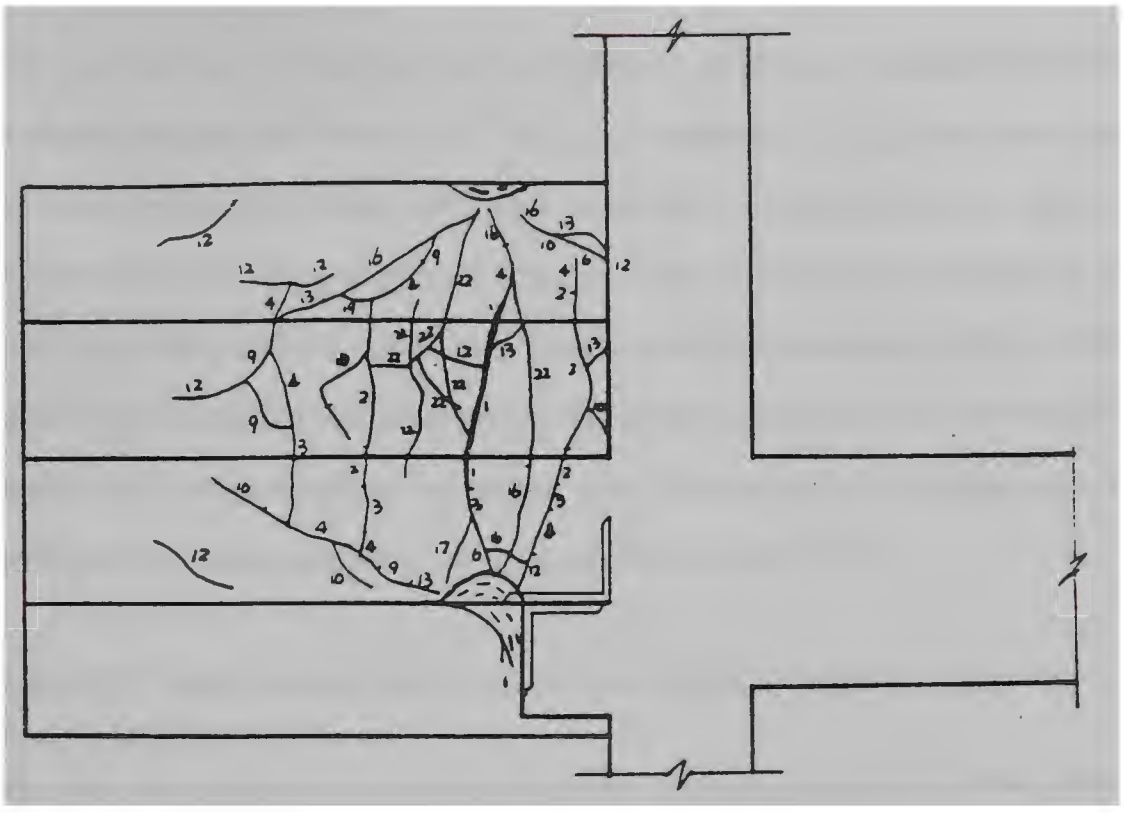

Fig. 5.2.12 Crack Pattern for Specimen RPB2

Plate 5.2.6 Crack Pattern for Specimen RPB2

For easy comparison, all the crack patterns are presented in the same diagram as shown in Fig 5.2.13. The loads corresponding to the first and second cracks of each specimen are given in Table 5.2.7. Fig. 5.2.13 indicates that the crack development and crack patterns at failure are largely identical for all specimens. Table 5.2.7 indicates that the first and second cracking loads of the precast specimens with a lower steel ratio were all higher than their monolithic counterpart, RM1. Although the cracking loads of the precast specimens with a higher steel ratio were a little bit lower than their monolithic counterpart RM2, the overall crack pattern and failure modes of the precast specimens were mostly the same as RM2.

Table 5.2.7 load values of first & second cracking for specimens tested under repeated loading

specimen	first crack load P_1 (kN)	P_1/P_u (%)	second crack load P_2 (kN)	P_2/P_u (%)
RM1	10	24	15	37
RPA1	15	32	25	53
RPB1	10	20	20	42
RM2	10	17	20	34
RPA2	10	15	30	44
RPB2	10	14	20	29

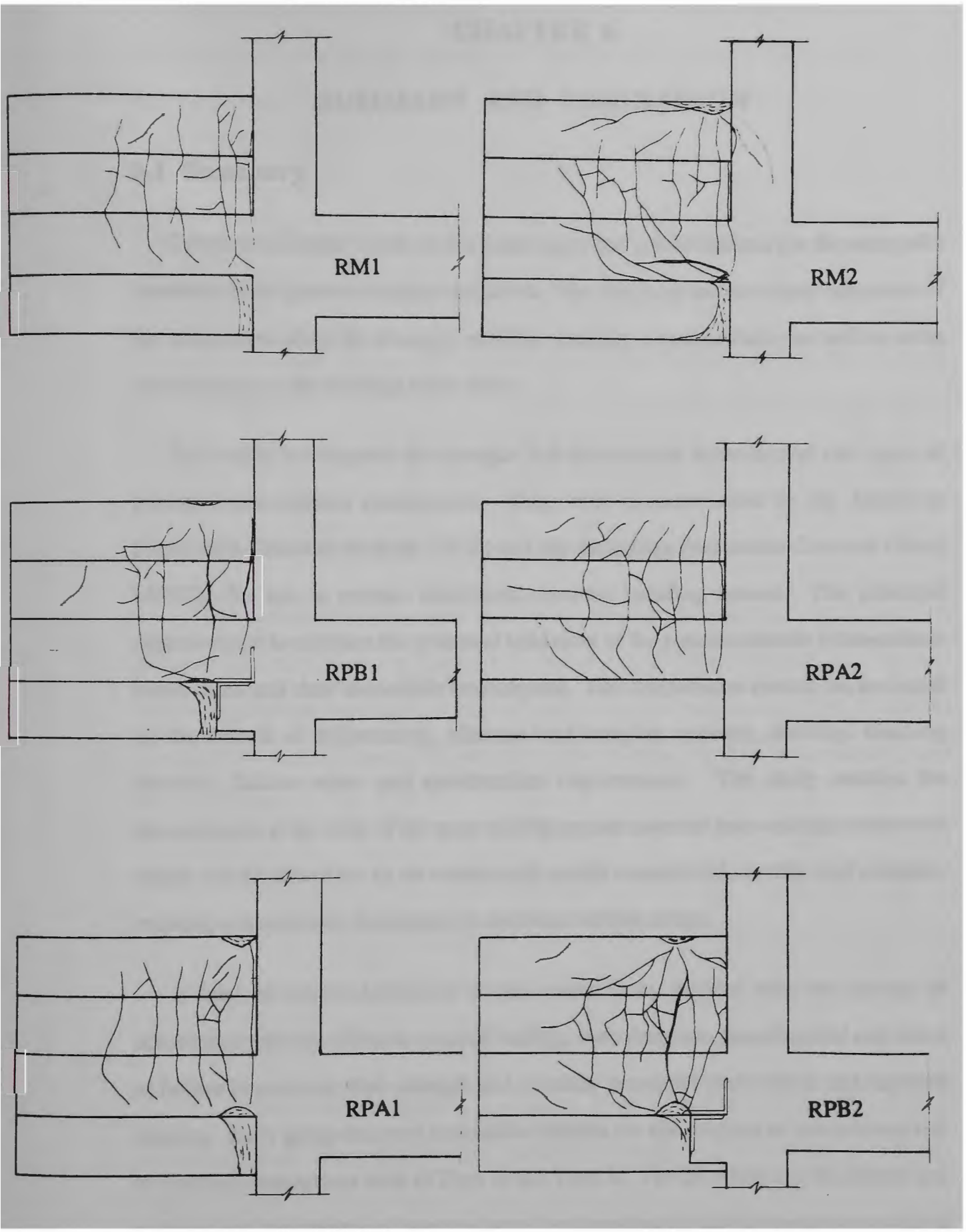

Fig. 5.2.13 Crack Patterns for All Specimens tested under Repeated Loading

CHAPTER 6

SUMMARY AND CONCLUSION

6.1 Summary

Connection design is one of the most important considerations for the successful construction of precast concrete structures. The detailing and structural behaviour of the connection affect the strength, stability, ductility, constructibility as well as stress redistribution of the building under loads.

This study investigates the strength and deformation behaviour of two types of precast beam-column connections. They were recommended by the American Prestressed Concrete Institute (PCI) and the Australian Prestressed Concrete Group (APCG) for use in precast reinforced concrete building frames. The principal objectives are to compare the structural behaviour of the precast concrete beam-column connections and their monolithic counterparts. The comparisons carried out are based on the criteria of deformation, ultimate load carrying capacity, ductility, cracking features, failure mode and construction requirements. The study enables the determination to be made of the most suitable precast concrete beam-column connection which can be classified as an economical, easily constructed, ductile, and moment-resisting connection in the context of moderate seismic design.

A total of twelve half-scale model connections, divided into two groups in accordance with the different types of loading, were designed, manufactured and tested to failure to evaluate their strength and ductility properties under static and repeated loading. Each group had two monolithic models for the purpose of comparison and two precast connections each of Type A and Type B. The dimensions of the beams and columns and the strength of concrete were kept constant for all the specimens to afford a direct comparative study of the connection behaviour. Each type of connections had

two steel ratios. This provided data for the study of the effects of the amount of reinforcement in the sub-assemblages on the behaviour of deformation, ultimate load carrying capacity, ductility, crack features, and failure mode.

6.2 Conclusions

Based on the test results of the twelve half-scale beam-column connection specimens investigated, the following conclusions can be drawn.

(1) As compared to the monolithic models tested under static loading, much improved behaviour was observed for all the precast models. These include higher load carrying capacity, larger displacement ductility and higher stiffness. The crack patterns, failure modes and load-strain curves for the reinforcing bars in tension were largely similar for both monolithic and precast models.

(2) As compared to the monolithic models tested under repeated loading, each of the two types of precast connection models had a higher load carrying capacity and larger displacement ductility as well as a better energy dissipation capability. The crack patterns and failure modes of the precast specimens were largely similar to that of the monolithic ones.

(3) In comparing the specimens with different steel ratios, it is found that the specimens with lower steel ratios had a higher ductility.

(4) Specimens subjected to repeated loading have a higher deflection ductility as compared to those subjected to static loading.

(5) In comparison to Type A specimens, Type B specimens had a higher load carrying capacity, larger displacement ductility and smaller crack width at the ultimate load.

(6) A comparison of the two types of precast specimens leads to the conclusion that connection Type B is more economical than Type A. This is because Type B does

not require any temporary props or formwork. This will save both time and money in construction. Furthermore, the second pour of the cast-in-place concrete*will provide the direct coupling with the precast floor system. This will further enhance the strength characteristics and integrity of the whole structure.

In summary, all the test results indicate that the two types of precast connections studied herein, if incorporated in precast concrete building frames, will develop adequate strength, stiffness and ductility to be classified as satisfactory moment-resisting connections. They can be adopted for use in the design and construction of precast concrete building frames located in moderate earthquake zones.

6.3 Recommendations for Future Research

The following recommendations for further study have emerged from the results of this investigation:

(1) One important drawback in the behaviour of connection Type A was the early appearance of the first cracks at the beam root, which quickly developed into excessively wide principal cracks. Although the surface was treated before pouring the cast-in-place concrete by roughing and wetting, the beneficial effect was not obvious. In order to increase the crack-resistance around the interface of precast and cast-in-place concrete at the connecting beam root, proprietary shear-key could perhaps be used. Or according to Park and Bill [54], the interface of the precast member could be roughened with an amplitude, typically, of 3 mm. This surface roughness may be achieved by chemical retardation of the surface after the initial setting. Then the surface cement paste from around the aggregate can be removed by washing with water and wire brushing. This problem deserves further investigation.

(2) Having been tested under static and repeated loading, the proposed beam-column connections for precast building frames are considered to be safe and reliable for use in areas of moderate earthquake. However, such connections would be subject

* The strength of the cast-in-place concrete was generally much higher than the precast concrete (see Table 3.6.3 and 3.6.4)

to moment reversals when the precast building frames are located in severe earthquake zones. Thus, further work should be carried out to investigate the behaviour of such connections under cyclic loading.

(3) Although the specimens have been tested under repeated loads, these loads were applied in a quasi-static manner. Further work should be carried out to investigate such connections under repeated or cyclic loads which are representative of true earthquake forces.

(4) Fibre reinforced concrete has been shown to have better structural characteristics such as higher levels of ductility and energy dissipation[75,76]. Further work should be carried out to investigate such connections using fibre concrete instead of the normal cast-in-place concrete.

REFERENCE

1 ABRAMS, D.P., "Scale Relations for Reinforced Concrete Beam-Column Joints", ACI Structural Journal, Vol. 84, No. 6, Nov.-Dec., 1987, pp. 502-512.

2 ADIN, M.A., YANKELEVSLY, D.Z., and FARHEY, D.N., "Cyclic Behaviour of Epoxy-Repaired Reinforced Concrete Beam-Column Joints", ACI Structural Journal, Vol. 90, No. 2, Mar.-Apr., 1993, pp. 170-179.

3 ALAMEDDINE, F., and EHSANI, M.R., "High-Strength RC Connections Subjected to Inelastic Cyclic Loading", ASCE Journal, Vol. 117, No. 3, March, 1991, pp 829-850.

4 ANNAMALAI, G., and BROWN, R.C., "Shear-Transfer Behavior of Post-Tensioned Grouted Shear-Key Connections in Precast Concrete-Framed Structures", ACI Structural Journal, Vol. 87, No. 1, Jan.-Feb., 1990, pp 53-59.

5 APCG (1990), "Connection Detail for Prestressed Concrete", Australia Prestressed Concrete Group Technical Committee on Connection Details, Sydney, Australia, pp. 45-70.

6 AUSTRALIA STANDARD, "Concrete Structures AS 3600-1988", Standards Association of Australia. 105p.

7 BETTERO, V.V., POPOV, E.P., and FORZANI,V., "Seismic Behaviour of Lightweight Concrete Beam-Column Subassemblages", ACI Journal, Proceedings, Vol. 77, No.1, Jan.- Feb., pp. 44-52.

8 BHATT, P., and KIRK, D.W., "Tests on an Improved Beam Column Connection for Precast Concrete", ACI Journal, Vol. 82, No. 6, November-December, 1985, pp. 834-843.

9 BIRKELAND, P.W., and BIRKELAND, H.W., "Connections in Precast Concrete Construction", ACI Journal, Vol. 63, No.3, March, 1966, pp. 345-353.

10 BIRSS, G.R., PAULAY, T., and PARK, R., "The Elastic Behaviour of Earthquake Resistant R.C. Interior Beam-Column Joints",Report 78-13, Univ. of Canterbury, Dept. of Civ. Engrg., Christchurch, New Zealand, Feb., 1978.

11 BLAKELEY, R.W.G., and PARK, R., "Seismic Resistance of Prstressed Concrete Beam-Column Assemblies", ACI Journal, Vol. 68, No.9, Sep., 1971, pp. 677-693.

12 BROWN, R.H., and JIRSA, J.O., "Reinforced Concrete Beams Under Load Reversals", ACI Journal, vol. 68, No. 5, May, 1971.pp. 380-390.

13 CASTRO, J.J., YAMAGUCHI, T., and IMAI, H., "Seismic Behaviour of Half Precast Beam-Column Joints", Translations of The Japan Concrete Institute, Vol. 13, 1991, pp. 327-334.

14 CHEOK, G.S., and LEW, H.S., "Performance of Precast Concrete Beam-to-Column Connections Subject to Cyclic Loading", PCI Journal, Vol. 36, No. 3, May-June, 1991, pp. 56-67.

15 CHEUNG, P.C., PAULAY, T., and PARK, R., "Behavoiur of Beam-Column Joints in Seismically-Loaded RC Frames." The Structural Engineer , Vol. 71, No. 8, April, 1993. pp. 129-138.

16 CRISP, B.C., "Practical Design and Constrution for Structural Precast Concrete", The Concrete Instutute of Australia. NSW Branch, Furture Directions-Precast Concrete in Buildings. Crisp/page 1-14.

17 DOLAN, C.W., STANTON, J.F., and ANDERSON,R.G., "Moment Resistant Connections and Simple Connections", PCI Journal, Vol. 32, No. 2, Mar.-Apr., 1987, pp. 62-75.

18 DOLAN, C.W., and PESSIKI, S.P., "Model Testing of Precast Concrete Connections", PCI Journal, Vol. 34 No. 2, March-April 1989, pp. 84-103.

19 DURRANI, A.J., and WIGHT, J.K., "Experimental and Analytical Study of Internal Beam-Column Connections Subjected to Reversed Cyclic Loading", Report No. UMEE 82R3, Univ. of Michigan, Ann Arbor, Mic., July, 1982.

20 DURRANI, A.J., and WIGHT, J.K.,"Earthquake Resistance of Reinforced Concrete Interior Connections Including a Floor Slab", ACI Structural Journal, Vol. 84, No. 5, Sep.-Oct., 1987, pp. 400-512.

21 EHSANI, M.R., and WIGHT, J.K., "Exterior Reinforced Concrete Beam-to-Column Connections Subjected to Earthquake-Type Loading", ACI Journal, Vol. 82, No.4, July-August 1985, pp. 492-499.

22 EHSANI, M.R., and ALAMEDDINE, F., "Design Recommendations for Type 2 High-Strength Reinforced Concrete Connections" ACI Journal, Vol. 88, No. 3, May-June, 1991, pp. 277-291.

23 EHSANI, M.R., and WIGHT, J.K., "Behaviour of External Reinforced Concrete Beam to Column Connections Subjected to Earthquake Type Loading", Report No. UMEE 82R5, Department of Civil Engineering, University of Michigan, Ann Arbor, July 1982, 243 p.

24 EI-METWALLY, S.E., and CHEN, W.F., "Mement-Rotation Modeling of Reinforced Concrete Beam-Column Connections", ACI Structural Journal, Vol. 85, No. 4, July-Aug., 1988. pp. 384-394.

25 ENGLEKIRK, R.E., "Precast Concrete for Seismic Resistance", PCI Journal, Vol. 31, No. 6, November-December, 1986, pp. 48-59.

26 ENGLEKIRK, R.E., "Overview of PCI Workshop on Effective Use of Precast Concrete for Seismic Resistance", PCI Journal, Vol. 32, No. 5, Sep.-Oct., 1987, pp. 131-137.

27 ENGLEKIRK, R.E., "Concepts for the Development of Earthquake Resistant Ductile Frames of Precast Concrete" PCI Journal, Vol. 32, No. 1, January-February, 1987, pp. 30-49.

28 FENWICK, R.C., and IRVINE, H.M., "Reinforced Concrete Beam-Column Joints for Seismic Loading", Report No. 142, Univ. of Auckland, Auckland, New Zealand, Mar., 1977.

29 FILIPPOU, F.C., POPOV, E.P., and BERTERO,V.V., "Analytical Studies of Hysteretic Behavior of R/C Joints", ASCE Journal, Vol. 112, No. 7,July, 1986, pp. 1605-1622.

30 FRENCH, C.W., AMU, O., and TARZIKHAN, C., "Connections Between Precast Elements Failure Outside Connection Region" ASCE Journal, Vol. 115, No. 2, Feb., 1989, pp, 316-317.

31 FRENCH, C.W., HAFNER, M., and JAYASHANKAR, V., "Connections Between Precast Elements-Failure Within Connection Region", ASCE Journal of Structural Engineering, Vol. 115, No. 12, December 1989, pp. 3171-3192.

32 FRENCH, C.W., THORP, G.A., and TSAI,W.J., " Epoxy Repair Techniques for Moderate Earthquake Damage", ACI Structural Journal , Vol. 87, No. 4 July-Aug., 1990. pp. 416-424.

33 GEFKEN, P.R., and RAMEY, M.R., "Increased Joint Hoop Spacing in Type 2 Seismic Joints Using Fiber Reinforced Concrete", ACI Structural Journal, Vol. 86, No. 2, Mar.-Apr., 1989. pp. 168-172.

34 " Guidelines for the Use of Structural Precst Concrete in Buildings", University of Canterbury,New Zealand, pp. 1-106.

35 GUIMARAES, G.N., KREGER, M.E., and JIRSA, J.O., "Evaluation of Joint-Shear Provisions for Interior Beam-Column-slab Connections Using High-Strength Materials", ACI Structural Journal, Vol. 89, No. 1,Jan.-Feb.,1992, pp. 89-98.

36 GULKAN, P., "The Inelastic Response of Repaired Reinforced Concrete Beam-Column Connections", Report on Project M46-372, Middle East Technical Univ., Ankara, Turkey, 1976.

37 HANSON, N.W., "Seismic Resistance of Concrete Frames with Grade 60 Reinforcement", ASCE Journal, Vol. 97. No. ST6, June, 1971, pp. 1685-1700.

38 HANSON, N.W., and CONNER, H.W., "Seismic Resistance of Reinforced Concrete Beam-Column Joints", ASCE Journal, Vol. 93, No. ST5, Oct., 1967, pp. 533-560.

39 HANSON, N.W., and CONNER, H.W., "Tests of Reinforced Concrete Beam Column Joints under Simulated Seismic Loading", RD012.01D, Portland Cement Association, Skokie, Illinois, 1972.

40 HAWKINS, N.M., and ENGLEKIRK, R.E., "U.S.-Japan Seminar on Precast Concrete Construction in Seismic Zones", PCI Journal, Vol. 32, No.2, March-April, 1987, pp. 75-85.

41 HIGASHI, Y., and OHWADA, Y.," Failing Behaviours of Reinforced Concrete Beam-Column Connections Subjected to Lateral Loads", Memoirs of Faculty of Technology, No. 19, Tokyo Metropolitan Univ., Tokyo, Japan, 1969.

42 JOHAL, L.S., JENNY, D.P., and SHAIKH, A.F., "Impact of Past Research and Future Research Needs of the Precast and Prestressed Concrete Industry", PCI Journal, Vol. 36, No. 6, Nov.-Dec., 1991, pp. 52-59.

43 KEONG, Y.S., and PARK, R., "Prestressed Concrete Beam-Column Joints", Report 78-2, Univ. of Canterbury, Dept, of Civ. Engrg., Christchurch, New Zealand, Feb., 1978.

44 KORDINA, K., and SCHAAFF, E., Tragverbalten von Rahmenknoten bei herabgesetzter Verankerungslange der Anschlusbewehrung unter Berucksichtigung der Bewehrungsfuhrung, Technical Univ. of Braunschweig, Braunschweig, W. Germany, No. 3263, 1972.

45 KUROSE, Y., NAGAMI, K., and SAITO,Y., "Beam-Column Joints in Precast Concrete Construction in Japan" JAMES O.JIRSA. Editor, American Concrete Institute, Michigan, U.S.A.1991, pp 492-517.

46 LEE, D.L.N., WIGHT, J.K., and HANSON, R.D., "RC Beam-Column Joints under Large Load Reversals", ASCE Journal, Vol. 103, No. ST12, Dec., 1977, pp. 2337-2350.

47 LEON, R.T., "Shear Strength and Hysteretic Behaviour of Interior Beam-Column Joints", ACI Structural Journal, Vol. 81, No. 1, Jan.-Feb., 1990, pp. 3-11.

48 LOO, Y.C. (1992), "Reinforced Concrete Analysis and Design with Emphasis on the Application of AS 3600-1988", University of Wollongong, Wollongong, Australia, 327 p.

49 LU, C.G., "Joint Connections for Precast Concrete Multi-Storey Buildings in China" FIP Notes, April, 1985, pp. 10-13.

50 MEINHEIT, D.F., and JIRSA, J.O., "The Shear Strength of Reinforced Concrete Beam-Column Joints",Report No. 77-1, Dept. of Civ. Engrg., Structures Res. Lab., Univ. of Texas at Austin, Jan., 1977.

51 MEINHEIT, D.F., and JIRSA, J.O., "Shear Strength of R/C Beam-Column Connections", ASCE Journal, Vol.107, No. ST11, November, 1981. pp. 2227- 2244.

52 MEGGET, L.M., and Park, R., "Reinforced Concrete Exterior beam-column Joints under Seismic Loading", New Zealand Engineering, 15 Nov., 1971, pp. 341-353.

53 NAKAKI, S.D., and ENGLEKIRK, R.E., "PRESSS Industry Seismic Workshops: Concept Development", PCI Journal, Vol. 36, No. 5, September-October,1991, pp. 54-61.

54 PARK,R., and BULL, D.K., " Seismic Resistance of Frames Incorporating Precast Prestressed Concrete Beam Shells", PCI Journal, Vol. 31, No. 4, July-August, 1986, pp. 54-93.

55 PARK, R., GAERTY, L., and STEVENSON, E.C., "Tests on an Interior reinforced Concrete Beam-Column Joint", Bulletin of the New Zealand National society for Earthquake Engineering, Vol. 14, No. 2, June, 1981.

56 PARK, R., and PAULAY. T., "Reinforced Concrete Structures", University of Canterbury of Canterbury, Christchurch, New Zealand, 1975, 769 p.

57 PARK,R., and THOMPSON,K.J., " Behavoiur of Prestressed, Partially Prestressed, and Reinforced Concrete Interior Beam-column Assemblies under Cyclic Loading: Test Results of Units 1 to 7,", Research Report 74-9, Dept. of Civ. Engrg., Univ. of Canterbury, Christchurch, New Zealand, 1974, 42 p.

58 PATTON, R.N., " Behaviour under Seismic Loading of Reinforced Concrete Beam-Column Joints with Anchor Blocks", Master of Engrg. Report, Univ. of Canterbury, Christchurch, New Zealand, 1972, 103p.

59 PAULAY, T. PARK, R., and PRIESTELEY, M.J.N., "Reinforced Concrete Beam-Column Joints Under Seismic Actions", ACI Journal, Vol. 75, No. 11, Nov., 1978. pp. 585-593.

60 PAULAY, T.,"Equilibrium Criteria for Reinforced Concrete Beam-Column Joints", ACI Structural Journal, Vol. 86, N0. 6, Nov-Dec., 1989. pp. 635-643.

61 PRIESTLEY, M.J.N., "Testing of Two Reinforced Concrete Beam-Column Assemblies under Simulated Seismic Loading", Report 5-75/1, New Zealand Ministry of Works and Development, 1975.

62 PCI (1982) "Connections for Precast Prestressed Concrete Buildings Including Earthquake Resistance", Prestressed Concrete Institute, Chicago, Illinois.

63 PCI (1988) "Design and Thpical Details of Connections for Precast and Prestressed Concrete", PCI Comittee on Connection Details.

64 PILLAI, S.U., and KIRK, D.W., "Ductile Beam-Column Connection in Precast Concrete", ACI Journal, Vol. 78, No. 6, Nov.-Dec., 1981, pp. 480-487.

65 PRIESTLEY, N.J.N., "Overview of PRESSS Research Program", PCI Journal, Vol. 36, No. 4, July-August 1991, pp. 55-57.

66 "Recommendations for Design of Beam-Column Joints in Monolithic Reinforced Concrete Structures", ACI-ASCE Joint Committee 352, ACI Journal, Proceedings, Vol,73, No. 7, July, 1976, pp. 375-393.

67 RENTON, G.W., "The Behavoiur of Reinforced Concrete Beam-Column Joints under Cyclic Loading", thesis submitted to the Univ. of Canterbury, at Christchurch, New Zealand, in 1972, in partial fulfillment of the requirements for the degree of Master of JEngineering in civil Engineering.

68 SCARPAS, A., "The Inelastic Behaviour of Earthquake Resistant Reinforced Concrete Exterior Beam-Column Joints", Report No.81-2, Department of Civil Engineering, University of Canterbury Christchurch, Feb, 1981, 84p.

69 SCRIBNER,C.F., and WIGHT, J.K., " Strength Decay in R/C Beams Under Load Reversals", ASCE Journal, Vol. 106, No.ST4, Apr.,1980. pp. 861-876.

70 SECKIN, M., and FU, H.C., "Beam-Column Connections in Precast Reinforced Concrete Construction", ACI Structural Journal, Vol. 87, No. 3, May-June, 1990, pp. 252-261

71 SMITH,B.J.,"Exterior Reinforced Concrete Joints with Low Axial Load under Seismic Loading", report submitted to the Univ. of Canterbury, at Christchurch, New Zealand, in 1972, in partial fulfillment of the requirements for the degree of Master of Engineering. 103p.

72 SOLEIMANI, D., POPOV, E.P., and BERTERO, V.V., "Hysteretic Behaviour of Reinforced Concrete Beam-Column Subassemblages", ACI Journal, Vol. 76, No. 11, November, 1979, pp. 1179-1195.

73 SOROUSHIAN, P., OBASEKI, K., and ROJAS, M.C., " Pullout Behaviour of Hooked Bar in Exterior Beam-Column Connections", ACI Structural Journal, Vol. 85, No. 3, May-June, 1988. pp. 269-276.

74 SOROUSHIAN, P., and CHOI,D.B.,"Analytical Evaluation of Straight Bar Anchorage Design in Exterior Joints", ACI Structural Journal, Vol. 88, No. 2, Mar.-Apr., 1991.pp. 161-168.

75 SOUBRA, K.S., WIGHT, J.K., and NAAMAN, A.E., "Fiber Reinforced Concrete Joints for Precast Construction in Seismic Areas", ACI Structural Journal, V. 88, No. 2, Mar.- Apr.,1991, pp. 214-221.

76 SOUBRA. K.S., WIGHT, J.K., and NAAMAN, A.E., "Cyclic Response of Fibrous Cast-in-place Connections in Precast Beam-Column Subassemblages", ACI Structural Journal, May-June 1993, pp. 316-323.

77 STANTON, J.F., HAWKINS, N.M., and HICKS, T.R., "PRESSS Project 1.3: Connection Classification and Evaluation", PCI Journal, September-October, 1991, pp. 62-71.

78 TOWNSEND, W.H., and HANSON, R.D., "Reinforced Concrete Connection Hysteresis Loops," Symposium on Reinforced Concrete Structures in Seismic Zones, ACI SP-53, American Concrete Institute, Detroit, Mich., 1977, PP. 351-370.

79 TSONOS, A.G., TEGOS, I.A., and PENELIS, G.Gr., "Seismic Resistance of Type 2 Exterior Beam-Column Joints Reinforced with Inclined Bars", ACI Structural Journal, Vol. 89, No.1,Jan.-Feb., 1992. pp. 3-12.

80 UZUMERI S.M., "Strength and Ductility of Cast-In-Place Beam-Column Joints," Symposium on Reinforced Concrete Structures in Seismic Zones. ACI SP-53, American concrete Institute, Detroit, Mich., 1977, pp. 293-350.

81 UZUMERI, S.M., and SECKIN, M., "Behavoiur of Reinforced Concrete Beam-Column Joints Subjected to Slow Load Reversals," Report 74-05, Dept. of Civ. Engrg., University of Toronto, Toronto, Ont., Canada, Mar., 1974.

82 YAO, B.Z., "Strength and Deformation Behaviour of Precast Beam-Column Connections for Reinforced Concrete Building Frames", M.E. Thesis, Univ. of Wollongong, Wollongong, N.E.W., Australia, 1992, 190 pp.

83 YOSHIOKA, K., and SEKINE, M., " Expermental Study on Prefabricated Beam-Column Subassemblages" JAMES O.JIRSA. Editor, American Concrete Institute, Michigan, U.S.A.1991, pp. 465-491.

APPENDIX 1

NOMALISED TEST DATA OF SPECIMEN TESTED

UNDER STATIC LOADING

Table A.1.1 Test Data of Deflection and Concrete Strain for Specemen SM1

load stage	load (kN)	P/P_u (%)	Deflection (mm)		Concrete Strain (10^{-3})		Remark
			Vertical	Horizontal	Tensional	Conpressive	
1	3	7.69	1.63	0.59	0.105	0.065	
2	6	15.38	2.10	0.65	0.462	0.178	first crack
3	9	23.08	2.60	0.70	0.868	0.308	
4	12	30.77	3.15	0.78	1.215	0.389	
5	15	38.46	3.74	0.85	1.636	0.486	
6	18	46.15	4.35	0.93	2.203	0.607	
7	21	53.85	5.02	1.04	2.859	0.656	
8	24	61.54	5.72	1.04	3.459	0.729	
9	27	69.23	6.51	1.25	4.042	0.923	
10	30	76.92	7.34	1.38	4.779	0.932	
11	33	84.61	8.07	1.49	5.646	1.013	first yield
12	36	92.30	9.23	1.64	6.828	1.094	
13	39	100	21.06	3.84		5.670	

Table A.1.2 Test Data of Strain of Steel Bar for Specemen SM1

load stage	load (kN)	Strain of steel Bar (10^{-6})					
		Gauge 1	Gauge 2	Gauge 3	Gauge 4	Gauge 9	Gauge 10
1	3	55	60	43	56	35	41
2	6	348	328	316	343	148	170
3	9	620	585	547	608	308	367
4	12	881	839	759	848	519	577
5	15	1124	1051	958	1064	707	784
6	18	1353	1222	1149	1228	957	1119
7	21	1677	1575	1363	1405	1190	1344
8	24	1972	1608	1559	1587	1428	1577
9	27	2294	1673	1757	1786	1664	1815
10	30	2602	1704	1966	2004	1913	2082
11	33	2879	1756	2148	2191	2111	2306
12	36	7596	1853	2265	2423	2386	2621
13	39			787	300	2766	1388

Table A.1.3 Test Data of Deflection and Concrete Strain for Specemen SPA1

load stage	load (kN)	P/P_u (%)	Deflection (mm)		Concrete Strain (10^{-3})		Remark
			Vertical	Horizontal	Tensional	Conpressive	
1	3	6.25	1.39	0.13	0.057	0.113	
2	6	12.50	1.77	0.27	0.138	0.194	
3	9	18.75	2.19	0.42	0.300	0.267	
4	12	25.00	2.73	0.60	0.535	0.308	first crack
5	15	31.25	3.27	0.76	0.786	0.34	
6	18	37.75	3.73	0.83	1.061	0.405	
7	21	43.75	4.06	0.95	1.353	0.527	
8	24	50.00	4.83	1.07	1.62	0.599	
9	27	56.25	5.43	1.22	1.92	0.672	
10	30	62.50	6.06	1.36	2.187	0.770	
11	33	68.75	6.68	1.48	2.543	0.778	
12	36	75.00	7.30	1.64	2.876	0.859	
13	39	81.25	8.03	1.77	3.240	1.061	first yield
14	42	87.50	12.83	2.35	7.371	1.377	
15	45	93.75	16.76	3.14	13.081	1.701	
16	46	95.83	29.51	3.56	14.29	1.790	
17	47	97	32.11	4.06	16.20		
18	48	100	34.71	4.46			

Table A.1.4 Test Data of Strain of Steel Bar for Specemen SPA1

load stage	load (kN)	Strain of Steel Bar (10^{-6})					
		Gauge 1	Gauge 2	Gauge 3	Gauge 4	Gauge 9	Gauge 10
1	3	132	102	48	40		
2	6	295	306	172	102		
3	9	453	510	332	211		
4	12	604	709	503	354		
5	15	774	916	644	509		
6	18	944	1110	806	664		
7	21	1139	1324	998	848		
8	24	1310	1504	1161	1011		
9	27	1479	1657	1341	1181		
10	30	1652	1844	1524	1369		
11	33	1811	2035	1690	1539		
12	36	1909	2162	1803	1658		
13	39	2329	2348	2038	1909		
14	42	2805	1704	2250	2097		
15	45	927	641	3501	2231		
16	46	1498	643	1672	2282		
17	47	1349	648	1681	2334		
18	48	659	624	2352	4039		

Table A.1.5 Test Data of Deflection and Concrete Strain for Specemen SPB1

load stage	load (kN)	P/P_u (%)	Deflection (mm)		Concrete Strain (10^{-3})		Remark
			Vertical	Horizontal	Tensional	Conpressive	
1	4	8.51	0.27	0.03	0.486	0.016	
2	8	17.02	0.67	0.07	0.203	0.039	first crack
3	12	25.53	1.29	0.15	0.437	0.056	
4	16	34.04	1.80	0.26	0.753	0.073	
5	20	42.55	2.33	0.39	1.069	0.859	
6	24	51.06	3.07	0.47	1.328	0.988	
7	28	59.57	3.63	0.57	1.547	1.094	
8	32	68.08	4.35	0.65	1.912	1.256	
9	36	76.60	4.97	0.77	2.438	1.296	
10	40	85.11	5.74	0.89	2.722	1.434	first yield
11	44	93.62	7.37	1.01	3.086	1.620	
12	45	95.74	9.37	2.01		2.106	
13	46	97.87	13.37	3.01			
14	47	100.00	18.71	4.01			

Table A.1.6 Test Data of Strain of Steel Bar for Specemen SPB1

load stage	load (kN)	Strain of Steel Bar (10^{-6})					
		Gauge 1	Gauge 2	Gauge3	Gauge 4	Gauge 9	Gauge 10
1	4	35	30	26	30	3	31
2	8	142	136	369	456	-6	136
3	12	309	276	351	803	-30	303
4	16	546	470	463	353	-40	503
5	20	762	690	562	361	-44	757
6	24	793	864	619	514	-23	985
7	28	1204	915	831		25	1098
8	32	1403	365	981		46	1338
9	36	1645	-525	1112		79	1586
10	40	1863				128	1793
11	44	2145				193	2069
12	45	2191				187	2127
13	46	2300				201	2191
14	47	2434				196	2288

Table A.1.7 Test Data of Deflection and Concrete Strain for Specemen SM2

load stage	load (kN)	P/P_u (%)	Deflection (mm)		Concrete Strain (10^{-3})		Remark
			Vertical	Horizontal	Tensional	Conpressive	
1	10	20	1.15	0.26	0.511	0.397	
2	20	40	2.92	0.66	1.377	0.761	
3	30	60	4.67	1.06	2.187	1.183	
4	40	80	7.05	1.56	3.240	1.612	first crack
5	45	90	9.87	1.76	3.650	1.934	
6	50	100	15.02	2.11	4.698	2.017	

Table A.1.8 Test Data of Strain of Steel of Bar for Specemen SM2

load stage	load (kN)	Strain of Steel Bar (10^{-6})					
		Gauge 1	Gauge 2	Gauge 3	Gauge 4	Gauge 9	Gauge 10
1	10	423	402	410	464	371	449
2	20	1099	1065	882	942	879	871
3	30	978	1589	1374	1403	1358	1297
4	40	895	2117	1695	1913	1930	1800
5	45	1056	2400	1612	2222	2915	2186
6	50	1217	2684	1529	2530	3900	2573

Table A.1.9 Test Data of Deflection and Concrete Strain for Specemen SPA2

load stage	load (kN)	P/P_u (%)	Deflection (mm)		Concrete Strain (10^{-3})		Remark
			Vertical	Horizontal	Tensional	Conpressive	
1	5	7.81	0.44	0.11	0.178		
2	10	15.63	0.96	0.24	0.324		first crack
3	15	23.44	1.42	0.37	0.559		
4	20	31.25	2.22	0.53	0.826		
5	25	39.06	2.90	0.67	1.061		
6	30	46.88	3.57	0.81	1.337		
7	35	54.68	4.47	0.98	1.571		
8	40	62.25	5.32	1.17	1.814	0.583	
9	45	70.31	6.22	1.35	2.203	0.697	
10	50	78.12	7.02	1.52	2.462	0.867	
11	55	85.94	8.20	1.45	2.843	0.875	first yield
12	60	93.75	11.72	1.93	6.269	0.988	
13	61	95.31	12.62	2.07	7.160	0.786	
14	62	96.88	14.12	2.27	8.699	1.069	
15	63	98.44	15.12	2.77	10.32	1.11	
16	64	100.00	28.20	3.77			

Table A.1.10 Test Data of Strain of Steel Bar for Specemen SPA2

load stage	load (kN)	Strain of Steel Bar (10^{-6})					
		Gauge 1	Gauge 2	Gauge 3	Gauge 4	Gauge 9	Gauge 10
1	5	148	140	82	60		
2	10	402	409	219	161		
3	15	654	715	388	293		
4	20	907	988	674	530		
5	25	1144	1207	917	750		
6	30	1392	1445	1124	954		
7	35	1630	1699	1353	1185		
8	40	1852	1911	1554	1383		
9	45	2082	2073	181	1881		
10	50	2303	2283	2043	2118		
11	55	2990	2534	2257	2372		
12	60	3526	2651	2334	2459		
13	61	2120	3728	2509	2774		
14	62	4810	1415	2669	2854		
15	63		1448	2914	2911		
16	64		1577	3094	3052		

Table A.1.11 Test Data of Deflection and Concrete Strain for Specemen SPB2

load stage	load (kN)	P/P_u (%)	Deflection (mm)		Concrete Strain (10^{-3})		Remark
			Vertical	Horizontal	Tensional	Conpressive	
1	5	7.58	0.07	0.00	0.057	0.170	
2	10	15.15	0.70	0.01	0.235	0.421	
3	15	22.73	1.22	0.10	0.348	0.599	first crack
4	20	30.30	1.83	0.21	0.535	0.705	
5	25	37.88	2.52	0.35	0.778	0.778	
6	30	45.45	3.15	0.50	1.061	0.964	
7	35	53.03	3.98	0.52	1.409	1.069	
8	40	60.61	4.80	0.80	1.733	1.191	
9	45	68.18	5.59	1.01	2.082	1.304	first yield
10	50	75.76	6.59	1.24	2.446	1.466	
11	55	83.33	7.75	1.48	2.738	1.661	
12	60	90.91	9.10	1.77	3.127	1.814	
13	61	92.42	9.51	1.83	3.208	1.879	
14	62	93.94	9.77	1.86	3.281	1.944	
15	63	95.45	10.14	1.92	3.426	2.001	
16	64	96.97	12.71	2.34	2.884	2.033	
17	65	98.48	13.71	2.83	7.663	2.503	
18	66	100.00	22.38	3.38	11712		

Table A.1.12 Test Data of Strain of Steel Bar for Specemen SPB2

load stage	load (kN)	Strain of Steel Bar (10^{-6})					
		Gaige 1	Gaige 2	Gaige 3	Gaige 4	Gaige 9	Gaige 10
1	5	40		157		110	
2	10	153		1481		264	
3	15	276		2037		418	
4	20	452		2230		630	
5	25	680		2560		851	
6	30	878		2792		1073	
7	35	1106		3200		1808	
8	40	1345		3386		1989	
9	45	1586		3426		2189	
10	50	1535		3709		2408	
11	55	1635		3736		2038	
12	60	1698		4157		2169	
13	61	1694		4262		2220	
14	62	1663		4518		2236	
15	63	1638		4732		2877	
16	64	1573		4746		2882	
17	65	1747				2300	
18	66	1792					

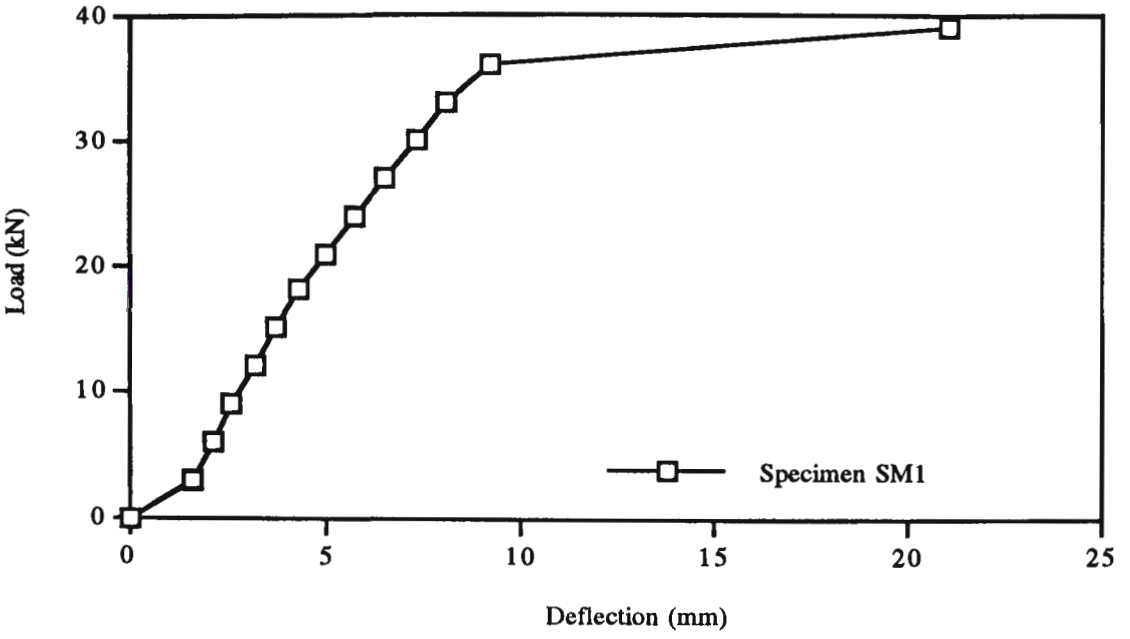

Fig.A.1.1 Load-Deflection Curve for Specimen SM1

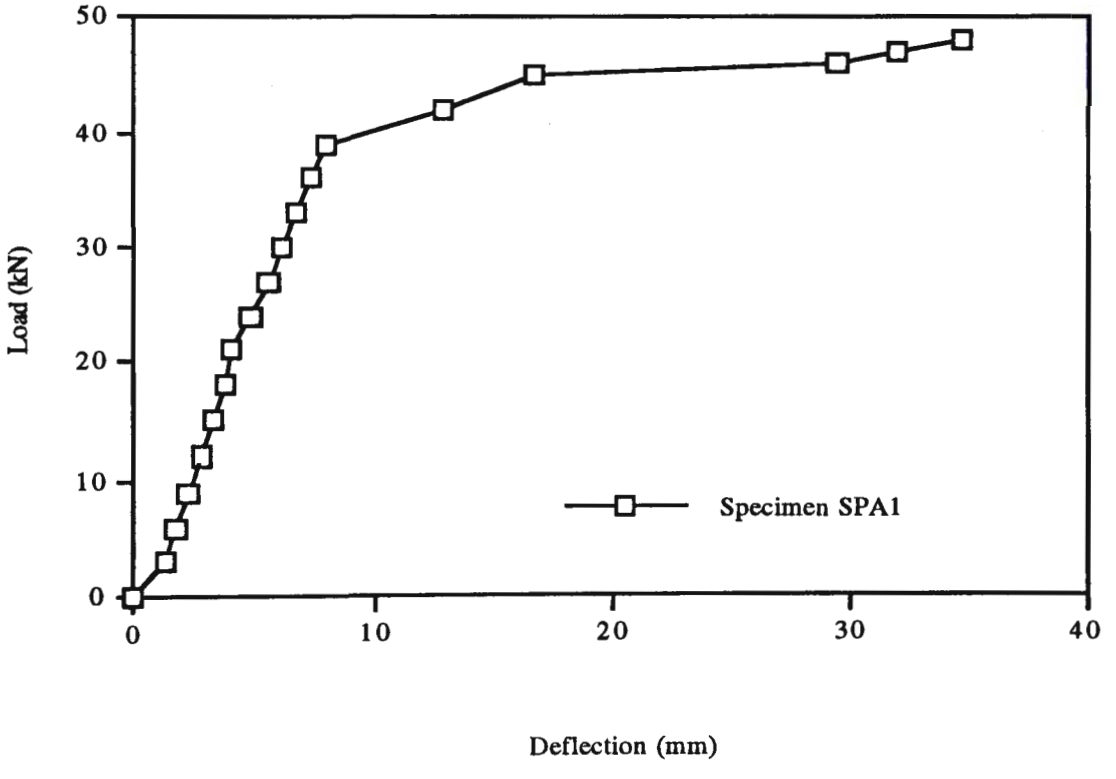

Fig. A.1.2 Load-Deflection Curve for Specimen SPA1

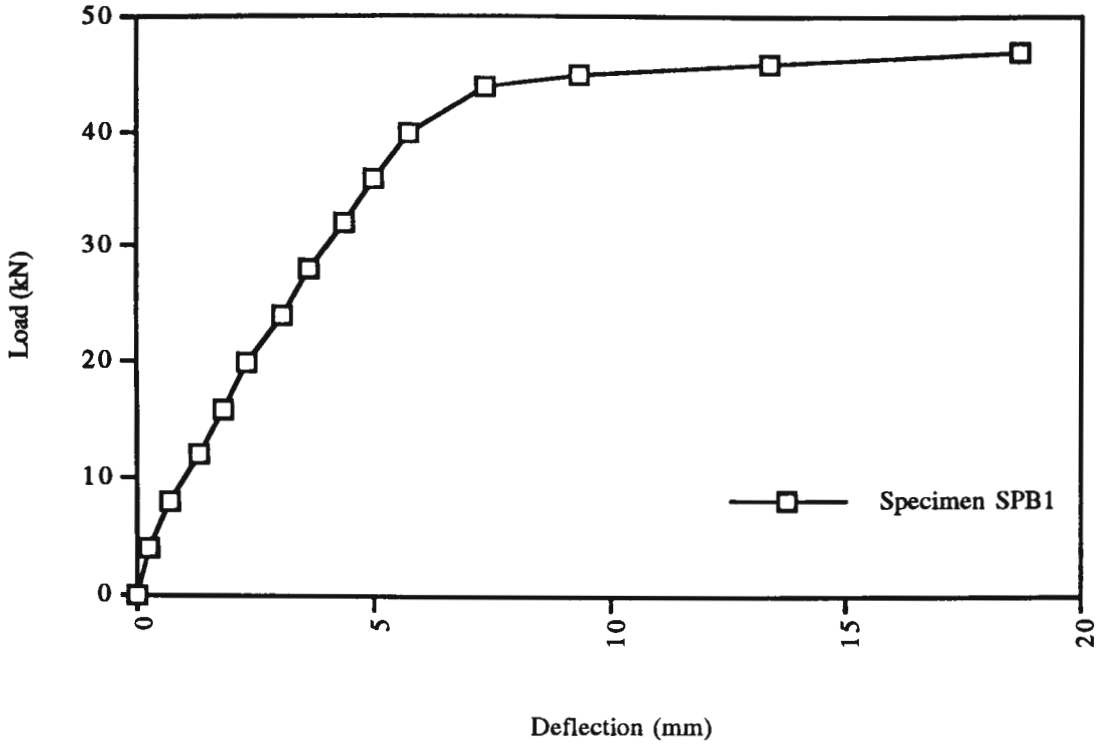

Fig. A.1.3 Load-Deflection Curve for Specimen SPB1

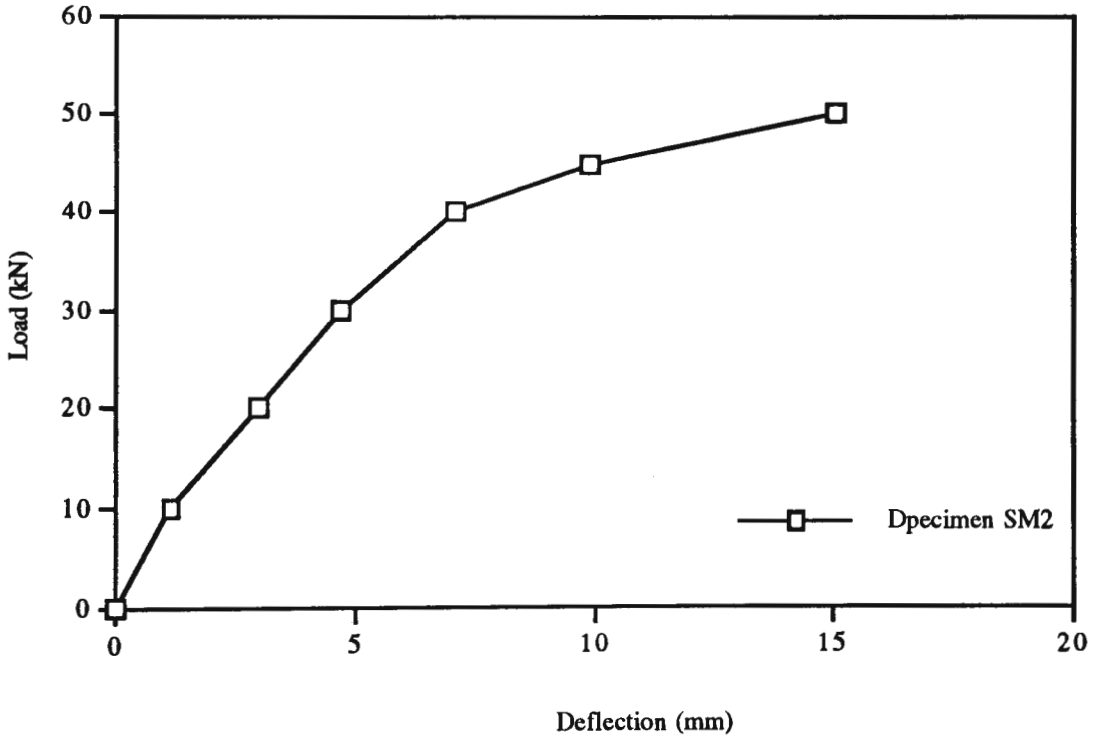

Fig. A.1.4 Load-Deflection Curve for Specimen SM2

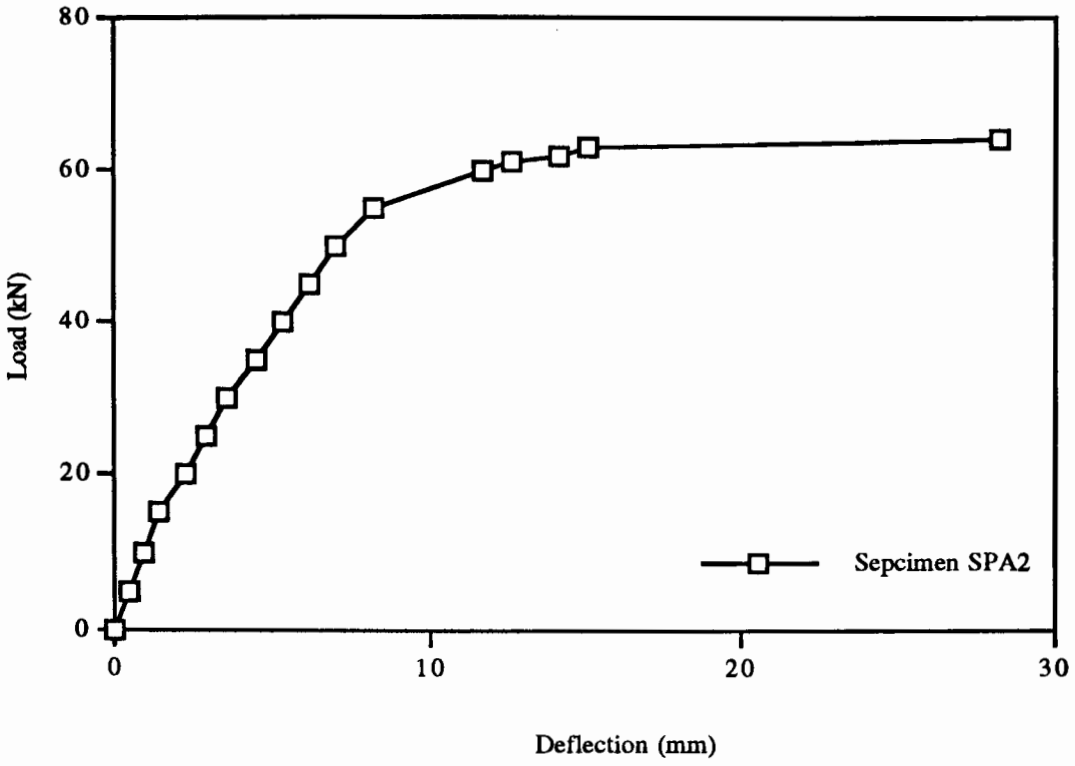

Fig. A.1.5 Load-Deflection Curve for Specimen SPA2

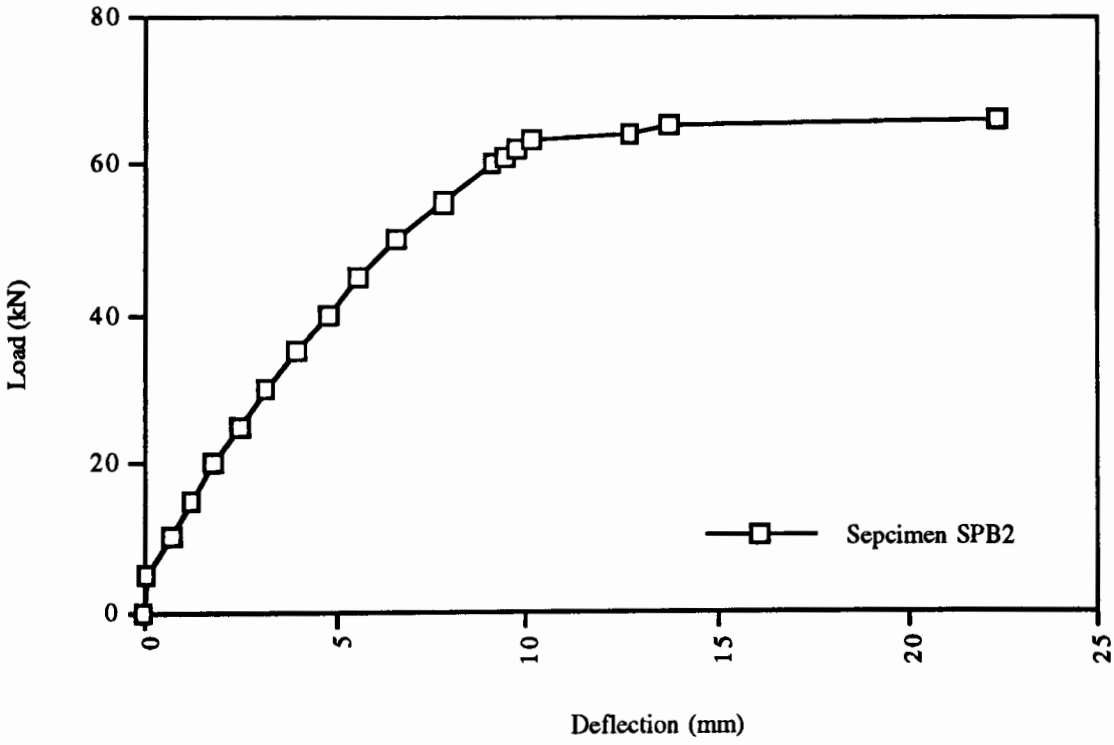

Fig. A.1.6 Load-Deflection Curve for Specimen SPB2

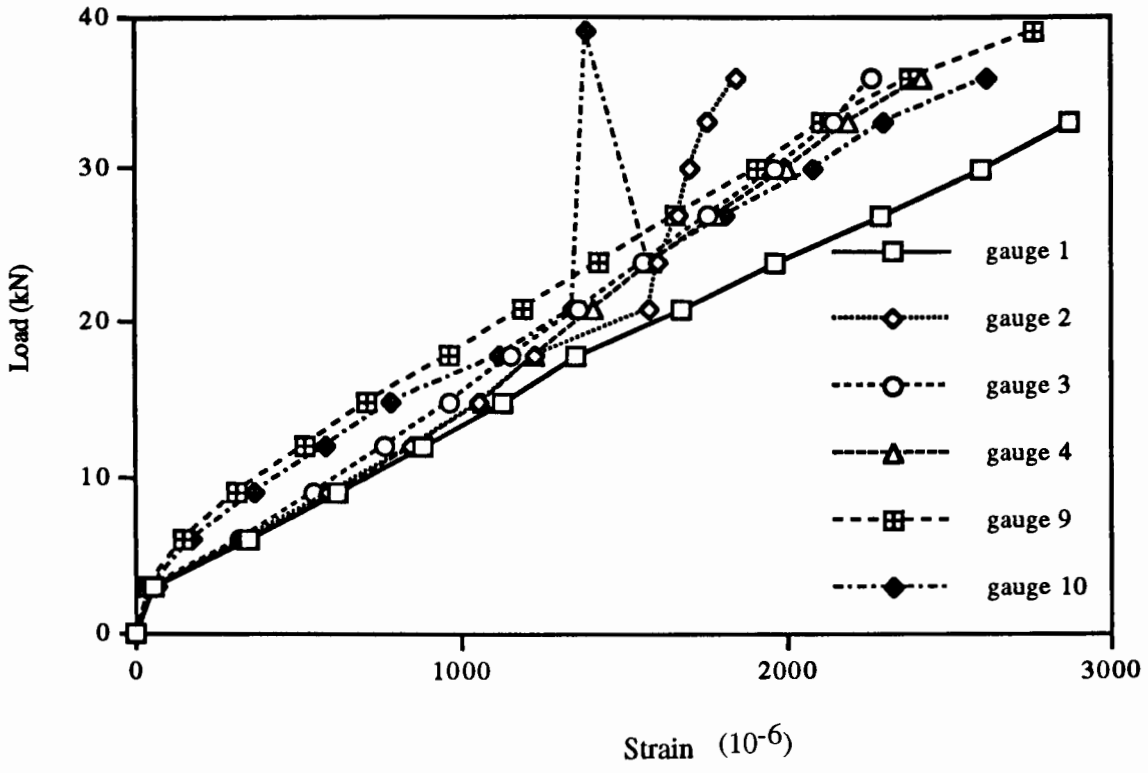

Fig. A.1.7 Load-Strain Curves for Specimen SM1

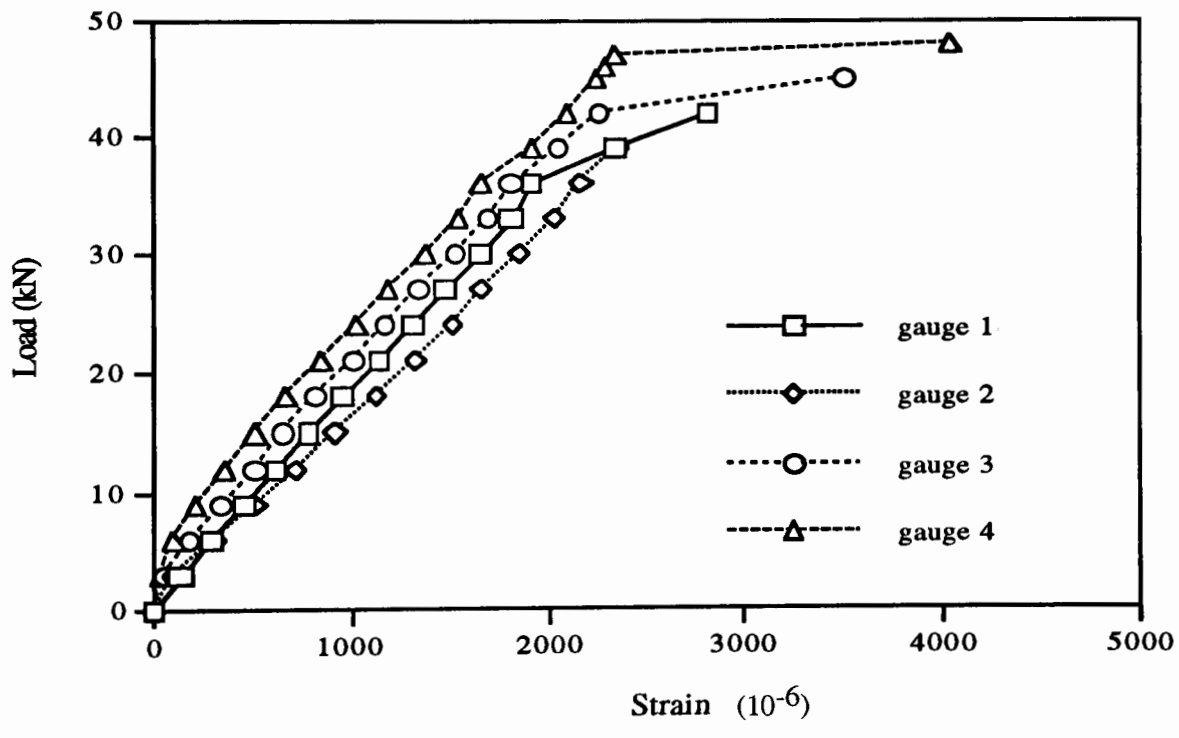

Fig. A.1.8 Load-Strain Curves for Specimen SPA1

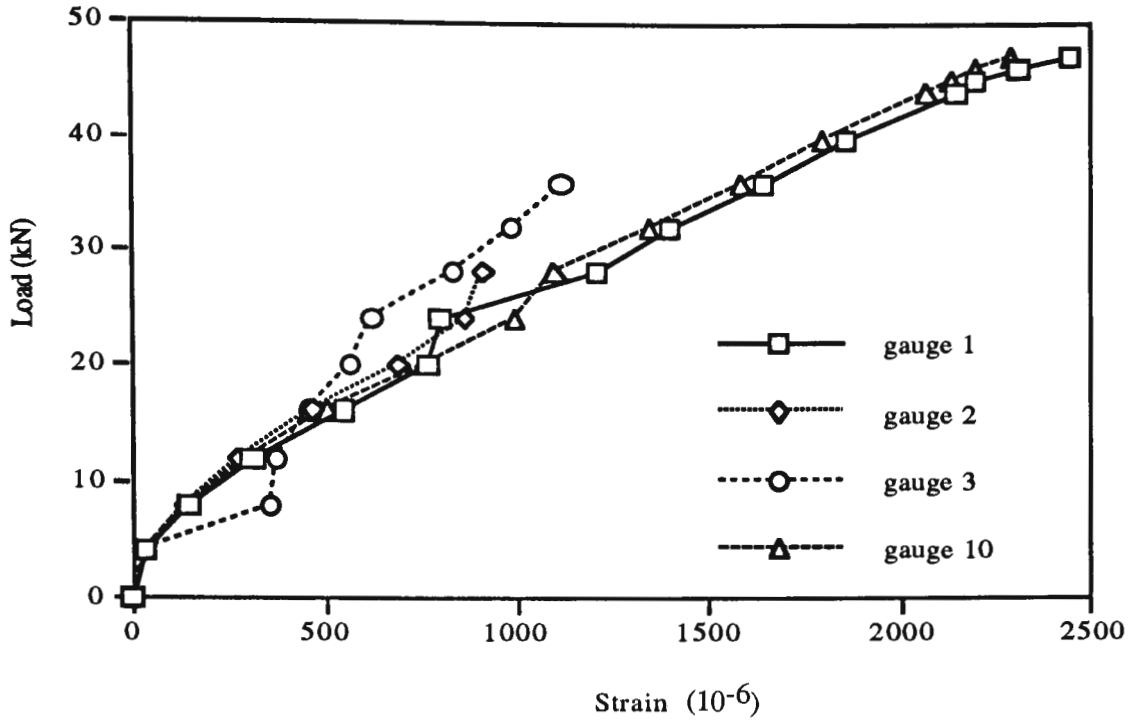

Fig. A.1.9 Load-Strain Curves for Specimen SPB1

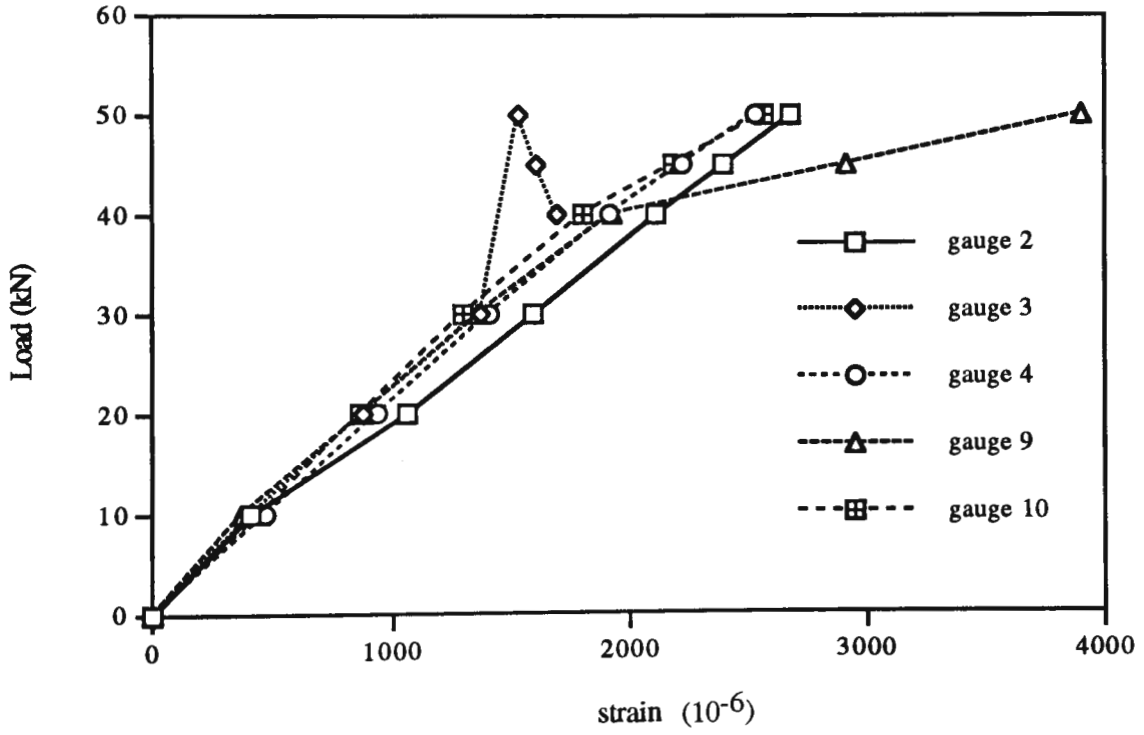

Fig. A.1.10 Load-Strain Curves for Specimen SM2

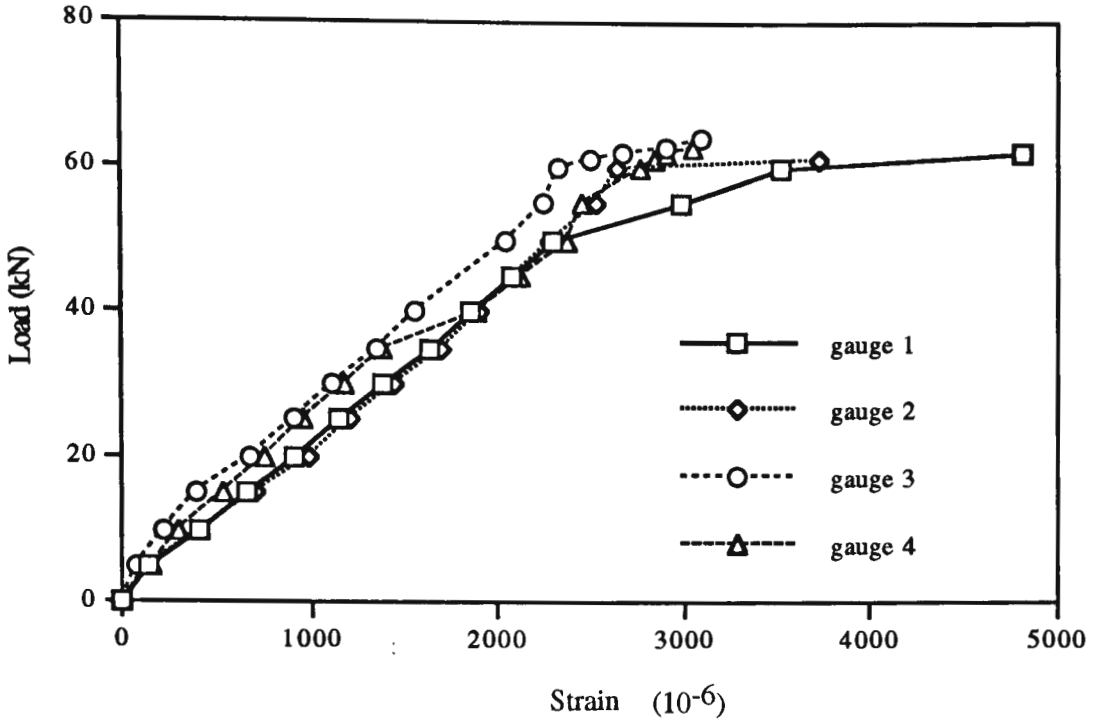

Fig. A.1.11 Load-Strain Curves for Specimen SPA2

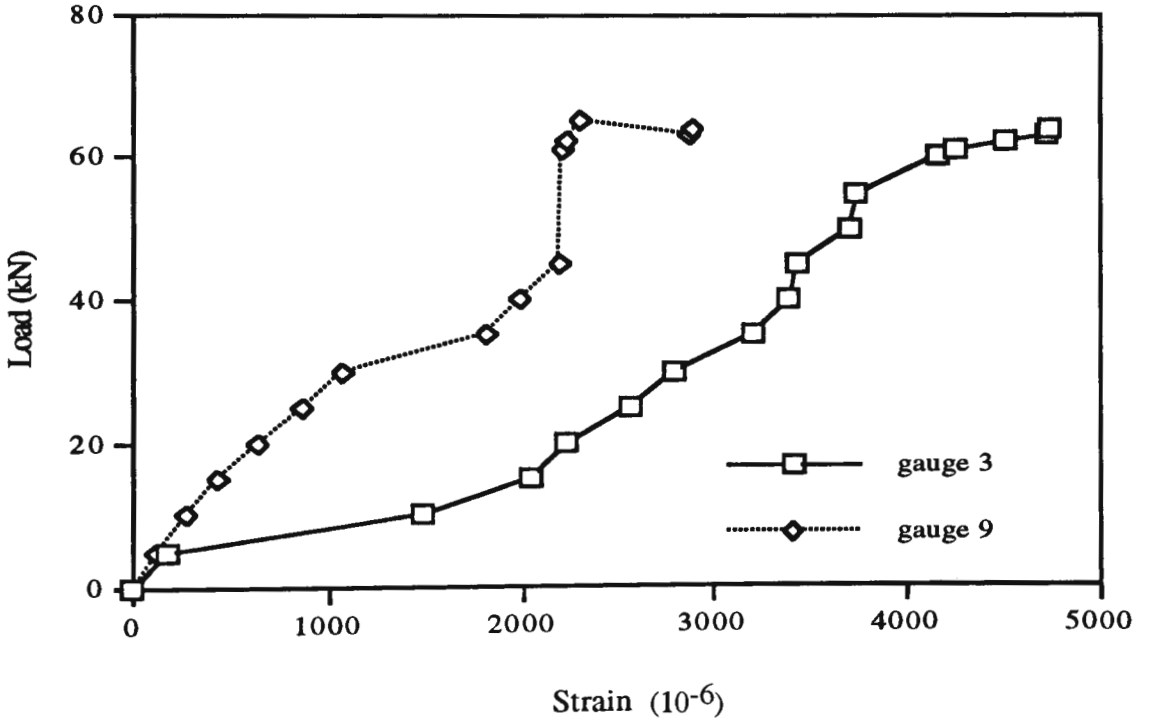

Fig. A.1.12 Load-Strain Curves for Specimen SPB2

APPENDIX 2

NOMALISED TEST DATA OF SPECIMEN TESTED

UNDER REPEATED LOADING

Table A.2.1 Test Data of Deflection and Concrete Strain for Specimen RM1

Load stage	Load (kN)	Deflection (mm)		Concrete Strain (10^{-6})				Remark
		Vertical	Horizontal	gauge 1	gauge 2	gauge 3	gauge 4	
0	0	0	0	0	0	0	0	
1	5	0.53	0.10	267	-111		-91	
2	10	1.46	0.25	1411	-274		-190	
3	15	2.31	0.39	2674	-449		-289	
4	20	3.42	0.59	3820	-623		-388	
5	25	4.37	0.74		-803		-490	Δ_y
6	20	3.99	0.67		-707		-413	
7	15	3.36	0.58		-579		-327	
8	10	2.71	0.49		-435		-237	
9	5	2.02	0.38		-290		-145	
10	0	1.27	0.23		-121		-49	
11	5	2.37	0.31		-249		-129	
12	10	2.52	0.43		-404		-277	
13	15	3.20	0.52		-551		-313	
14	20	3.89	0.64		-700		-409	
15	30.7	5.74	0.96		-1067		-618	$1.3\Delta_y$
16	20	4.57	0.75		-817		-436	
17	10	3.16	0.53		-521		-256	
18	0	1.57	0.25		-163		-62	
19	10	2.80	0.46		-461		-239	
20	20	4.72	0.69		-771		-423	
21	30	5.84	0.96		-1077		-615	
22	40	11.42	1.76		-1607		-852	$2.6\Delta_y$
23	30	9.92	1.57		-1589		-708	
24	20	8.46	1.31		-1341		-535	
25	10	6.72	1.02		-1027		-337	
26	0	5.92	0.70		-566		-135	
27	10	6.26	0.93		-903		-307	
28	20	7.95	1.20		-1237		-505	
29	30	8.98	1.52		-1558		-696	
30	40	11.84	2.00		-2020		-893	
31	41.1	14.87	2.92		-2153		-956	$3.4\Delta_y$
32	30	14.22	2.66		-2319		-789	
33	20	13.53	2.31		-2441		-610	
34	10	12.59	1.87		-2059		-416	
35	0	9.42	1.36		-1484		-212	
36	10	10.92	1.65		-1906		-381	
37	20	11.92	1.95		-2303		-571	
38	30	13.84	2.25		-2629		-757	
39	40	14.80	2.96		-2963		-942	
40	41	16.92	4.96		-773			
41	41	33.70	7.67					$7.7\Delta_y$

Table A.2.2 Test Data of Deflection and Concrete Strain for Specimen RPA1

Load stage	Load (kN)	Deflection (mm)		Concrete Strain (10^{-6})				Remark
		Vertical	Horizontal	gauge 1	gauge 2	gauge 3	gauge 4	
0	0	0	0		0	0	0	
1	5	0.51	0.05		-50	76	-50	
2	10	1.14	0.23		-161	-492	-125	
3	15	1.81	0.35		-226	-941	-199	
4	20	2.58	0.52		-302	-1583	-281	
5	25	3.47	0.70		-634	-2004	-383	
6	30	5.43	1.61		-703		-473	Δ_y
7	20	4.42	1.48		-566		-342	
8	10	3.19	1.27		-600		-195	
9	20	4.28	1.42		-730		-336	
10	31	5.53	1.69		-893		-493	Δ_y
11	20	4.56	1.52		-642		-244	
12	10	3.28	1.30		-492		-197	
13	20	4.35	1.46		-638		-339	
14	30	5.63	1.67		-780		-480	
15	35	6.38	1.83		-850		-551	
16	40	7.65	1.70		-899		-643	
17	42	10.83	2.34		-936		-694	$2\Delta_y$
18	10	5.15	1.63		-774		-522	
19	30	7.63	1.59		-846		-592	
20	35	8.33	1.78		-951		-709	
21	42.4	10.56	2.78		-658		-247	$2\Delta_y$
22	10	6.19	1.71		-948		-535	
23	30	9.86	1.94		-1089		-678	
24	40	10.33	2.63		-1075		-620	
25	47.2	16.48	4.37		-741		-307	$3\Delta_y$
26	10	14.45	2.97		-1008		-597	
27	30	16.48	3.61		-1148		-737	
28	40	17.53	4.09					$3\Delta_y$
29	10							
30	43.6	34.33	8.01					$6.3\Delta_y$

Table A.2.3 Test Data of Deflection and Concrete Strain for Specimen RPB1

Load stage	Load (kN)	Deflection (mm)		Concrete Strain (10^{-6})				Remark
		Vertical	Horizontal	gauge 1	gauge 2	gauge 3	gauge 4	
0	0	0	0		0			
1	10	1.49	0.48		-36			
2	20	3.54	0.85		-78			
3	25	4.40	1		-94			Δ_y
4	0	1.26	0.04		-2			
5	10	2.56	0.43		-18			
6	15	4.40	0.74		-41			Δ_y
7	0	1.22	0.02		-11			
8	10	2.60	0.36		-10			
9	20	3.98	0.85		-55			Δ_y
10	25	4.61	0.98		-72			
11	30	5.41	1.13		-86			
12	35	6.37	1.32		-99			
13	40	7.34	1.52		-117			
14	46	8.80	1.81		-143			$2\Delta_y$
15	0	2.41	0.09		-26			
16	30	6.84	1.38		-71			
17	44	8.80	1.79		-126			$2\Delta_y$
18	0	2.45	0.04		-28			
19	40	8.48	1.68		-103			
20	47	12.39	2.31					$3\Delta_y$
21	0	7.33	0.81					
22	46	13.04	2.94					$3\Delta_y$
23	0	8.49	0.80					
24	48	30.79	9.50					$7\Delta_y$

Table A.2.4 Test Data of Deflection and Concrete Strain for Specimen RM2

Load stage	Load (kN)	Deflection (mm)		Concrete Strain (10^{-6})				Remark
		Vertical	Horizontal	gauge 1	gauge 2	gauge 3	gauge 4	
0	0	0	0		0	0	0	
1	10	1.41	0.51		-283	569	-169	
2	20	3.81	0.77		-556	1290	-345	
3	25	3.56	0.87		-699	1713	-435	
4	30	4.38	1.03		-854	2127	-538	
5	35	5.28	1.14		-1014	2567	-633	
6	40	6.63	1.52		-1210		-740	Δ_y
7	0	1.49	0.30		-178		-51	
8	30	5.18	1.11		-990		-585	
9	38.6	6.56	1.49		-1203		-729	Δ_y
10	0	1.50	0.30		183		-54	
11	40	6.28	1.08		-1257		-760	
12	50	8.83	1.70		-1589		-985	
13	55	9.41	1.83		-1710		-1161	
14	59	13.25	2.36		-1974		-1231	$2\Delta_y$
15	0	4.69	1.62		-675		-208	
16	50	11.28	1.15		-1595		-1193	
17	54.3	13.16	2.29		2143		-1277	$2\Delta_y$
18	0	4.83	0.67		-693		-218	
19	50	11.31	2.23		-2083		-1218	
20	58.5	19.89	4.36					$3\Delta_y$
21	0	6.91	2.24				-355	
22	49.0	38.06	6.49				-343	$5.74\Delta_y$

Table A.2.5 Test Data of Deflection and Concrete Strain for Specimen RPA2

Load stage	Load (kN)	Deflection (mm)		Concrete Strain (10^{-6})				Remark
		Vertical	Horizontal	gauge 1	gauge 2	gauge 3	gauge 4	
0	0	0	0		0	0	0	
1	10	2.04	1.34		-139	154	-108	
2	20	3.12	1.62		-325	688	-239	
3	30	4.45	1.98		-519	1338	-374	
4	35	5.20	2.18		-615	1595	-441	
5	40	5.98	2.39		-714		-523	
6	45	7.04	2.81		818		-595	Δ_y
7	0	2.26	1.53		-61		-58	
8	44.5	7.04	2.79		-813		-599	Δ_y
9	0	2.28	1.53		-61		-58-553	
10	40	6.75	2.75		-741		-613	
11	45	7.25	2.91		-829		-770	
12	55	9.86	3.28		-1040		-1008	
13	65	14.27	4.53		-1694		-173	$2\Delta_y$
14	0	7	2.33		-403		-924	
15	58	14.12	4.28		-1571		-174	$2\Delta_y$
16	0	7.02	2.32		-406		-834	
17	50	13.23	4.10		-1410		-924	
18	63	21.24	6.97		-156		-288	$3\Delta_y$
19	0	9.82	4.53				-1127	
20	66	21.27	7.27				-297	$3\Delta_y$
21	0	19.89	4.70				-1137	
22	68	41.15	12.31					$5.8\Delta_y$

Table A.2.6 Test Data of Deflection and Concrete Strain for Specimen RPB2

Load stage	Load (kN)	Deflection (mm)		Concrete Strain (10^{-6})				Remark
		Vertical	Horizontal	gauge 1	gauge 2	gauge 3	gauge 4	
0	0	0	0	0	0		0	
1	10	0.97	0.18	52	-37		-256	
2	20	3.17	0.38	1561	-93		-458	
3	30	4.54	0.59		-131		-609	
4	44	6.6	0.94		-132		-826	
5	0	0.23	0.09		-26		-108	
6	30	5.30	0.65		-107		-636	Δ_y
7	42.5	6.60	0.92		-127		-803	
8	0	2.29	0.09		-25		-109	Δ_y
9	40	6.39	0.86		-123		-771	
10	50	8.17	1.43		-148		-919	
11	60	10.11	2.15		-147		-1078	
12	70	13.40	2.78		-136		-1278	
13	0	5.20	0.54		-83		-257	$2\Delta_y$
14	52	13.20	2.45		-173		-1219	
15	0	5.22	1.51					$2\Delta_y$
16	60	13.04	2.40					
17	70	19.75	4.93					
18a	0	15.29	1.84					
18	64	19.79	4.62					$3\Delta_y$
19	0	16.94	2.53					
20	50	17.69	4.19					$3\Delta_y$
21	63.5	26.34	6.15					
22	0	24.49	3.73				-275	
23	61	40.66	8.62				-1234	$5.8\Delta_y$

APPENDIX 3

APPENDIX 3

MEASURED PROPERTIES OF REINFORCING BAR

There were four types of reinforcing bars used for the specimens. These were deformed bars Y16 for top longitudinal steel of beams; deformed bars Y12 for the longitudinal steel of columns; plain bar R10 for the bottom longitudinal steel of beams and plain bar R6 for all the stirrups.

Four 400 mm long samples were taken from each type of bars. Each of these four samples were cut from different 6 m length bars to get average test results. The samples was tested uniaxially in tension to obtain the yield and ultimate strength, and ultimate elongation over a gauge length of 200 mm. At each loading stage the load and the elongation were recorded. The results are given in Table A.3.1 to A.3.6. Load-extension curves for different diameter reinforcing bars are given in Fig A.3.1 through A.3.3.

Table A.3.1 Test Data of Tension steel Bar (1) (10mmbar):

No. of sample	Load (kN)	Division	ε (10^{-4})	α=P/A (MPa)	Es=α/ε (MPa)	Es (MPa)	Aver.Es (MPa)
1	0.00	930				244100	227600
	3.65	962	2.592	45.56	175800		
	8.70	980	4.05	108.59	268100		
	13.80	1007	6.237	172.24	276200		
	18.70	1035	8.505	233.40	274400		
	23.00	1080	12.15	287.07	236300		
	28.80	1120	15.39	359.46	233600		
2	0.00	900				217000	
	4.50	940	3.24	56.39	174000		
	9.30	967	5.427	116.54	214700		
	14.00	996	7.776	175.44	225600		
	19.00	1028	10.368	238.10	229600		
	23.7	1058	12.798	296.99	232100		
	28.50	1095	15.795	357.14	226100		
3	0.00	815				221800	
	3.80	850	2.835	48.4	170700		
	9.00	877	5.022	114.59	228200		
	14.5	910	7.695	184.62	239900		
	18.6	935	4.86	236.82	243600		
	23.4	973	12.798	297.94	232800		
	29.50	1030	17.415	375.60	215700		

Note: one division = 0.81 x 10^{-6} strain.

Table A.3.2 Test Data of Tension Steel Bar(1) (12mm bar):

No. of sample	Load (kN)	Division	ε (10^{-4})	α=P/A (MPa)	Es=α/ε (MPa)	Es (MPa)	Aver.Es (MPa)
1	0.00	1004				243500	230300
	9.40	1048	3.564	88.95	249600		
	19.00	1092	7.128	179.79	252200		
	29.00	1145	11.142	274.41	240300		
	39.10	1195	15.471	369.98	239100		
	49.80	1250	15.926	471.23	236500		
2	0.00	935				212000	
	9.60	986	4.151	89.29	216100		
	18.60	1033	7.938	173.01	218000		
	29.25	1095	12.960	272.07	209900		
	39.20	1152	17.577	364.62	207400		
	50.30	1212	22.437	467.86	208500		
3	0.00	937				235300	
	8.50	988	4.131	80.43	194700		
	19.10	1037	8.100	180.73	223100		
	28.40	1075	11.178	268.74	240400		
	39.30	1116	14.499	372.88	257200		
	49.20	1157	17.820	465.56	261300		

Note: one division = 0.81 x 10^{-6} strain.

Table A.3.3 Test Data of Tension Steel Bar (1) (16mm bar):

No. of sample	Load (kN)	Division	ε (10^{-4})	α=P/A (MPa)	Es=α/ε (MPa)	Es (MPa)	Aver.Es (MPa)
1	0.00	1002				220700	215000
	13.00	1043	3.321	72.475	218230		
	28.70	1088	6.966	154.077	221180		
	43.20	1135	10.773	231.920	215300		
	57.80	1175	14.013	310.302	221440		
	72.80	1215	17.253	390.081	226530		
	89.50	1270	10.854	480.485	221340		
2	0.00	953				22490	
	13.90	996	3.483	75.605	434000		
	27.70	1032	6.399	150.666	235500		
	43.80	1081	10.368	238.238	229800		
	58.00	1128	14.175	315.475	222600		
	72.90	1175	17.982	396.519	220500		
	89.70	1222	21.789	487.898	223900		
3	0.00	902				213500	
	14.80	946	3.564	76.839	215600		
	29.30	988	6.966	152.121	218400		
	43.60	1030	10.368	226.364	218300		
	59.20	1078	14.256	307.357	215600		
	74.30	1130	18.468	385.754	208900		
	88.60	1180	22.518	459.997	204300		
4	0.00	944				200700	
	13.20	990	3.726	71.23	191200		
	27.00	1040	7.776	145.71	187400		
	42.60	1090	11.826	229.90	194400		
	58.90	1130	15.066	317.86	211000		
	72.50	1177	18.873	391.26	207300		
	88.40	1221	22.437	477.06	212600		

Note: one division = 0.81 x 10^{-6} strain.

Table A.3.4 Test Data of Tension Steel Bar (2) (10mm bar)

name of samples	diameter (mm)	area (mm^2)	yield load (kN)	yield strength (MPa)	yield strain (10^{-3})	Max. load (kN)
1	10.10	80.12	30.06	375.19	1.648	38.02
2	10.08	79.80	30.00	375.94	1.652	38.27
3	10.00	78.54	29.60	376.88	1.656	38.00
4	10.10	80.12	29.20	364.45	1.601	38.30
average	10.07	79.65	29.72	373.11	1.639	38.15
normalise	10.00	80.00	29.72	371.50	1.639	38.15

Table A.3.5 Test Data of Tension Steel Bar (2) (12mm bar)

name of samples	diametre (mm)	area (mm^2)	yield load (kN)	yield strength (MPa)	yield strain (10^{-3})	Max. load (kN)
1	11.60	105.68	52.60	497.73	2.161	63.67
2	11.70	107.51	52.60	489.26	2.124	64.50
3	11.60	105.68	52.40	495.84	2.153	63.30
4	11.68	107.15	51.40	477.83	2.075	62.04
average	11.65	106.51	52.20	490.17	2.128	63.38
normalise	12.00	110.00	52.20	470	2.128	63.38

Table A.3.6 Test Data of Tension Steel Bar (2) (16mm bar)

name of samples	diametre (mm)	area (mm^2)	yield load (kN)	yield strength (MPa)	yield strain (mm)	Max. load (kN)
1	15.40	186.27	87.00	467.06	2.172	112.50
2	15.30	183.85	88.00	478.65	2.226	113.30
3	15.66	192.61	88.00	456.88	2.125	113.70
4	15.36	185.30	88.00	474.91	2.209	112.30
average	15.43	187.01	87.75	469.38	2.183	112.95
normalise	16.00	200.00	87.75	440.00	2.183	112.95

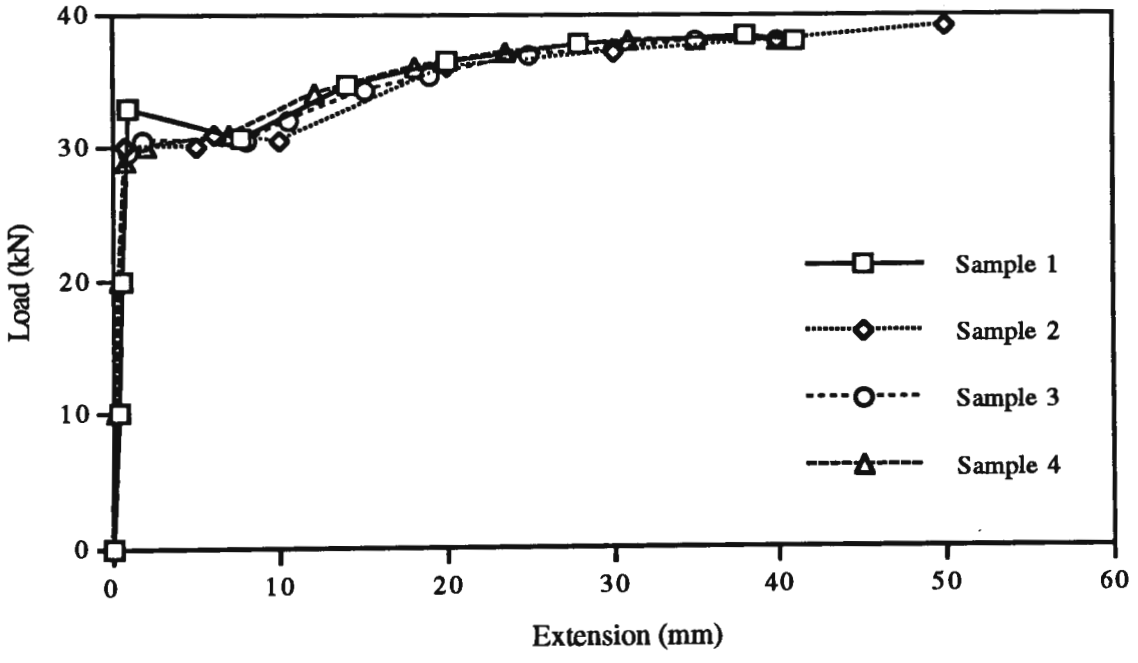

Fig. A.3.1 Load-Extension Curves for R10 Bar

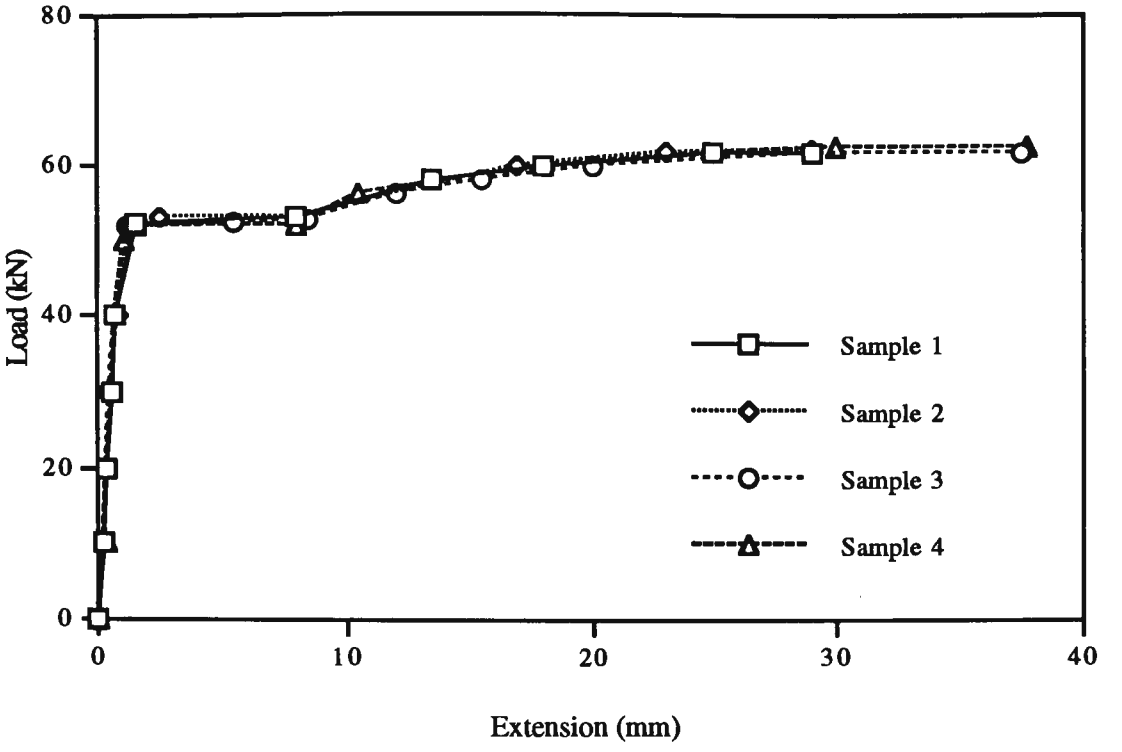

Fig.A.3.2 Load-Extension Curves for Y12 Bar

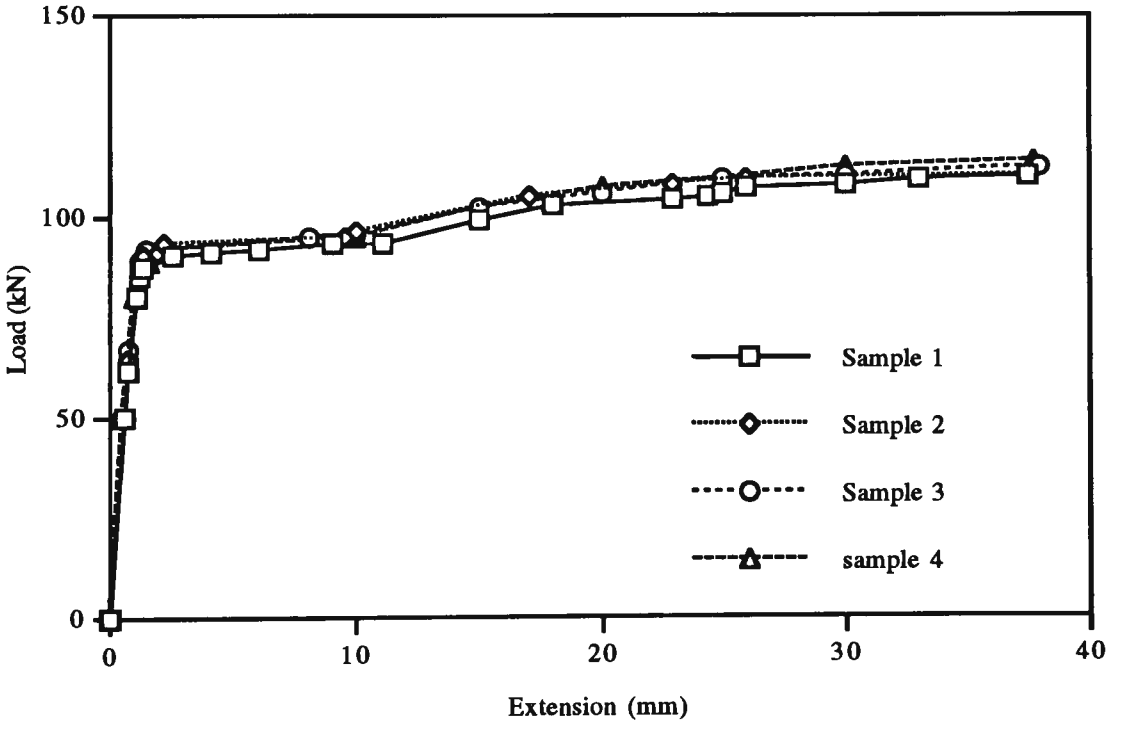

Fig.A.3.3 Load-Extension Curves for Y16 Bar

APPENDIX 4

APPENDIX 4

DESIGN OF CAST-IN-PLACE CONCRETE

Cast-in-place concrete is a very important material for precast concrete structures, because it is used to assemble two different precast parts into a whole structure. Therefore the characteristics of cast-in-place concrete affects the whole structure, directly.

The object of mix design is to determine the most appropriate proportions in which to use the constituent materials to meet the needs of construction work. In particular, the concrete should comply with the specification requirement for structural strength which is usually stated in terms of the compressive strength of standard test specimens, and have satisfactory durability in the environment in which the structure is placed.

The procedure of mix design is describedas follows:

A. Selection of target strength

Generally, in order to avoid connection failure prior to that of the structure, the characteristic strength of cast-in-place concrete should be at least 10MPa higher than that of the precast concrete. So, the target strength can be calculated from the following:

target strength = Strength of precast concrete + 10MPa

Here:

Strength of precast concrete: 32MPa

Target strength of cast-in-place concrete = 42MPa

B. Selection of water / cement ratio:

The compressive strength of fully compacted concrete can generally be assumed to be dependent only on the water / cement ratio of the mix, provided that the properties of the cement and the curing conditions remain the same. According to Australian code, for 42MPa target strength, a 0.42 water / cement ratio is needed.

C. Getting proportions by weight for 1 Cubic Metre of concrete under 80 mm slump

For a given value of target strength and water/cement ratio, the proportions of constituents may be obtained by AS Code. Following is the proportions by weight for 1 cubic metre of concrete under 80 mm slump.

Table A.4.1 Proportion by weight for 1 cubic metre of concrete under 80 mm slump

Max.Agg. size (mm)	F'c (MPa)	W / C (%)	Total water (kg)	Cement (kg)	Sand (kg)	Coarse Agg. (kg)
10	42	42	220	520	730	800

The concrete obtained to make precast models at different times usually have different strengths. Therefore the strength of cast-in-place concrete had to be changed accordingly. In order to verify the required strength of cast-in-place concrete, some small cylinders were made in small trial batches. Type B high early strength cement was used to decrease the curing time and avoid shrinkage cracking during curing.

The details of the first trial mixture of cast-in-place concrete are shown in Table A.4.2. Table A.4.3 gives the strength and slump of first trial.

Table A.4.2 The proportion of first trial mixture of cast-in-place concrete

Name	pouring date	total vol (m^3)	Max Agg size (mm)	W / C (%)	Total water (kg)	Cement (kg)	Sand (kg)	Corse Agg (kg)	Eexp. strength (MPa)	Exp. Slump (mm)
T1	1/9	0.02	10	42	4.4	14.6	45.4	16	40	80
T2	1/9	0.015	10	36	3.3	9	9.9	12	50	80
T3	1/9	0.015	10	30	3.3	11.25	7.875	12	60	80

Table A.4.3 The strength of first trial mixture of cast-in-place concrete.

Name	pouring date	exp. strength. (MPa)	exp. slump (mm)	7 days strength (MPa)	14 days strength. (MPa)	slump (mm)
T1	1/9	40	80	41.76	47.05	160
T2	1/9	50	80	47.91	53.60	105
T3	1/9	60	80	54.43	56.00	15

From table A.4.3, we know that the slump is not quite well. So the second trial mixtures were made as follows:

Table A.4.4 The proportion of second trial mixture of cast-in-place concrete

Name	pouring date	total vol (m^3)	Max Agg size (mm)	W / C (%)	Total water (kg)	Cement (kg)	Sand (kg)	Corse Agg (kg)	Eexp. strength (MPa)	Exp. Slump (mm)
T4	13/9	0.0075	10	42	1.5	3.575	5.75	6.3	40	80
T5	13/9	0.0075	10	35	1.625	4.45	5.00	6.05	50	80
T6	13/9	0.0075	10	30	1.725	5.75	3.79	5.85	60	80

Table A.4.5 The strength of second trial mixture of cast-in-place concrete.

Name	pouring date	expected. strength. (MPa)	expected. slump (mm)	7 days strength (MPa)	14 days strength. (MPa)	slump (mm)
T4	13/9	40	80	41.5	59	50
T5	13/9	50	80	45.0	60.5	70
T6	13/9	60	80	49.0	65	50

Base on the information from two trial mixtures, the suitable proportion of cast-in-place concrete were chosen as the same as T5.